Government of **Western Australia**
Department of **Mines and Petroleum**

**RECORD 2010/19**

# A TIME TRANSECT THROUGH THE HADEAN TO NEOARCHEAN GEOLOGY OF THE WESTERN YILGARN CRATON — A FIELD GUIDE

**compiled by**

**MJ Van Kranendonk, TJ Ivanic, S Wyche, SA Wilde, and I Zibra**

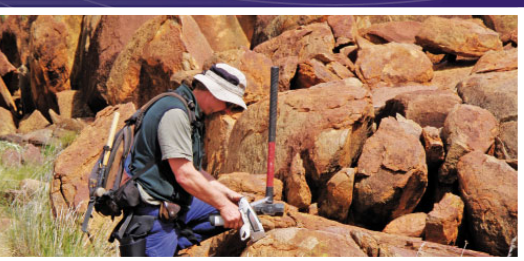

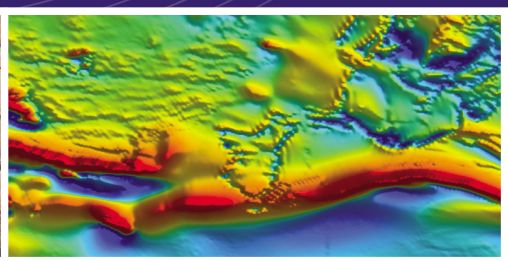

**Geological Survey of Western Australia**

Government of **Western Australia**
Department of **Mines and Petroleum**

**Record 2010/19**

# A TIME TRANSECT THROUGH THE HADEAN TO NEOARCHEAN GEOLOGY OF THE WESTERN YILGARN CRATON — A FIELD GUIDE

**compiled by**
**MJ Van Kranendonk[1], TJ Ivanic[1], S Wyche[1], SA Wilde[2], and I Zibra[1]**

[1] Geological Survey of Western Australia
[2] Curtin University of Technology

**Perth 2010**

Geological Survey of Western Australia

**MINISTER FOR MINES AND PETROLEUM**
**Hon. Norman Moore MLC**

**DIRECTOR GENERAL, DEPARTMENT OF MINES AND PETROLEUM**
**Richard Sellers**

**ACTING EXECUTIVE DIRECTOR, GEOLOGICAL SURVEY OF WESTERN AUSTRALIA**
**Rick Rogerson**

**REFERENCE**
**The recommended reference for this publication is:**
Van Kranendonk, MJ, Ivanic, TJ, Wyche, S, Wilde, SA and Zibra, I 2010, A time transect through the Hadean to Neoarchean geology of the western Yilgarn Craton — a field guide: Geological Survey of Western Australia, Record 2010/19, 69p.

**National Library of Australia Card Number and ISBN 978-1-74168-325-7 (PDF); 978-1-74168-326-4 (printed)**

**Grid references in this publication refer to the Geocentric Datum of Australia 1994 (GDA94). Locations mentioned in the text are referenced using Map Grid Australia (MGA) coordinates, Zone 50. All locations are quoted to at least the nearest 100 m.**

**Published 2010 by Geological Survey of Western Australia**
**This Record is published in digital format (PDF), as part of a digital dataset on CD, and is available online at <http://www.dmp.wa.gov.au/GSWApublications>. Laser-printed copies can be ordered from the Information Centre for the cost of printing and binding.**

**Further details of geological publications and maps produced by the Geological Survey of Western Australia are available from:**
Information Centre
Department of Mines and Petroleum
100 Plain Street
EAST PERTH, WESTERN AUSTRALIA 6004
Telephone: +61 8 9222 3459 Facsimile: +61 8 9222 3444
**www.dmp.wa.gov.au/GSWApublications**

# Contents

## Mid-Murchison Domain (by I Zibra)



## Part 3: Windimurra and Narndee Igneous Complexes (by TJ Ivanic)



# Figures

## Tables

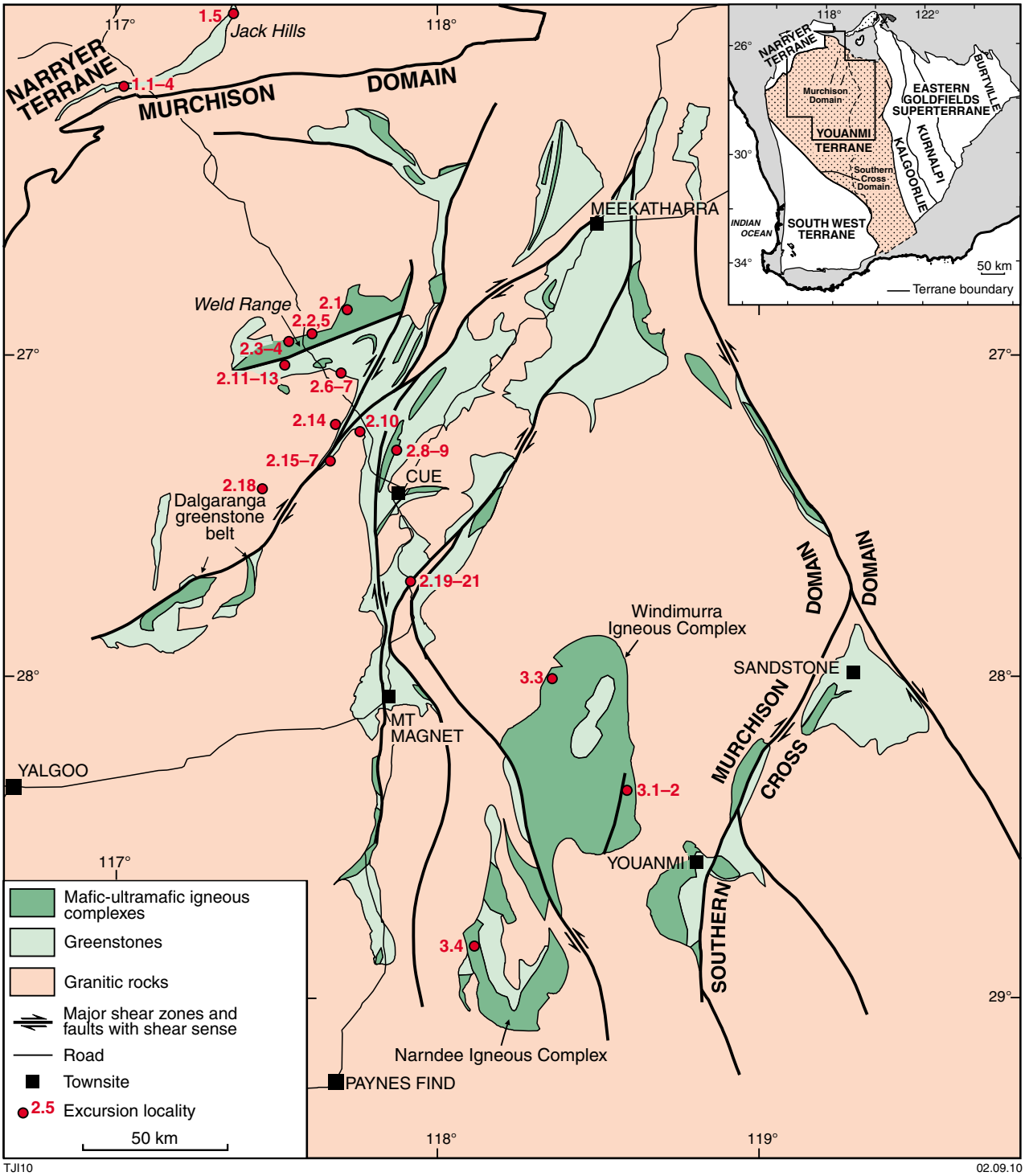


**Figure 1. Simplified geology of the northwestern part of the Yilgarn Craton showing excursion localities**

# A time transect through the Hadean to Neoarchean geology of the western Yilgarn Craton — a field guide

**compiled by**

**MJ Van Kranendonk[1], TJ Ivanic[1], S Wyche[1], SA Wilde[2], and I Zibra[1]**

## Preface

Rocks of every Archean era are present in the western Yilgarn Craton, with zircons dating back to the Hadean also represented in clastic sedimentary rocks. This excursion will investigate a time slice from the Hadean zircons at Jack Hills through Eo-, Paleo-, Meso- and Neoarchean rocks of the Narryer and Youanmi Terranes. A wealth of new isotopic, geochronological, geochemical, and geophysical data will be presented, in the context of new geological mapping, to see what insights they give into evolving early Earth processes and the development of related mineral systems.

Starting in the Jack Hills, site of the oldest known zircons on Earth, the excursion will visit Eo- to Paleoarchean gneisses of the Narryer Terrane, and then the recently documented Meso- to Neoarchean stratigraphy of the Youanmi Terrane, including the large layered mafic–ultramafic intrusions such as the Windimurra Igneous Complex — among the oldest of these features on Earth. Representative granite suites will be placed in the context of the overall tectonic history.

1 Geological Survey of Western Australia
2 Curtin University of Technology

# Part 1: Narryer Terrane

by SA Wilde

## Introduction

The Narryer Terrane, in the northwestern Yilgarn Craton of Western Australia, occupies an area of approximately 30 000 km$^2$ (Figs 1, 2). It is composed predominantly of granites and gneisses with U–Pb zircon ages up to 3730 Ma, which make these the oldest known rocks in Australia (Nutman et al., 1991). In addition, the gneisses contain lenses and more extensive areas of supracrustal rocks that range in metamorphic grade from greenschist to granulite facies and include belts of clastic metasedimentary rocks which, at Mount Narryer and Jack Hills, contain abundant detrital zircon grains >4 Ga in age, including the oldest terrestrial material on Earth. An overview of the history of investigations in the Narryer Terrane has recently been published (Wilde and Spaggiari, 2007) and only a brief outline will be given here; sufficient to place the rocks we will visit on the excursion into context.

As part of an extensive program by the Geological Survey of Western Australia (GSWA) to map the whole State of Western Australia at a scale of 1:250 000, the Narryer Terrane was investigated in the mid to late 1970s and the maps and accompanying explanatory notes published in the early 1980s. Of particular relevance to this excursion are the Belele* (Elias, 1982), Byro (Williams et al., 1983) and Robinson Range (Elias and Williams, 1980) sheets that each contain segments of the Jack Hills belt and environs. At the time these investigations were in progress, the Narryer area was considered to be part of the 'Western Gneiss Terrain' of Gee (1979) and Gee et al. (1981), defined as a belt of high-grade gneisses, deformed and undeformed granites, metasedimentary belts, and rare greenstone belts that made up the western margin of the Yilgarn Craton. This had long been considered the oldest part of the craton (Arriens, 1971) and as such became a focus for those interested in the early evolution of the Australian continent. Arriens (1971) had obtained several Rb–Sr whole rock ages in excess of >3 Ga from the southwestern margin of the Yilgarn Craton and it was decided by GSWA to test if the gneisses in the northwest recorded similar ages. Pioneering Rb–Sr whole-rock geochronological investigations were thus undertaken on granitic gneisses in the vicinity of Mount Narryer, where Ian Williams had identified a belt of quartzites that appeared remarkably similar to those exposed in the southwestern Yilgarn Craton near Toodyay (Wilde and Low, 1978). A date of 3348 ± 43 Ma was obtained by de Laeter et al. (1981a) and appeared to substantiate a connection between the southern and northern parts of the 'Western Gneiss Terrain' (Fig. 3). Dating of two of these samples using the Sm–Nd whole-rock technique (de Laeter at al., 1981b) yielded $T_{CHUR}$ model ages of 3630 ± 40 Ma and 3510 ± 50 Ma, considerably older than any ages previously obtained from the Yilgarn Craton.

Myers (1988) introduced the term 'Narryer Gneiss Terrane' for those areas in the northern part of the Yilgarn Craton where reconnaissance mapping indicated older gneisses were predominant. Later, Myers (1990) referred to the whole area, including those parts where late Archean granites were dominant over ancient gneisses, as the 'Narryer Terrane' and this is still the current usage of the term. The western margin of the Narryer Terrane is delineated by the Darling Fault, the northern margin by the Errabiddy Shear Zone, and the southern margin by the Balbalinga and Yalgar Faults (Fig. 4). The northern margin defines where the Glenburgh Terrane was accreted to the Yilgarn Craton during the 2005 to 1960 Ma Glenburgh Orogeny (Occhipinti et al., 2004; Occhipinti and Reddy, 2004). The southern margin marks the boundary with the Murchison Domain of the Younami Terrane, a major Archean granite–greenstone province in the west-central Yilgarn Craton (Cassidy et al., 2006) (Fig. 2). The early Archean gneisses of the Narryer Terrane have been interpreted as an allochthonous unit that was thrust over c. 3 Ga crust of the Youanmi Terrane, just prior to, or during, Late Archean granitic magmatism that stitched the two terranes (Nutman et al., 1993).

The gneisses have been subdivided into four main components (Myers and Williams, 1985; Nutman et al., 1991). The **Meeberrie Gneiss** belongs to the tonalite–trondhjemite–granodiorite (TTG) suite, with the oldest known component being a tonalite collected 3 km south of the Jack Hills. With a SHRIMP U–Pb date of 3731 ± 4 Ma (Nutman et al., 1991) this is the oldest known rock in Australia. Kinny and Nutman (1996) emphasized that it is impossible to quote a single age for the Meeberrie Gneiss in the Mount Narryer region as it is a polyphase migmatite that has been metamorphosed to granulite facies, with ages ranging from 3730 to 3300 Ma. The **Dugel Gneiss** occupies large areas of the Narryer Terrane and is dominantly syenogranite, ranging to monzogranite in composition. It forms veins that crosscut the Meeberrie Gneiss in low-strain zones, but is commonly brought into layer parallelism with the Meeberrie Gneiss and both underwent high-grade metamorphism. Zircon cores

* Capitalized names refer to standard 1:250 000 map sheets

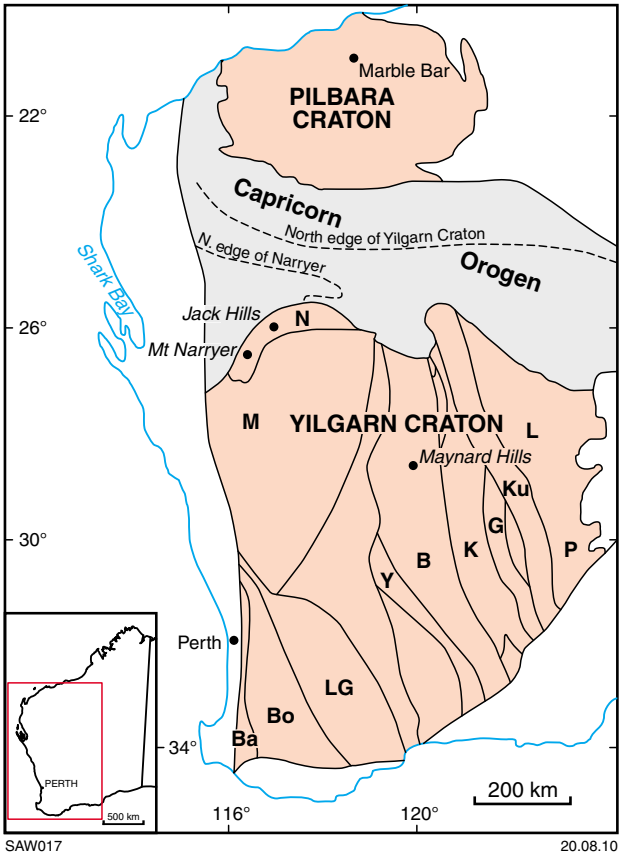


**Figure 2.** **Simplified geological map showing the main subdivisions of the Yilgarn Craton (after Wilde et al., 1996) and the relationship to the Pilbara Craton. Also shown are the three sites (including Jack Hills) where >4 Ga detrital zircons have been recorded. Map legend for terranes: B = Barlee; Ba = Balingup; Bo = Boddington; G = Gindalbie; K = Kalgoorlie; Ku = Kurnalpi; L = Linden; LG = Lake Grace; M = Murchison; N = Narryer; P = Pinjin; Y = Yellowdine**


**Figure 3.** **One of the original sample sites where TTG gneisses >3.6 Ga were first identified in the Yilgarn Craton of Western Australia ('site C' as recorded in de Laeter et al., 1981a,b)**

from the Dugel Gneiss record a SHRIMP U–Pb upper intercept date of 3375 ± 26 Ma, with rims defining an age of 3284 ± 9 Ma (Nutman et al., 1991). Although this age is similar to the c. 3300 Ma component of the Meeberrie Gneiss, the two are quite distinct and there is no evidence of anatexis or migmatization of the Dugel Gneiss at c. 3300 Ma (Kinny and Nutman, 1996). Within the Dugel Gneiss, fragments of a dismembered layered basic intrusion are referred to as the **Manfred Complex** (Myers and Williams, 1985; Williams and Myers, 1987). Anorthosite from the Manfred Complex records U–Pb zircon dates of 3730 ± 6 Ma (Kinny et al., 1988). Finally, Nutman et al. (1991) recognized a suite of younger tonalitic gneisses that had not undergone granulite facies metamorphism, referred to as the **Eurada Gneiss**, that record SHRIMP U–Pb zircon dates of 3470 to 3440 Ma. A population of distinctly younger grains gave a $^{207}Pb/^{206}Pb$ age of 3055 ± 3 Ma, which was interpreted to reflect pegmatite intrusion into the gneiss or else to record a partial melting event (Nutman et al., 1991).

In the Paleoproterozoic, a series of orogenic events record the collision of the Pilbara and Yilgarn Cratons and these variously affected the Narryer Terrane. The Capricorn Orogeny (1830–1780 Ma) was predominantly a greenschist-facies intracratonic event, which resulted in reworking of both the northern and southern margins of the Narryer Terrane through dextral transpression. Deformation extended south to the northern end of the Mingah Range greenstone belt within the Murchison Domain (Spaggiari, 2007a; Spaggiari et al., 2007).

## Mount Narryer and Jack Hills

On the basis of the discovery of gneisses with $T_{CHUR}$ model ages in excess of 3.6 Ga, more-detailed mapping of the Mount Narryer area was undertaken by Ian Williams in 1981–82 and John Myers in 1983 (Williams and Myers, 1987), with particular emphasis on determining the distribution of metasedimentary and anorthositic components identified on Mount Narryer itself. A complementary U–Pb geochronological investigation of these granulite-facies metasedimentary rocks on Mount Narryer was undertaken by geoscientists at the Australian National University (ANU), following a similar investigation of c. 3 Ga gneisses and quartzites in the Toodyay area of the southwest Yilgarn Craton by Nieuwland and Compston (1981) using conventional multigrain zircon U–Pb methods. However, with the development of the Sensitive High-Resolution Ion MicroProbe (SHRIMP I) at ANU, a new U–Pb method of more rapid investigation was available.

The culmination of this work was the discovery, within a quartzite (sample 71932, collected about 2.5 km north-northeast of Mount Narryer), of four detrital zircon cores with ages ranging from 4110 to 4190 Ma, the oldest crustal remnants identified on Earth at that time (Froude et al., 1983). There was considerable international interest in this discovery and extensive work was undertaken throughout the Narryer Terrane by ANU as part of the 'First Billion Years' project. The terrane was mapped by Allen Nutman and Peter Kinny from ANU and John Myers at GSWA. The age and distribution of the gneisses became

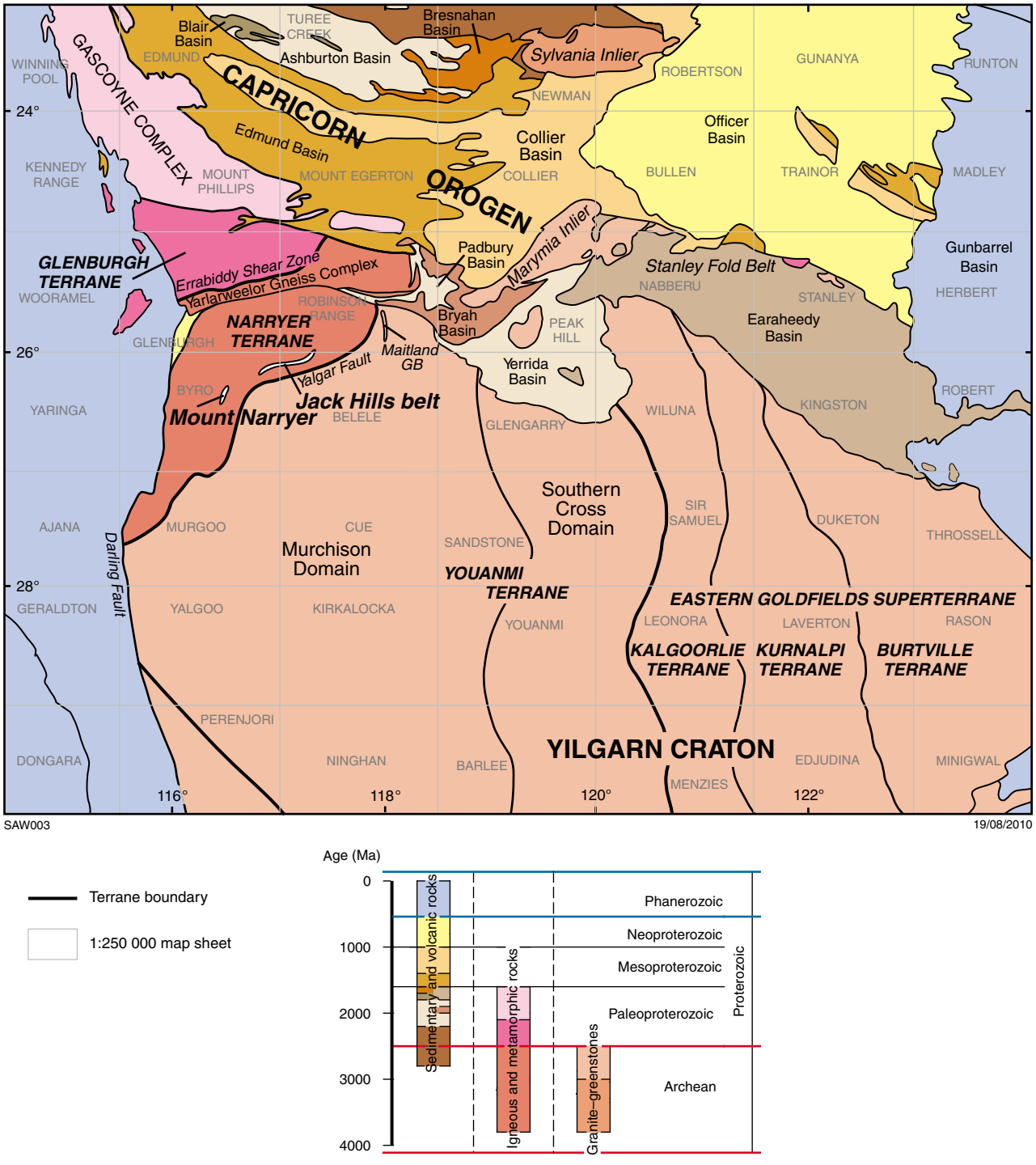


**Figure 4. The location of the Narryer Terrane with respect to the Yilgarn Craton and adjacent Proterozoic Capricorn Orogen (from Spaggiari, 2007b)**

well-established, including the identification of the oldest rock near Jack Hills, as mentioned above. However, no older material was identified from Mount Narryer and interest in this regard had already moved to Jack Hills, as outlined below.

## Early investigations of the Jack Hills belt

Jack Hills forms a low, about 80 km-long, sigmoidal-shaped range (Fig. 5), located approximately 150 km north of Cue in the Murchison district of Western Australia. In 1983, as part of an Australian Research Council (ARC) program to examine the five greenstone belts that had been identified within the Western Gneiss Terrain by Gee et al. (1981), the first detailed mapping of the Jacks Hills at a scale of 1:10 000 was completed by third-year undergraduate students of the Western Australian Institute of Technology (now Curtin University of Technology) under the guidance of John Baxter, Robert Pidgeon, and Simon Wilde. The Jack Hills was initially considered to be a greenstone belt (Elias, 1982), but was found to consist predominantly of metasedimentary rocks, including both chemical and clastic varieties, enclosed by granitic gneisses (Baxter et al., 1984). However, unlike at Mount Narryer, some 60 km to the southwest, where the rocks are predominantly at granulite facies (Williams and Myers, 1987), the metamorphic grade at Jack Hills is greenschist to amphibolite facies (Baxter et al., 1984).

The student mapping exercise was repeated in 1984 to refine the map and some 31 samples were collected for geochronology over the two-year period. Samples included quartzites, granites, rare volcanic rocks, and a conglomerate from a rather prominent outcrop on the eastern flank of Eranondoo Hill (Fig. 6). To test if there was any similarity with the Mount Narryer metasedimentary rocks, zircons obtained from the latter sample (W74) were extracted and run on the ANU SHRIMP. Two zircons with ages of 4276 ± 12 Ma were identified, making these the oldest known crustal

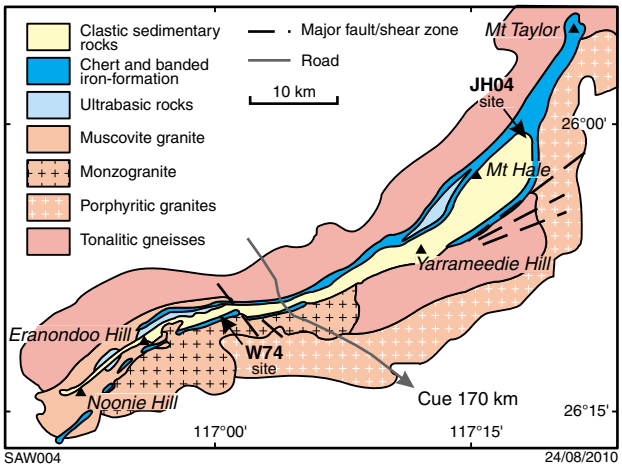


**Figure 5. Simplified map of the Jack Hills showing the distribution of the main lithological packages and the location of the W74 'Discovery' site**

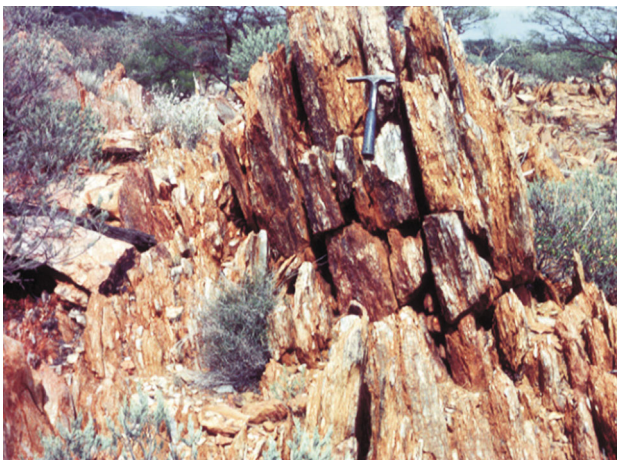


**Figure 6. The original W74 site as it appeared in 1984**

components on Earth at that time (Compston and Pidgeon, 1986), some 80 million years older than at Mount Narryer.

Following publication of the results (Compston and Pidgeon, 1986), additional work was carried out on the same suite of zircons in sample W74 from Eranondoo Hill. Both Köber et al. (1989) and Amelin (1998) reproduced the earlier SHRIMP results, the former by stepwise evaporation of single zircon grains and the latter by Thermal Ionization Mass Spectrometry (TIMS) using selected crystal fragments. However, no older material was identified and, by the mid 1990s, interest in the area had started to wane.

Interest was re-ignited in 1998 when a team from Curtin University and the University of Wisconsin collected both SHRIMP U–Pb and Cameca IMS 4f oxygen data on a new suite of zircon grains extracted from the same W74 sample initially analysed by Compston and Pidgeon (1986). This led to the identification of a zircon that contained a portion with an date of 4404 ± 8 Ma (2σ) (Wilde et al., 2001) — by far the oldest age ever obtained from crustal material on Earth. A companion investigation began in 1999, involving a team from UCLA and Curtin University, and included collection of new material from the W74 site (Mojzsis et al., 2001). Importantly, both studies obtained evidence for elevated $\delta^{18}$ oxygen values in the ancient zircon fraction, implying zircon growth in a magma generated from rocks that had previously interacted with surface waters (Wilde et al., 2001; Mojzsis et al., 2001; Peck et al, 2001). This implied the early development of continents and oceans on the planet at a time when it had previously been considered too hot and inhospitable — with the term 'Hadean' coined by Preston Cloud to cover this period of Earth history, and believed to have extended to as late as 3.6 Ga by some workers.

## Significance of the Eranondoo Hill W74 site

Following initial publication of results in 2001, much additional work has been undertaken at Jack Hills, focused initially on the older crystals at the W74 site, but extending

to other sedimentary and rare volcanic rocks. This has led to a number of very significant findings about the early Earth that are summarized below:

a) **A cool early Earth**: this hypothesis evolved from the initial oxygen work (Wilde et al, 2001; Mojzsis et al., 2001; Peck et al., 2001) and was more precisely formulated in Valley et al. (2002). As alluded to above, the elevated oxygen values of the Jack Hills' zircons, including grains 4.4–4.3 Ga old, required interaction of the magmatic protolith of the crystals with cool surface waters. The surface temperature would need to be below about 200°C and the fact the $\delta^{18}O$ values appeared to record a similar range at this time as they did in the Archean at 2.7 Ga, where a much larger database was available, especially from the Superior Province in Canada (King et al., 1998), led to the view that magmatic processes showed no major change throughout this time interval. This questioned whether the Earth was really 'hell-like' at 4.4 Ga; and thus the appropriateness of using the term 'Hadean' for the Eon prior to 4 Ga, which is still under consideration by the International Stratigraphic Commission. Later work by Cavosie et al. (2005) highlighted a significant shift to higher $\delta^{18}O$ values at 4.2 Ga, suggesting that reworking of continental crust became especially important from that time onward.

b) **Nature of the earliest crust**: the favoured interpretation for the origin of the ancient zircon crystals, based on their chemistry and suite of inclusions, is that they crystallized in granites (Maas et al., 1992; Wilde et al., 2001; Cavosie et al., 2006; Harrison et al., 2005, 2007). It has been debated whether these actually formed within continental crust, with some workers proposing that differentiated mafic rocks in an oceanic setting could produce the observed chemistry (Coogan and Hinton, 2006; Rollinson, 2008). However, the work of Grimes et al. (2007) has shown that plots of U versus Yb and U/Yb versus Hf and Y discriminate zircons crystallized in oceanic crust from zircon derived from continental crust. Significantly, the ancient suite from Jack Hills plots within the continental fields on these diagrams. Also, amongst those favouring a continental origin, there has also been much debate as to the nature of the host rocks. The low temperatures of about 700°C obtained by Ti-in-zircon thermometry (Watson and Harrison, 2005) and the interpretation of white mica inclusions in a >4 Ga zircon as a primary feature (Hopkins et al., 2008) have been used to argue that the hosts were wet, minimum-melt S-type granites. However, a comprehensive study by Fu et al. (2008) has shown that titanium thermometry is a poor discriminator of rock type, based on calculated temperatures of zircons obtained from a wide variety of rock types. Indeed, the ancient Jack Hills zircons with ages of 4.4–3.9 Ga record an average temperature of 718 ± 63°C, which is similar to that calculated by Watson and Harrison (2005), but overlapping with felsic, intermediate and mafic rocks, so that the source of such zircons cannot be uniquely defined by this technique. Alternatively, other workers have considered that the most likely source of the ancient zircons was from rocks of the tonalite–trondhjemite–granodiorite (TTG) suite (Blichert-Toft and Albarède, 2008). Such rocks dominate the early Archean record and provide a more consistent interpretation, given the similarity of the oxygen isotope systematics of the ancient crystals with the 2.7 Ga Superior Province record, as discussed above. With respect to inclusions in >4 Ga zircon, no published data have identified any 'inclusion' that is older than the host. Of relevance is a study of xenotime and monazite in the matrix of the conglomerate at the W74 site, which shows that these are considerably younger than the ancient zircons (Rasmussen et al., 2010). This throws considerable doubt as to whether the inclusions reported by Hopkins et al. (2008) are primary.

c) **Formation age of the earliest crust and its possible preservation**: notwithstanding some contrary opinions (Nemchin et al., 2006; Pidgeon and Nemchin, 2006), the consensus is that at least some portions of the ancient Jack Hills zircon crystals retain primary isotopic information as to their age, magmatic origin, and somewhat elevated oxygen signatures (Cavosie et al., 2006; Harrison, 2009). Given that the oldest known zircons are magmatic and require the melting of precursor rocks that interacted with liquid water for their generation, requires that there be an even older protolith. By way of timing, the upper age constraint must be the accretion of the Earth but, more likely, is the time of its differentiation into a core and mantle (and possible ?protocrust). These events are placed at 4.55 Ga (Chambers, 2004) and c. 4.50 Ga (see Harrison, 2009), respectively. Further constraints can be placed by utilizing the Lu–Hf system in zircon, which provides a tracer of this pre-history. However, there is also a divergence of opinion here, with different studies leading to quite different conclusions. Harrison et al. (2005, 2008) presented a range of εHf values from >4 Ga Jack Hills zircons, with both depleted and undepleted signatures, and argued that this reflected massive recycling of continental crust into the mantle. However, a recent study by Kemp et al. (2010) found that all ancient zircons had subchondritic εHf values and there was no evidence for extensive recycling of crust back into the mantle. These conflicting views lead to very different interpretations as to the processes operative in the early Earth. For example, it has been argued that plate tectonics operated from c. 4.5 Ga with magmas generated at and above subduction zones, based on inferred thermal gradients and the view that extensive recycling had taken place (Harrison et al., 2005; Hopkins et al., 2008). However, Kemp et al. (2010) have shown that granites adjacent to the Jack Hills belt, ranging in age from 3.6 to 2.65 Ga also show evidence of an ancient hafnium component, consistent with multiple reworking of a protocrust extracted from the mantle c. 4.5 Ga ago (see also Blichert-Toft and Albarède, 2008; Harrison et al., 2005). There is also a marked similarity in the Hf isotopic signature of the ancient Jack Hills zircons with that of lunar zircons, leading to the possibility they were derived from similar mafic components, perhaps formed initially during final crystallization of a terrestrial magma ocean, in a manner analogous to lunar KREEP (Blichert-Toft and Albarède, 2008; Kemp et al., 2010). Multiple reworking and extraction of granitic magmas

into the Neoarchean further indicates that instead of being recycled back into the mantle, some early crust survived into the late Archean. This leaves the question as to why no rocks older than 4.03 Ga (Bowring and Williams, 1999) are known to have survived on Earth. One explanation may be contained in the zircon lithium record from Jack Hills (Ushikubo et al., 2008), where not only do the zircons contain higher than expected total lithium, but the $\delta^7$Li values match the range found in whole-rock lithium studies of highly weathered rocks; consistent with extensive weathering at the Earth's surface, possibly in a $CO_2$-rich atmosphere. Such rapid weathering would have destroyed the earliest rocks; the only survivors being the few zircon grains that later became incorporated in the Jack Hills metasedimentary rocks.

d) **The presence of diamonds**: one of the more intriguing discoveries from the ancient zircon suite at Jack Hills has been the recognition of microdiamond and graphite inclusions in crystals ranging in age from 3.06 to 4.25 Ga (Menneken et al., 2007). However, although the Raman spectroscopic features of the diamonds most closely resemble those resulting from ultrahigh-pressure metamorphism (UHP), no other minerals characteristic of UHP conditions have so far been reported. Furthermore, several of the diamond and graphite inclusions are located within oscillatory-zoned portions of the crystals that record high Th/U ratios and are thus considered to be of magmatic origin. This is in stark contrast to other areas in the world, where such inclusions are clearly associated with zircon domains that have recrystallized under UHP metamorphic conditions (e.g. at Dabieshan; Liu et al., 2007). Also of interest is that the carbon isotope data obtained from the diamond and graphite inclusions have strongly negative $\delta^{13}$C values, a feature not inconsistent with generation from the deep subduction of biogenic carbon (Nemchin et al., 2008). However, although this signature is non-unique and may have resulted from inorganic chemical reactions, the results indicate that a low $\delta^{13}$C reservoir must have existed on the early Earth. Further work is clearly required to resolve the enigma of diamond and graphite inclusions in the zircons from Jack Hills, especially when virtually all other mineral inclusions so far described are consistent with a granite origin for the zircon.

## Nature and timing of sedimentation and volcanism at Jack Hills

### *Sedimentary rocks*

The traditional view of the age of the Jack Hills belt was that it formed in the Archean, based on the youngest detrital zircons obtained from the conglomerate at the initial W74 'discovery site' on Eranondoo Hill, where numerous studies indicate that the youngest detrital zircon grains are c. 3.0 Ga (Compston and Pidgeon, 1986; Mojzsis et al., 2001; Peck et al., 2001; Cavosie et al., 2004; Dunn et al., 2005; Crowley et al., 2005; Pidgeon and Nemchin, 2006). The Archean age of this site has recently been confirmed from metamorphic monazite in the conglomerate matrix yielding a weighted mean $^{207}$Pb/$^{206}$Pb date of 2653 ± 5 Ma, interpreted to represent the time of low-grade metamorphism and therefore a minimum age for sedimentation (Rasmussen et al., 2010). In addition, banded iron-formation near Mount Hale (Fig. 5) contains detrital monazite and xenotime, as well as monazite and xenotime inclusions in detrital quartz, that record an age of 3080 ± 20 Ma. The banded iron-formation forms part of an older succession at Jack Hills (see **Field localities**, below) that includes chert and mafic–ultramafic rocks (Wilde and Pidgeon, 1990; Spaggiari, 2007a,b). If this lithological association is a conformable sequence, then it must also be older than 3080 ± 20 Ma (Rasmussen et al., 2010). These results confirm that at least some of the succession at Jack Hills is amongst the oldest in the Yilgarn Craton, where most sedimentary and volcanic rocks were deposited after c. 2.8 Ga (Wyche, 2008).

However, a surprising finding in recent years has been that the Jack Hills belt cannot be entirely of Archean age. Cavosie et al. (2004) and Dunn et al. (2005) both reported the presence of Proterozoic detrital zircons in several clastic sedimentary units, including one about 50 m from the W74 site. More recently, Grange et al. (2010) have described numerous Proterozoic grains within actual quartzite cobbles from a conglomerate band approximately one km west of the W74 site, including one grain as young as 1220 ± 42 Ma (1σ): the youngest so far reported from Jack Hills. This latter grain shows magmatic oscillatory zoning and its presence implies at least two Proterozoic sedimentary cycles: the first involving erosion of an igneous precursor and incorporation of zircon into a clastic sediment, with subsequent induration or metamorphism to produce the quartzite; and the second following further erosion and transport, resulting in the incorporation of the quartzite cobble in the conglomerate. The nearest sedimentary source for rocks of this age is the Bangemall Supergroup in the Collier Basin, about 100 km northeast of Jack Hills, in the Capricorn Orogen. This would require an original extension of the basin farther to the southwest, with subsequent tectonic interleaving, possibly related to activity along the Cargarah Shear Zone that traverses the Jack Hills belt (Fig. 5). Some evidence for Proterozoic metamorphism and deformation has also been provided by the monazite and xenotime study of Rasmussen et al. (2010) and an earlier argon study by Spaggiari et al. (2008). Quartz–mica schist from the central part of the Jack Hills belt contains metamorphic monazite formed at both c. 2.65 Ga and 1858 ± 6 Ma. The younger age coincides with the broad range of dates obtained by $^{40}$Ar/$^{39}$Ar from this region (Spaggiari et al., 2008), and is interpreted to record the timing of shearing and heating associated with movement along the Cargarah Shear Zone (Rasmussen et al., 2010). In addition, authigenic xenotime from the conglomerate at the W74 site recorded an age of 800 ± 25 Ma (Rasmussen et al., 2010). Although similar ages have been reported from the Gascoyne Complex to the north using $^{40}$Ar/$^{39}$Ar (Occhipinti and Reddy, 2009), these were attributed to uplift that is unlikely to result in monazite growth: the significance of this event at Jack Hills thus awaits further resolution.

In terms of sedimentation, only the Archean components of the succession have so far been examined in any detail (Eriksson and Wilde, 2010). The facies associations

SAW006 12/08/2010

**Figure 7. Well-developed cross-bedding on the hill 100 m east of the W74 site**

indicate a prograding fan delta setting, with the source of the alluvial fans being proximal highland areas. The fans built directly into either a lake or shallow sea and were characterized by high gradients and high flow velocities. Near the W74 site on Eranondoo Hill, the succession is capped by an approximately 25 m-thick unit of cross-bedded quartz arenite–gritstone. This has a similar spectrum of U–Pb detrital zircon ages to the W74 site, suggesting it is related to the underlying facies associations. The quartz arenite–gritstone facies association is interpreted to record transgressive tidal reworking of the fan delta, as it contains abundant herringbone cross-bedding (Fig. 7).

### *Volcanic rocks*

Further evidence for Proterozoic activity in the area is provided by a study of rare intermediate to felsic volcanic rocks interleaved with amphibolite and quartzite in the central part of the Jack Hills belt (Wilde, 2010). These contain a range of magmatic zircons with ages extending from 3470 Ma to 1775 Ma, commonly grouped into populations at 3.3–3.4 Ga, c. 3.0–3.1 Ga, c. 2.6 Ga and c. 1.8–1.9 Ga. The youngest magmatic group with ages of 1970 to 1775 Ma were interpreted as recording the time of volcanism, thus providing the first evidence of Proterozoic magmatism along the northern margin of the Yilgarn Craton. A further implication of this study comes from the fact that the volcanic rocks are metamorphosed from upper greenschist to amphibolite facies, indicating that this too must have occurred in the Proterozoic.

An interesting point regarding both the Proterozoic sedimentary and volcanic rocks is their general lack of >4 Ga zircons (Cavosie et al., 2004; Grange et al., 2010; Wilde, 2010). This might imply that the ancient source rocks were either buried or completely destroyed by this time.

# Field locations

## Rock types at Jack Hills

### *Sedimentary associations*

Wilde and Pidgeon (1990) divided the supracrustal rocks of the Jack Hills belt into three informal associations: (i) chemical sediment association; (ii) pelite–semipelite association; and (iii) clastic sedimentary association. This was later refined by Spaggiari et al. (2007a,b) to incorporate (iv) Proterozoic sedimentary association.

**Association 1**: The main components are chert (Fig. 8) and banded iron-formation (Fig. 9), accompanied by thin amphibolite and ultramafic units. The cherts are fine grained and commonly banded from white to black. There are also locally recrystallized cherts, now converted into quartzite. The banded iron-formation units are particularly well developed in the northern part of the belt near Mount Hale (Fig. 5), where mining is currently taking place. The

SAW007 12/08/2010

**Figure 8. Chert recrystallized to quartzite on Yarrameedie Hill, central Jack Hills belt**

SAW008 12/08/2010

**Figure 9. Folded BIF in Association 1 at northern margin of the Jack Hills belt near Yarrameedie Hill**

fresh mineral assemblage consists of quartz–hematite and quartz–magnetite, with the local development of grunerite in Fe-rich bands. There are also banded rocks containing very little quartz where the Fe-rich components alternate with layers composed mainly of talc. The amphibolite units are best developed along the northern margin of the belt. Massive and banded varieties consist mainly of hornblende and andesine, with local biotite. Most units probably represent mafic lava flows, as some are interlayered with bands of dacite and rhyolite. However, some may be mafic intrusions, although they are now in layer parallelism with the adjacent units. Local ultramafic units are present at both the southern and northern margins of the belt, although some cross-cutting units also occur in gneisses south of the belt.

**Association 2**: These rocks occupy the central core of the Jack Hills belt and also are present along the southern margin in the central and southern portions. They are poorly exposed and strongly schistose (Fig. 10), consisting mainly of quartz–biotite and quartz–chlorite schists with gradations to varieties containing muscovite. There is also local development of andalusite in more aluminous components in the central part of the belt. The chloritic schists are Fe-rich, commonly with magnetite porphyroblasts that have developed during metamorphism. Sedimentary structures such as graded bedding are locally preserved and many of the schists were probably derived from turbidites. However, some units of quartz–chlorite schist adjacent to thin amphibolite units probably represent sheared amphibolite. There are also thin units of schistose ultramafic rocks interleaved with the above types, especially in the southern part of the belt. More semipelitic units are present as granofelsic microgneiss, especially to the north of Eranondoo Hill. A complicating factor near Eranondoo Hill is that a late granite intrusion that cuts the belt (Fig. 5) is also extensively sheared along its contacts and these shear zones extend eastward into the pelitic schists, making it difficult to discriminate between metasedimentary rocks and extensively sheared granite.

**Association 3**: This is composed of mature clastic rocks that include weakly metamorphosed conglomerate, gritstone, sandstone, quartzite, and siltstone (Fig. 11). The rocks are well developed at Eranondoo Hill, on Yarrameedie Hill, and in the northern part of the belt, south of Mount Hale (Fig. 5). The metaconglomerates have sharp basal contacts and gradational tops, passing upward into coarse-grained quartzites, commonly with cross-bedding. The metasandstones fine upwards and some are planar bedded. In many of the finer grained units, there is an increase in the amount of muscovite. Some cycles have graded bedding. The sequence was interpreted by Baxter et al. (1986) and Wilde and Pidgeon (1990) as having been deposited in the medial to distal part of an alluvial-fan delta, and this has been confirmed by subsequent work (Eriksson and Wilde, 2010).

**Association 4**: These are the known Proterozoic rock units and they are essentially identical to Association 3, and perhaps components of Association 2; the only distinction being they contain detrital Proterozoic zircon. They have been recognized on the southeastern flank of Eranondoo Hill, within about 50 m of the W74 site and also south of Mount Hale (Dunn et al., 2005), where zircons as young as 1884 ± 32 Ma occur in a schistose metaconglomerate with a high matrix content. This unit has abundant poikiloblasts of andalusite set within a fine-grained matrix of quartz and muscovite. Further work is currently in progress to ascertain what proportion of the sedimentary sequence at Jack Hills is Proterozoic in age.

SAW009 12/08/2010

**Figure 10. Kinks cutting pelitic schist of Association 2 in the central part of the Jack Hills belt, northeast of Eranondoo Hill**

SAW010 12/08/2010

**Figure 11. Sharp transition from sandstone and quartzite to pebble conglomerate in Association 3, about 1 km east-northeast of the W74 site on Eranondoo Hill**

### *Granites*

There has only been one comprehensive study published on the granites adjacent to the Jack Hills belt (Pidgeon and Wilde, 1998), although additional information on gneisses to the south of the belt is included in Nutman et al. (1991). In general, there are several differences from granites described from elsewhere in the Narryer Terrane, as briefly outlined above. The most significant feature is that the rocks are generally less deformed and retain more of their primary igneous characteristics, including phenocrysts. For the older components, although all rocks show some degree of deformation, many are best classified as deformed granites rather than as orthogneisses, with deformation increasing toward discrete shear zones. In addition, pluton-scale bodies of TTG rocks are present.

There is a marked similarity in the ages obtained from the granites at Jack Hills with those obtained from Mount Narryer, about 60 km to the southwest, with a range of SHRIMP U–Pb zircon dates from 3.7 to 3.3 Ga (Pidgeon and Wilde, 1998). Discrete age peaks are evident at 3.75 – 3.65 Ga, c. 3.50 Ga, and at 3.3 Ga, and these have been interpreted to define both periods of magmatic activity and disturbance to the isotopic systems in existing rocks. The presence of c. 3.3 Ga zircon rims around older cores in several granites suggests metamorphism also took place at this time and that this was a major event in the area. However, based on the limited database, it appears that 3.3 Ga activity was restricted to the southern side of the Jack Hills belt, suggesting that the belt may lie along a major suture within the Narryer Terrane.

Based on the geochronological and geochemical datasets, an evolutionary trend has been identified within the TTG suite (Pidgeon and Wilde, 1998). The earliest tonalites and trondhjemites have weak to negligible negative Eu anomalies and record $^{207}Pb/^{206}Pb$ dates of 3608 ± 22 Ma, but do contain zircons as old as 3756 ± 7 Ma — the oldest material so far identified from the Narryer Terrane. A granodiorite immediately north of the belt has a slightly more prominent negative Eu anomaly and an age of 3516 ± 32 Ma. In rocks south of the belt, younger granodiorite and porphyritic granite with $^{207}Pb/^{206}Pb$ dates of c. 3300 Ma have much more prominent negative Eu anomalies and appear to be the result of remelting of the older tonalite–trondhjemite, as cores as old as 3707 ± 12 Ma are present in some samples. This time sequence also shows a distinct trend on the $CaO–Na_2O–K_2O$ diagram, with the oldest rocks plotting along the TTG line, but the younger rocks becoming more $K_2O$ rich and trending toward the calc-alkaline trend (Pidgeon and Wilde, 1998), suggesting progressive remelting of the ancient crustal source. All these rocks have also undergone a late Archean disturbance at c. 2700 Ma, similar in age to the event recognized near Mount Narryer (Kinny et al., 1990).

Besides the older TTG suite, there is also a suite of younger, generally less-deformed monzogranites (Fig. 12) developed throughout the area, and locally cross-cutting the TTG rocks. Two monzogranites gave SHRIMP U–Pb zircon dates of 2643 ± 7 Ma and 2654 ± 7 Ma (Wilde and Pidgeon, 1990), similar within error to the age obtained for monzogranite at Mount Narryer by Kinny et al. (1990). This implies that the Narryer Terrane was assembled by this time as similar ages are ubiquitous throughout the Yilgarn Craton. Zircon cores with significantly older ages are not common in monzogranite at Jack Hills, with only two xenocrysts, with dates of c. 3.6 and 3.5 Ga, reported by Pidgeon and Wilde (1998). Not all monzogranites are undeformed and many have been affected by Proterozoic shearing (Spaggiari, 2007a,b) and this appears to be reflected in the non-zero disturbance of the zircon isotopic systems in both the younger and older granites (Pidgeon and Wilde, 1998).

In the southwest, near Noonie Hill (Fig. 5), the Jack Hills belt is intruded by extensive areas of muscovite-bearing granites and pegmatite or aplite dykes (Fig. 13). These

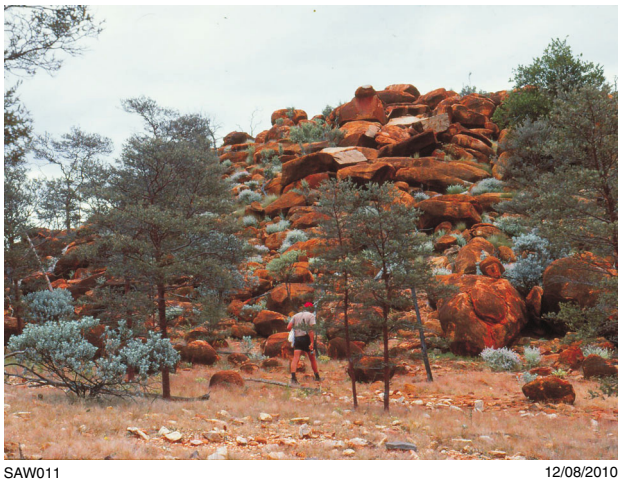

SAW011 12/08/2010

**Figure 12. Monzogranite intruding the Jack Hills belt at the 'Blob' on Eranondoo Hill**

SAW012 12/08/2010

**Figure 13. Late-stage pegmatite dyke cutting chloritic schist near Noonie Hill in the southern part of the Jack Hills belt**

pervasively dismember the belt, enveloping rafts of metasedimentary rocks (especially banded iron-formation). The muscovite-bearing granites are devoid of major deformation and therefore post-date the monzogranites. No U–Pb ages are available for these rocks, but data from a Rb–Sr and K–Ca study of their white micas (Fletcher et al., 1997) produced a range of rather imprecise dates. The Rb–Sr ages have large errors and range from 2556 to 2530 Ma for the granite and from 2595 to 2569 Ma for the pegmatite, whereas the K–Ca ages are younger, ranging from 2117 to 2099 Ma in the granite and between 2435 and 2383 Ma in the pegmatite. These data are difficult to interpret, as the ages are older in the pegmatites, yet these clearly cross-cut the muscovite granite in the field.

# Field localities

A number of localities are described below. The W74 'discovery site' is a 'must' to visit, but the others will be selected at the time of the excursion, based on access conditions and time constraints.

# Locality 1.1: W74 site, Eranondoo Hill

*From the Cue–Berringarra Road, turn onto a track leading west (MGA 506680E 7107025N). You will come to a gate after about 300 m, and after about 7.4 km will come to an intersection with a track heading north (MGA 499820E 7105090N). Follow this track up the gully as far as it goes and park near the small creek. Walk up the gully to the W74 sample site on the side of the hill (at MGA 499137E 7105845N).*

Considerable information has been presented in the literature based on work at this site, and many of the highlights have been listed above under '**Significance of the Eranondoo Hill W74 site**'. A geological map of the site and its environs is presented as Figure 14 (from Wilde and Pidgeon, 1990) and a more-detailed map of the site (Fig. 15) is from Spaggiari (2007b). A number of detailed traverses have been documented and also from the hill to the east, copies of which will be provided on the excursion.

# Locality 1.2: Early Archean gneisses

*From about 20 m east of the turnoff to Locality 1.1 (MGA 499842E 7105090N), follow a track to the south for about 2.9 km to Boundary Bore (MGA 498222E 7102281N). Staying on the northern side of the fence, drive about 400 m to the southwest, across the creek, into the area of patchy outcrop of Meeberrie Gneiss, which continues for several kilometres on either side of the track.*

As mentioned above, the Meeberrie Gneisses in the Jack Hills area are commonly less deformed than in the Mount Narryer region, and many are better described as deformed granites. Just south of the Jack Hills belt, a series of gneisses were sampled along the Nookawarra–Berringarra fence line by the ANU, of which three were dated (see Nutman and Kinny, 1990). The rocks are migmatites, composed of grey, fine- to medium-grained tonalite–granodiorite gneiss cut by paler, coarser grained syenogranite. Sample MT–21 of the grey tonalitic–granodioritic component of the migmatite, from about 50 m north of the fence, was dated by SHRIMP and the dominant population of zircons yielded a weighted mean $^{207}Pb/^{206}Pb$ date of 3731 ± 14 Ma, interpreted to be the age of the igneous protolith of the gneiss, and making it the oldest rock known in Australia. Samples of the syenogranite component record ages of c. 3300 Ma, but do include inherited grains with ages >3700 Ma (Nutman and Kinny, 1990).

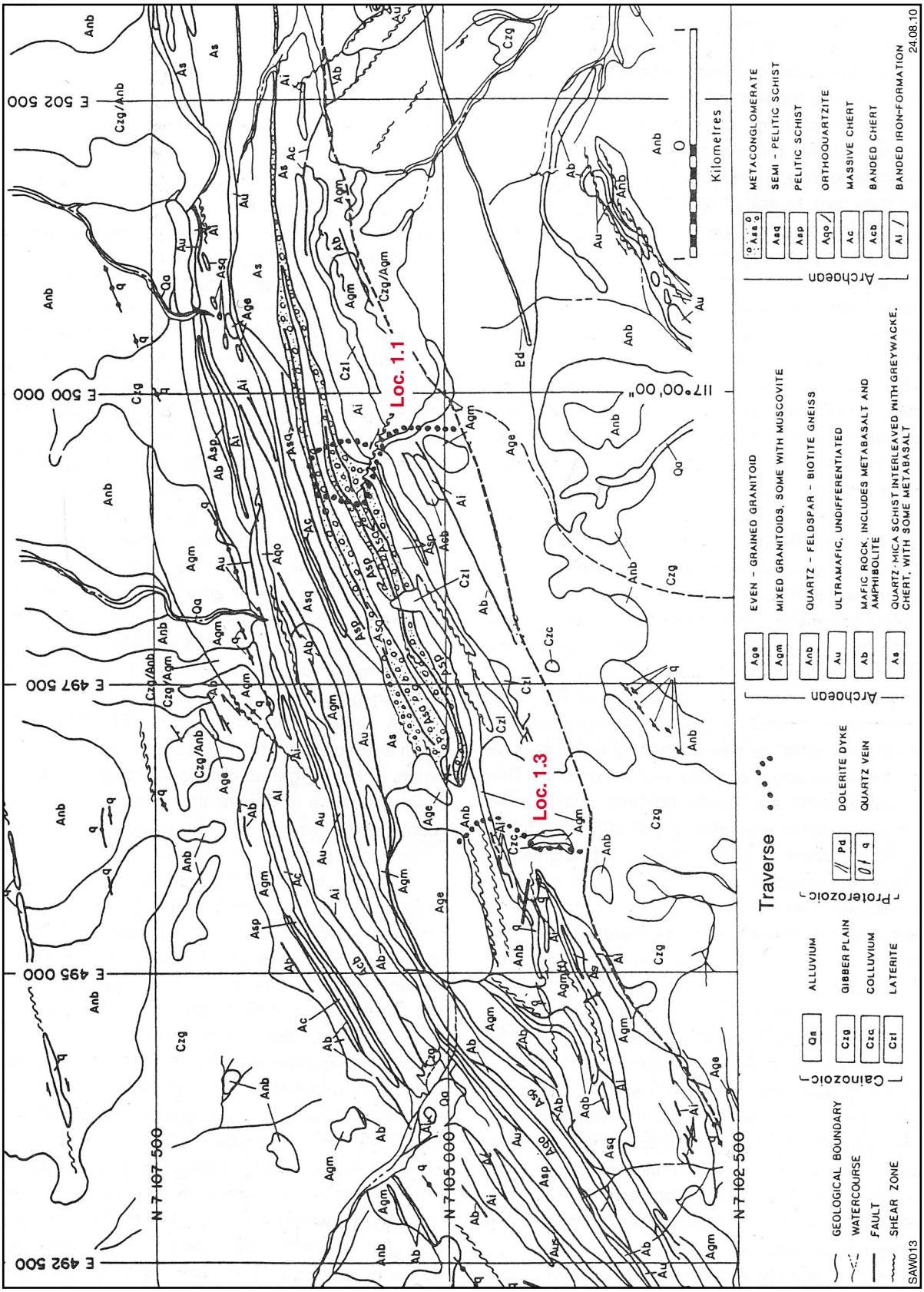


**Figure 14. Detailed lithological map of the central Jack Hills belt showing excursion localities (from Pidgeon and Wilde, 1990). Note that the map grid has AMG coordinates**

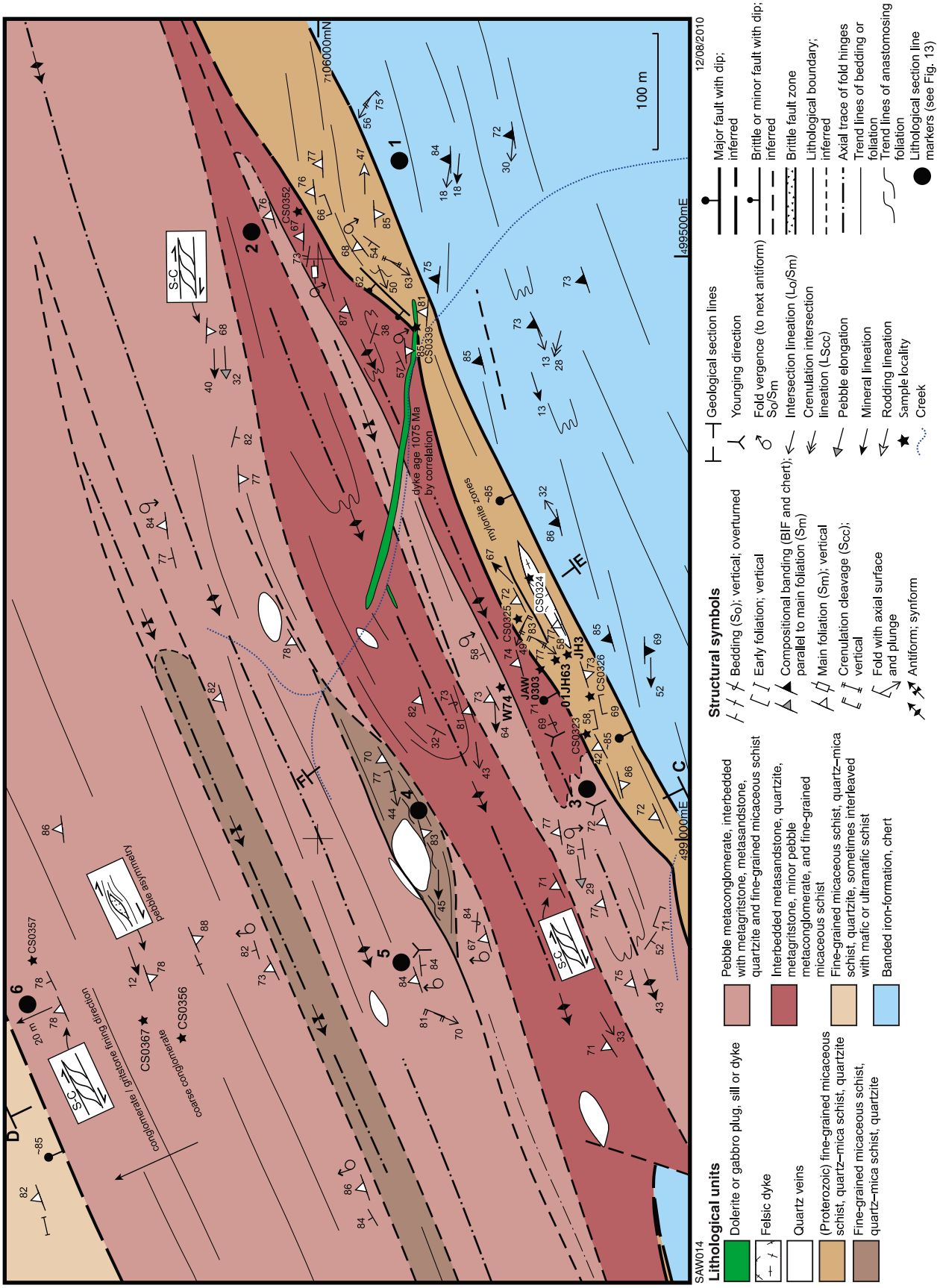


**Figure 15. Detailed geological map of the W74 site and its environs (from Spaggiari, 2007a,b)**

## Locality 1.3: Late Archean granites of the Narryer Terrane

*From the turnoff to Locality 1.1 (MGA 499820E 7105090N), continue west-southwest along the main track for about 3.7 km to an intersection with a track heading north (MGA 496346E 7104018N). Turn onto this track and follow it for about one km to an area of granite outcrop for the 'Blob' locality. The 'Gallery' locality lies beside the Cue–Berringarra Road, about 3.5 km northwest of its junction with the road to the Jack Hills iron mine (MGA 507650E 7106150N).*

We will visit either the Gallery granite or the 'Blob'; the latter being intrusive into the Jack Hills belt to the west of the W74 'discovery site'. Both are fairly homogeneous monzogranites, composed of an allotriomorphic granular aggregate of plagioclase, potash feldspar, quartz, and biotite. At Yarrameedie Gallery (Fig. 16), the granite records a $^{207}Pb/^{206}Pb$ zircon date of c. 2650 Ma (sample W158 of Pidgeon, 1992).

The rocks at the 'Blob' are more complex. Between the southern margin of the intrusion and the main east–west access track, amphibolite facies granitic gneisses have a general 060° trend. Veins of pegmatite cross-cut the gneiss, although they tend to be subparallel to the gneissosity; and both are locally folded together. Thin veins of weakly deformed monzogranite are present further north, and are also subparallel to the gneissic layering. They increase in size and abundance northward over a distance of about 40 m, until the rock is composed of equal proportions of gneiss and monzogranite. Later shearing along a trend of 080° affects all rock units, locally reducing the monzogranite to a quartz–sericite schist. The central stock of monzogranite is fairly homogeneous (Fig. 17), although there is local nebulitic banding near the southern margin. A U–Pb zircon date of c. 2650 Ma has been obtained from this granite (Sample W67 of Pidgeon and Wilde, 1998). An interesting feature is the way the shear fabric wraps around the 'Blob' and, especially to the east, it becomes increasingly difficult to distinguish sheared monzogranite from the quartz–mica schist of the layered Jack Hills succession into which it is intruded.

## Locality 1.4: Proterozoic intermediate to acid volcanic rocks

*From the turnoff to Locality 1.1 (MGA 499820E 7105090N), drive about 6.3 km back towards the Cue–Berringarra Road (MGA 505415E 7106435N). The outcrop lies in a creekbed about 50 m south of the track (MGA 505483E 7106280N).*

A number of rare intermediate to acid volcanic rocks were discovered in 1983 and 1984 during 1:10 000-scale mapping. Although large volumes of rock were collected, the zircon yield was low and insufficient for multi-grain zircon U–Pb analysis at the time. It was eventually decided to re-investigate these upon determination that sufficient grains were available for SHRIMP analysis (Wilde, 2010).

Zircons from four identified intermediate/felsic volcanic units reveal an almost identical age distribution pattern, with populations at c. 3.3–3.4 Ga, c. 3.0–3.1 Ga, c. 2.6 Ga, and c. 1.8–1.9 Ga. The c. 3.3–3.4 Ga zircons show well-developed oscillatory zoning in cathodoluminescence (CL) images and are considered to be inherited igneous zircon derived from the c. 3.3 Ga trondhjemitic granites of the Narryer Terrane. The c. 3.0–3.1 Ga zircons also have well-developed oscillatory zoning in CL but rocks of this age have so far not been recorded from the Narryer Terrane, although granite and volcanic rocks of this age are recorded in the Murchison Domain to the south. The c. 2.6 Ga population is also igneous and matches the age of nearby late Archean granites intruding the Jack Hills

SAW015 12/08/2010

**Figure 16. Monzogranite outcrop (site of sample 158 of Pidgeon and Wilde, 1998) along the Cue to Beringarra Road at Yarrameedie Gallery in the central Jack Hills**

SAW016 12/08/2010

**Figure 17. Sample site W67 (Pidgeon and Wilde, 1998) in the monzogranite at the 'Blob', Eranondoo Hill**

belt, suggesting derivation from this source. The youngest group of zircon grains, with ages ranging from c. 1970 to c. 1775 Ma, show strong oscillatory zoning and average Th/U ratios of 0.76, features consistent with an igneous origin. These younger zircons were therefore interpreted as defining the age of crystallization of the volcanic rocks (Wilde, 2010). These results indicate that both volcanic and sedimentary rocks of Proterozoic age are incorporated in the Jack hills belt. The volcanic rocks have undergone upper greenschist to amphibolite facies metamorphism and so a further implication is a post-1775 Ma metamorphic event affected part of the northern Yilgarn Craton.

Approximately one km south of the main belt (Fig. 5), there is a coherent unit of metadacite in a small creek (MGA 505747E 7106522N). The contact with adjacent rocks is not exposed, but amphibolite is present along the track about 100 m to the north. This unit was sampled in both 1983 (sample W44) and again in 1984 (sample W73) and consists of fine-grained, dark grey, meso- to melanocratic dacite, with large amphibole crystals up to 2 mm long. Some areas of greenish epidote alteration are present and there are also discrete layers of coarser grained amphibolite. In thin section, ovoid to elongate areas composed of aggregates of quartz (10%) with curved to amoeboid boundaries are set in a groundmass of epidote (35%), quartz (25%), white mica (8%), and chlorite (7%). The proportion of these minerals varies considerably and much of the epidote is associated with white mica as a replacement of original plagioclase. Randomly oriented, poikiloblastic blades of colourless to mid-green amphibole (15%) overprint the fabric, being preferentially associated with areas rich in quartz. The overall features indicate epidote-amphibolite regional metamorphism.

## Locality 1.5: Jack Hills iron ore mine

Jack Hills was long recognized as a potential source of iron ore although, with the opening up of the vast Hamersley deposits in the 1960s, little interest was shown in the area until recently. The original Ministerial Reserves were taken up by Murchison Metals and Midwest Corporation and serious exploration and testing of the reserves commenced in 2000. The main resource is on Mount Hale (Fig. 5) and an openpit mine commenced operation in 2006.

# Part 2: Murchison Domain, Youanmi Terrane

by MJ Van Kranendonk and TJ Ivanic

## Introduction

The roughly 300 000 km$^2$ Youanmi Terrane, and the South West and Narryer Terranes, form the western half of the Archean Yilgarn Craton (Fig. 18). The Youanmi Terrane is distinguished from the Eastern Goldfields Superterrane in the eastern half of the craton on the basis of its higher metamorphic grade, older and more dismembered greenstones, and the widespread presence of banded iron-formation. The well-preserved, older geological history of the Youanmi Terrane is recorded in greenstones (2.95 Ga) and granitic rocks (3.2 Ga, with xenocrystic zircons up to 4.0 Ga), and reflected in Nd isotope data (Pidgeon and Wilde, 1990; Watkins et al., 1991; Wiedenbeck and Watkins, 1993; Mueller et al., 1996; Schiøtte and Campbell, 1996; Yeats et al., 1996; Nelson et al., 2000; Pidgeon and Hallberg, 2000; Champion and Cassidy, 2007).

The Youanmi Terrane is subdivided into the Murchison and Southern Cross Domains. Although these domains have common elements in their stratigraphic assemblages, the successions in the Murchison Domain appear to have a more complex history with a number of identifiable volcanic cycles (Fig. 19). The Southern Cross Domain consists of undated, dominantly mafic volcanic and chemical and clastic sedimentary rocks that are unconformably overlain by isolated felsic volcanic complexes such as the c. 2735 Ma calc-alkaline Marda Complex. Some greenstone belts also contain clastic sedimentary rocks that unconformably overlie the main greenstone successions (Chen et al., 2003). The boundary between the Southern Cross and Murchison Domains is a late-tectonic, anastomosing, strike-slip shear zone.

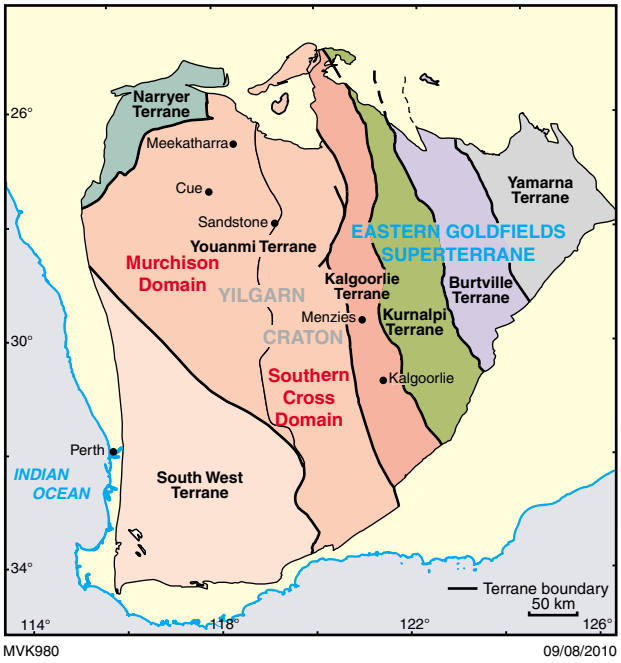


**Figure 18. The Yilgarn Craton showing terrane subdivisions within the Eastern Goldfields Superterrane, and the domain subdivision of the Youanmi Terrane (modified from Cassidy et al., 2006)**

To the east, the Youanmi Terrane is fault bounded against the Eastern Goldfields Superterrane along the northerly trending, long-lived Ida Fault. The Youanmi Terrane is also fault-bounded against the Narryer Terrane in the northwest (famous for its Hadean detrital zircons and Paleoarchean crustal remnants, e.g. Nutman et al., 1993; Wilde et al., 2001), and against the South West Terrane, which has a long and complex Meso- to Neoarchean history (Wilde et al., 1996; Wilde, 2001).

Recent mapping by the Geological Survey of Western Australia in the Murchison Domain, in combination with new and previous precise U–Pb zircon and baddeleyite geochronological data, has shown that, although the northern Murchison Domain preserves an older crustal history than the Eastern Goldfields Superterrane, it also contains a Neoarchean history of events that is remarkably similar to those across the Eastern Goldfields Superterrane, including eruption of mafic to felsic volcanic rocks, widespread and long-lived emplacement of granitic rocks, ductile strike-slip shearing, and gold mineralization.

Map, geochemical, and geochronological data have been used to develop a new stratigraphic scheme (Van Kranendonk and Ivanic, 2009) for the northern part of the Murchison Domain (Figs 19, 20). Greenstones are divided into four groups: 1) the 2960–2930 Ma Golden Grove Group of mafic and felsic volcanic and volcaniclastic rocks, in the southern part of the domain; 2) the widespread 2820–2805 Ma Norie Group of mafic volcanic rocks, felsic volcaniclastic sandstones, and banded iron-formation; 3) the 2800–2735 Ma Polelle Group of mafic–ultramafic volcanic rocks, intermediate to felsic volcanic and volcaniclastic sedimentary rocks, and banded iron-formation; and 4) the 2735–2700 Ma Glen Group of coarse clastic sedimentary rocks, komatiitic basalt, and minor rhyolite.

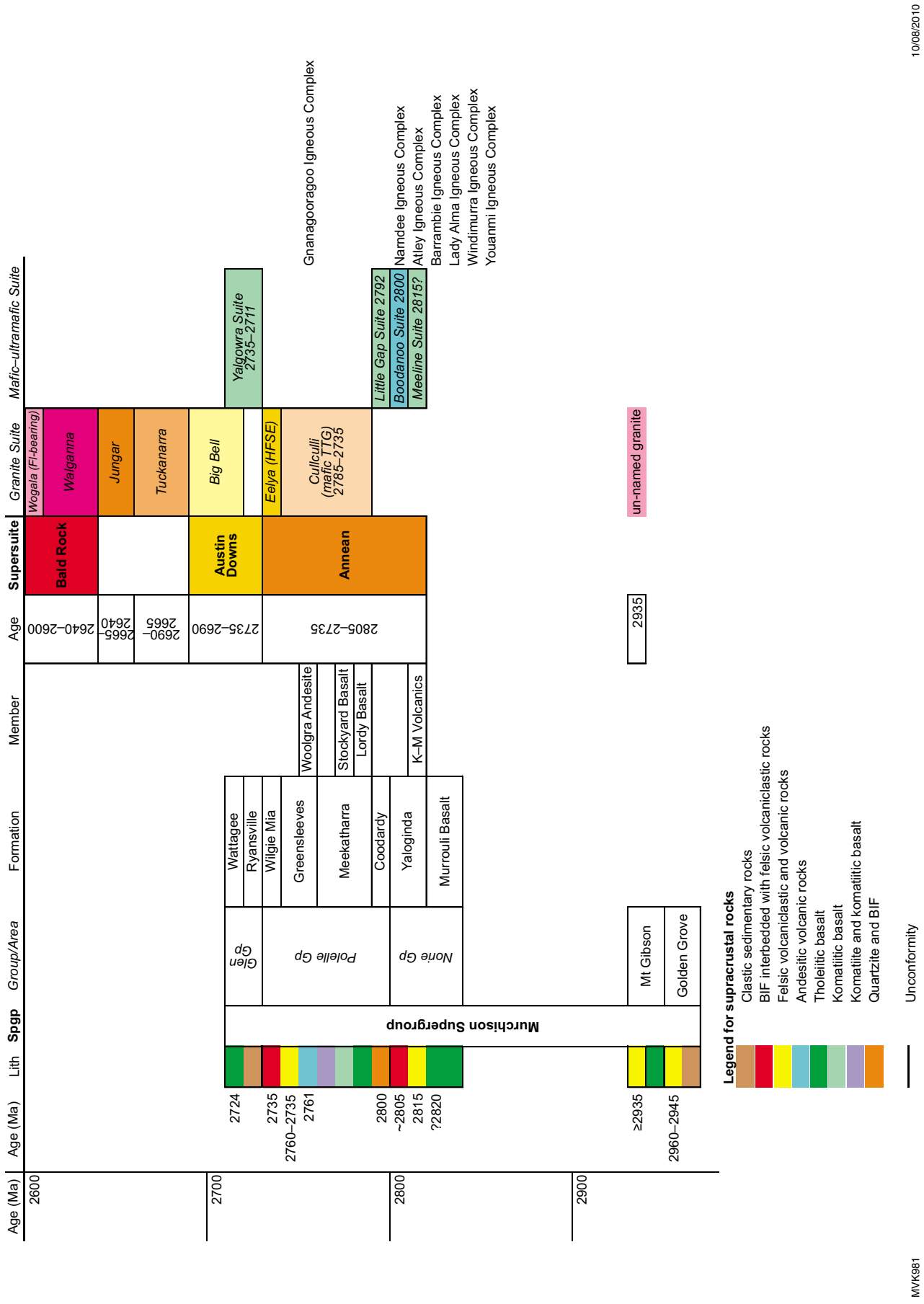


**Figure 19. Stratigraphic scheme for the northeastern Murchison Domain (modified from Van Kranendonk and Ivanic, 2009)**

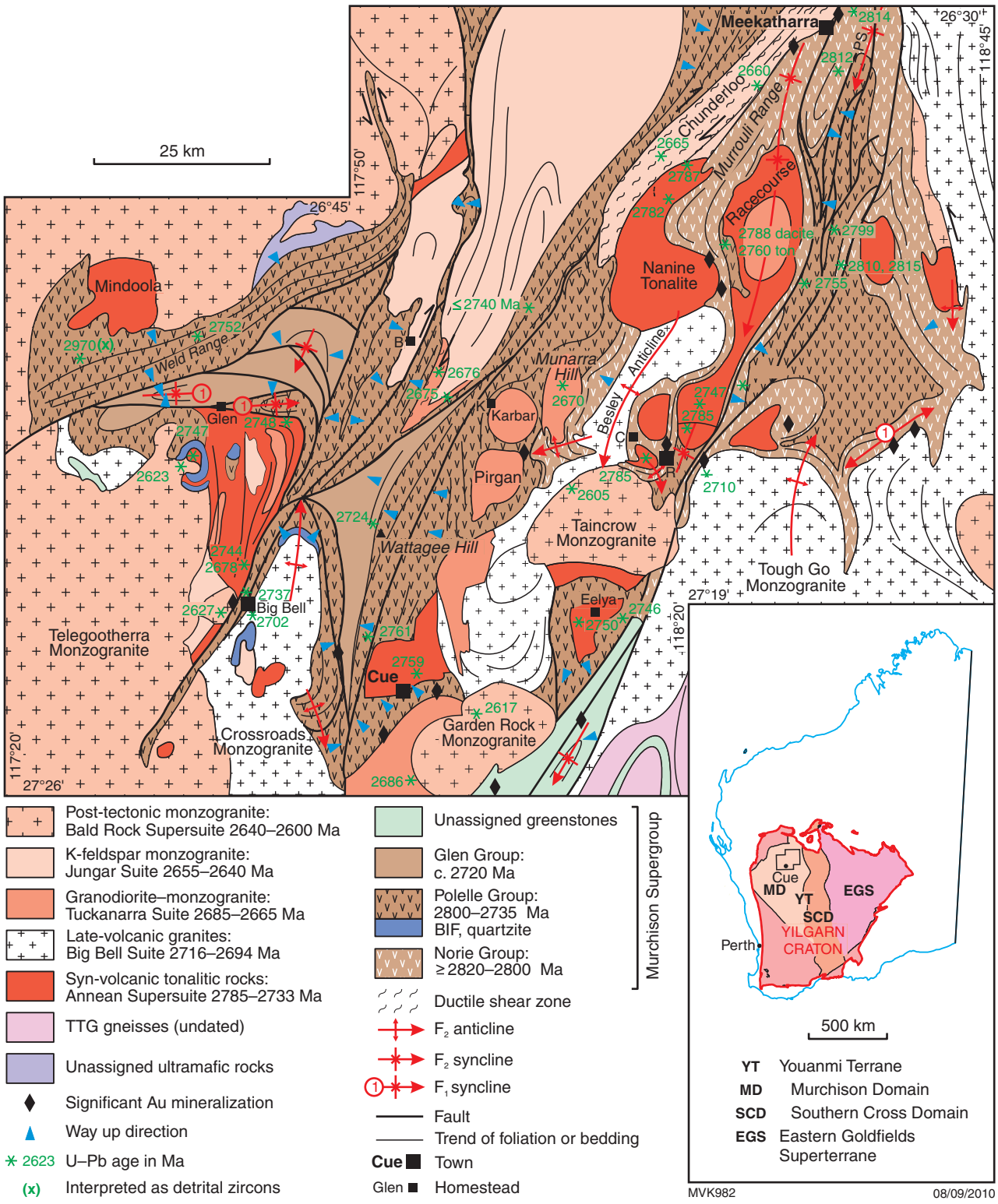


**Figure 20. Interpreted geological map of the northeastern Murchison Domain**

Younger groups have unconformable relationships with older greenstones, as exposed locally, whereas the base of the Golden Grove Group is intruded by younger granites. Very large layered mafic–ultramafic complexes of the Meeline Suite (e.g. Windimurra Igneous Complex) and Boodanoo Suite (Narndee Igneous Complex) accompanied eruption of the Norie Group during crustal extension between 2820 and 2800 Ma. Less voluminous mafic–ultramafic intrusive suites accompanied eruption of the Polelle and Glen Groups.

Deposition of the Golden Grove, Polelle, and Glen Groups was accompanied by widespread intrusion of synvolcanic plutons. This was followed by 120 Ma of widespread and voluminous granitic magmatism, between 2720 and 2600 Ma, including 2640 to 2600 Ma post-tectonic granites. All granites are crustal melts and represent an extremely long period of crustal melting and associated external thermal input, with or without the effects of thermal blanketing from newly erupted greenstones. Common c. 2950 Ma xenocrystic zircons in these rocks, combined with detrital zircons of a similar age in 2820 to 2720 Ma greenstones, indicate autochthonous development on older crust.

Deformation consists of four events, including two early periods of greenstone tilting ($D_1$ = 2930–2825 Ma; $D_2$ = 2735 Ma) — possibly associated with crustal extension — and two later (c. 2680–2640 Ma) periods of deformation resulting in tight to isoclinal folding of greenstones. $D_3$ structures include steeply plunging, easterly trending folds of greenstones and open domes of granitic rocks, which formed during a period of inferred partial convective overturn of dense greenstone upper crust and partially molten granitic middle crust at c. 2675 Ma. Subsequent overprinting $D_4$ structures (developed in response to strong east–west compression) are broad, splayed, north-northeasterly striking dextral shear zones, upright, northerly to north-northeasterly trending folds, and minor north-northwesterly striking sinistral shear zones. Gold mineralization tends to be focused in regions of $D_4$ dextral shear and/or low-pressure domains in fold interference structures.

Much of the late history of the domain, from 2720 to 2630 Ma, is similar and contemporaneous with events that also affected the Eastern Goldfield Superterrane. Specifically, we note shared komatiitic–basaltic volcanism at c. 2720 Ma, followed by widespread felsic magmatism (from 2690 to 2660 Ma), early deformation at 2675 Ma, shear-hosted gold mineralization at 2660 to 2630 Ma, and post-tectonic granites at c. 2630 Ma. In addition, we note that the whole craton experienced a period of mafic–ultramafic magmatism (komatiitic and basaltic volcanic rocks, layered mafic–ultramafic complexes, and gabbros) at c. 2810 Ma, indicating a shared early history. These findings, together with a lack of evidence for significant thrusting, low overall metamorphic grade, and lack of passive margin/foreland basin/accretionary prism successions suggest that a re-evaluation of subduction–accretion tectonic models for craton development is warranted.

## Locality 2.1: Subaerial komatiitic basalt and contemporaneous felsic volcaniclastic rocks, Weld Range

*From the Jack Hills, follow the sealed road south through the Weld Range, continuing for 4.4 km and turn left at MGA 560347E 7015966N* into the Sinosteel camp to pick up Sinosteel representatives and undertake site induction. Return to the main road and turn right, heading north for 4.4 km back through the Weld Range. Turn into the exploration road for access to the northern edge of the Weld Range, at MGA 557750E 7017750N. Keep left and follow the main track east-northeast for about 16 km until a sharp left turn (MGA 568750E 7026200N). At this point, follow a minor track straight ahead (east-northeast) for a further 1.8 km onto a rubbly brown hill at MGA 569760E 7026620N and park the vehicle. Walk uphill and to the left for about 40 m to Locality 2.1 at MGA 569836E 7026607N.*

At this locality (Fig. 21), we are at the transition from the Meekatharra Formation into the Greensleeves Formation of the Polelle Group. For reasons presented below, the Weld Range area is interpreted to represent a cross section through a c. 2.75 Ga supervolcano, tilted to the south as a result of $D_1$ deformation at c. 2676 Ma (Localities **2.11 – 2.14**, marked on Fig. 1). The observations at this locality, and in the surrounding outcrops, show that the whole of the Polelle Group is linked to a major episode of mantle melting, which erupted a thick succession of interbedded komatiitic and tholeiitic basalts, caused crustal melting to produce felsic volcanic and volcaniclastic rocks, which, in turn, gave rise to hydrothermal circulation and the deposition of banded iron-formation within the collapsed caldera of the initial volcanic eruptions. The lines of evidence used to develop this model are that: 1) the Meekatharra and Greensleeves Formations are linked through transitional volcanism, as seen at this locality; 2) the Greensleeves Formation is interbedded with banded iron-formation of the Wilgie Mia Formation and thus is contemporaneous with it; 3) isotopic data from Wilgie Mia banded iron-formation show that the jaspilitic chert precursor was precipitated abiogenically through hydrothermal processes (Czaja et al., 2010); and 4) enrichment of the jaspilitic chert to form magnetite and pyrite-rich units was effected through localized hydrothermal enrichment by circulation of highly reduced fluids prior to emplacement of the c. 2750 Ma Gnanagooragoo Igneous Complex into the Weld Range banded iron-formations, intrusion of c. 2740 Ma granitic rocks, and deposition of the unconformably overlying (c. 2735 Ma) Glen Group (Locality **2.13**). The origin of the reducing fluids that transformed hematite into magnetite is linked to green-black (organic-rich) shales within the Wilgie Mia Formation (Locality **2.5**).

* All grid references are quoted with respect to datum GDA94, and lie within MGA Zone 50.

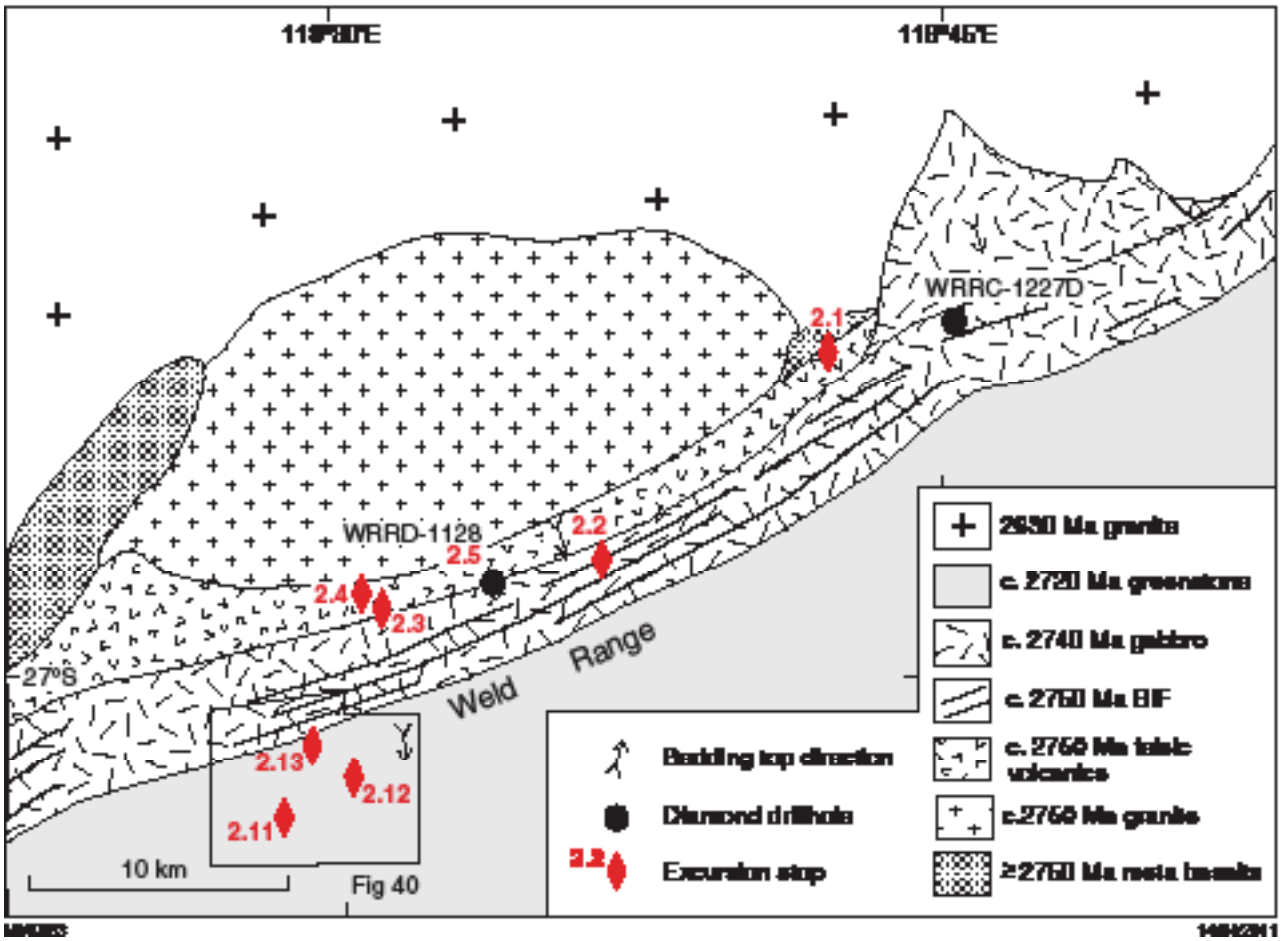


**Figure 21. Simplified geological map of the Weld Range showing excursion localities**

## Locality 2.1.1

The small outcrop at this locality shows what appears to be a fine chilled pillow rind, and adjacent blocks show centimetre-sized varioles. These textures are typical of submarine pillowed komatiitic basalts, but thin section analysis reveals the 'rinds' are not chilled pillow margins after all, but syn- to post-metamorphic alteration fractures.

## Locality 2.1.2

Walk uphill 20 m (to MGA 569831E 7026592N). At this locality, fine-grained komatiitic basalt is weakly brecciated, possibly representing the base of a subaerial flow unit (unit 2 on the section shown in Fig. 22). This finer grained unit grades up into medium-grained komatiitic basalt within the middle part of the flow unit. Petrographic analysis of a similarly textured unit higher up in the section (base of unit 3) shows that this rock type is a cumulate of euhedral, zoned clinopyroxene (augite) crystals in a fine-grained matrix.

## Locality 2.1.3

Walk a few metres further uphill to MGA 569833E 7026583N. Here we see a fine-grained komatiitic basalt near the top of unit 2 that contains sulfides.

## Locality 2.1.4

Walk 30 m southwest to MGA 56986E 7026554N. At this locality we see the coarse-grained component of the thick flow unit 3, consisting of euhedral, zoned augite crystals in a finer grained matrix (Fig. 22).

## Locality 2.1.5

Proceed 30 m south to 569795E 7026504N. At this locality, we are nearing the top of flow unit 3, and the komatiitic basalt shows good pyroxene-spinifex texture as well as common, 1–2 mm spherical vesicles, now filled by quartz (Fig. 22). It is these vesicles that first suggested a subaerial origin for this unit and that the coarse-grained phase was a cumulate component of a thick subaerial flow unit.

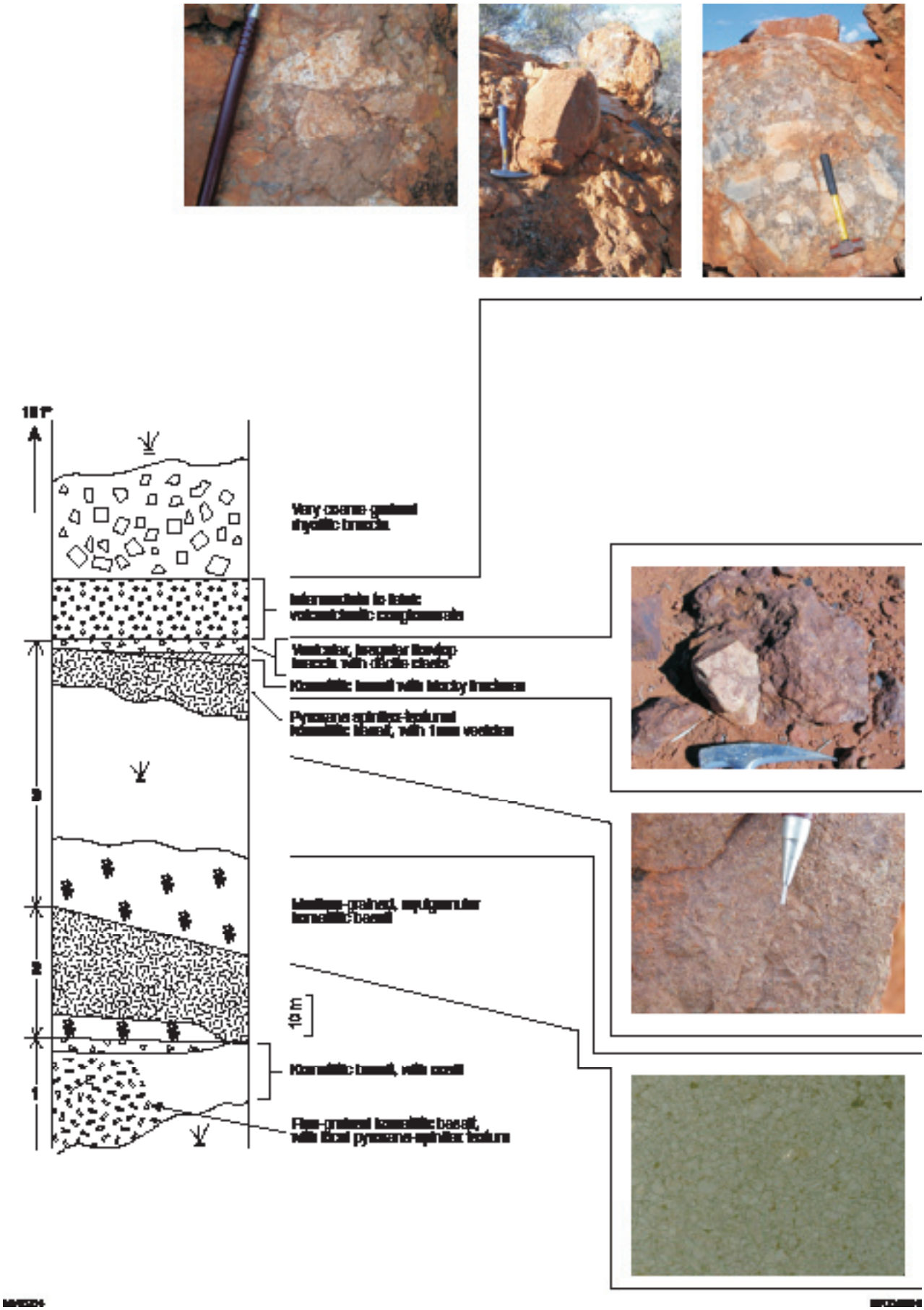


**Figure 22. Stratigraphic section and accompanying photographs of the subaerial komatiite–rhyolite transition at excursion locality 2.1**

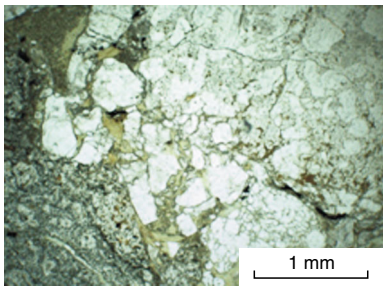


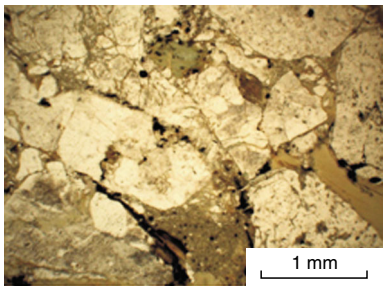


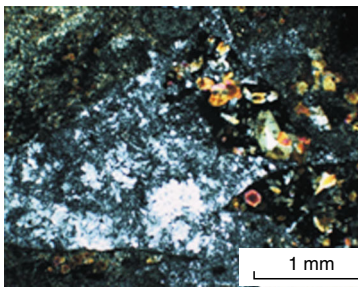


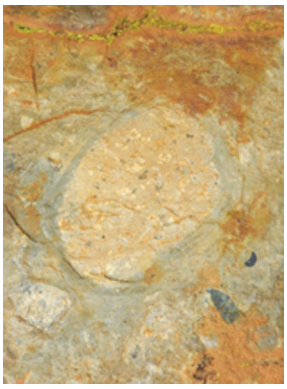

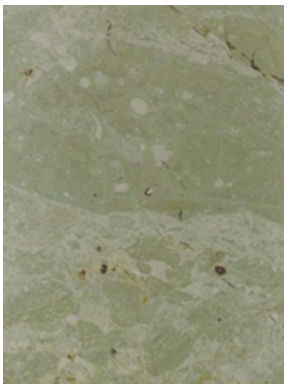

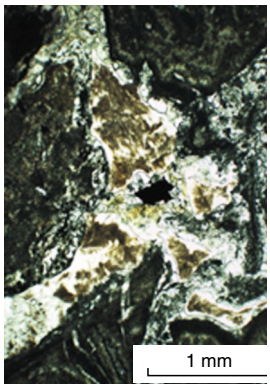


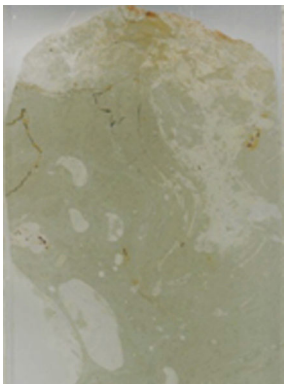

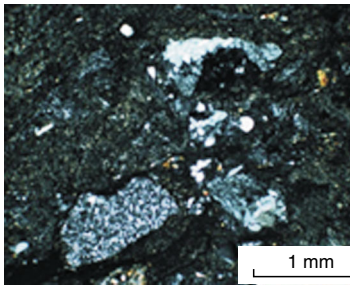


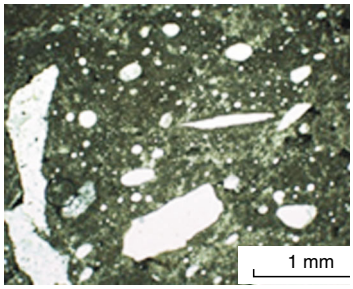


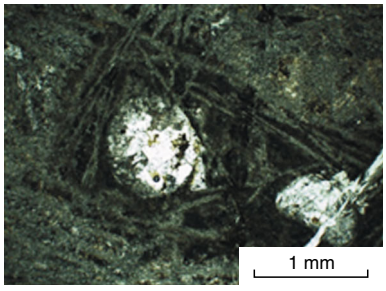


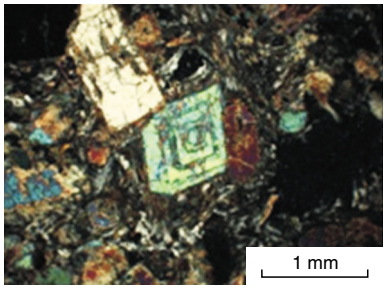


MVK984 18/(

## Locality 2.1.6

Walk 15 m southeast to MGA 569811E 7026490N. Here we are in the rubbly flowtop breccia of flow unit 3, consisting of irregular fragments of slightly silicified komatiitic basalt, surrounding more angular fragments of darker brown komatiitic basalt. Vesicles here are more sparse than further down, but larger, up to 1 cm in diameter (Fig. 22). Also contained in this flowtop breccia are sparse, angular clasts of dacite (Fig. 22), interpreted (for reasons described at the next localities) as having been dropped in from an adjacent, contemporaneous, explosive felsic volcano.

## Locality 2.1.7

Two metres further south at MGA 569813E 7026489N, we reach a more silicic component of the flowtop breccia, with a silicic matrix surrounding fragments of komatiitic basalt (main component) and clasts of felsic volcanic material.

## Locality 2.1.8

Five metres east-southeast (at MGA 569818E 7026486N) we pass into an intermediate volcaniclastic rock with abundant angular felsic volcanic clasts to 5 cm in a mafic–intermediate, green, volcanic matrix. This grades upwards into coarse-grained intermediate to acid volcaniclastic rocks. Note that bedding is not evident in this unit except as defined by changes in composition. Petrographic analysis of thin sections indicate the rock consists of fragments of felsic volcanic material in komatiitic basalt as well as fragments of komatiitic basalt within a felsic matrix, suggesting the rock is a hybrid of mixed magmas.

## Locality 2.1.9

Ten metres farther south (at MGA 569819E 7026473N), the volcaniclastic rocks are slightly more felsic (light orange-weathering) and contain more well-rounded felsic clasts, although the matrix is still intermediate to mafic in composition (Fig. 22). Thin sections reveal a felsic matrix to fragments of vesicular komatiitic basalt and an unusual matrix texture of highly clouded, anhedral feldspars (?glassy), with cuspate margins developed along the contacts of komatiitic basalt clasts (Fig. 22).

## Locality 2.1.10

Walk 30 m south-southwest to the prominent outcrop at MGA 569800E 7026435N. This spectacular outcrop of very coarse grained felsic volcanic breccia shows that we are now very close to the throat of the erupting felsic volcano. Angular felsic blocks up to 40 cm (microgranite, rhyolite, and medium-grained granite) lie packed together with smaller blocks of dominantly felsic composition in a matrix of still smaller, slightly more polymict clasts (including layered chert and a variety of felsic volcanic rocks) and rock flour (Fig. 22). Larger matrix clasts show blocky fracturing, whereas smaller clasts show evidence of in situ disaggregation, suggestive of deformation during volcanic-associated seismic events. Thin section petrography shows that the large granitic blocks within the breccia contain spherulitic texture, with bow-tie, plumose, and fan-shaped sheafs of fibres (Fig. 23; Lofgren, 1974). These textures are indicative of devitrification of rhyolitic volcanic glass at temperatures of 400 to 650°C (Lofgren, 1971).

Walk to the east along strike and observe other outcrops of this spectacular volcanic breccia. At MGA 569920E 7026490N, note the presence of long, disrupted panels of medium-grained granite within the breccia that may represent disrupted feeder dykes to this volcanic episode.

# Locality 2.2: Weld Range banded iron-formation in outcrop

*Return to the vehicle and follow the track back out towards the highway. Just before reaching the end of the range, park the vehicle (at MGA 558026E 7017812N) and climb up the low ridge to the south of the track to MGA 558087E 7017735N.*

This locality shows a good example of typical banded iron-formation of the Wilgie Mia Formation in the type area of the Weld Range. The banded iron-formation here consists of layers of hematite-bearing (jaspilitic) chert alternating with pure magnetite (Fig. 24). Although this may look like bedding, closer inspection of outcrop and drillcore samples (see Locality **2.5** below) shows that, whereas the jaspilitic chert does appear to contain millimetre-scale 'primary' bedding consisting of jaspilitic chert and clear chert, the magnetite layers diverge and splay and locally surround remnant pods of layered jaspilitic chert, indicating that the magnetite is of secondary origin (e.g. Fig. 25). Indeed, the local observation of tight to isoclinal folds of this layering suggests that much of the outcrop-scale layering is highly transposed.

The Weld Range project of Sinosteel Midwest Corporation Limited is a direct shipping ore (DSO) resource expected to produce 15 Mt per annum for export out of the proposed Oakajee port. The project is at an advanced stage of a Bankable Feasibility Study, due for completion in 2010, and should be ready for production by 2013. The Weld Range project includes a confirmed total resource of 155.5 Mt of hematitic mineralization at 58.0% Fe at a cutoff grade of 50% Fe, with grades as high as 66.9% Fe having been recorded (69.9% Fe being pure hematite). The areas covered by the mineral resource estimate have low contents of deleterious contaminant elements and have acceptable strip (waste:ore) ratios. The Weld Range project has high-grade outcrops over a total 16 km strike length. The current resource estimate represents only 6 km of the strike length.

Sinosteel Midwest has also commenced a drilling program at Weld Range aimed at determining a magnetite resource. Initial indications have identified two significant potential magnetite products — one similar to the relatively coarse-grind material at Jack Hills, and the other similar to the finer grind magnetite product found at Koolanooka to the south.

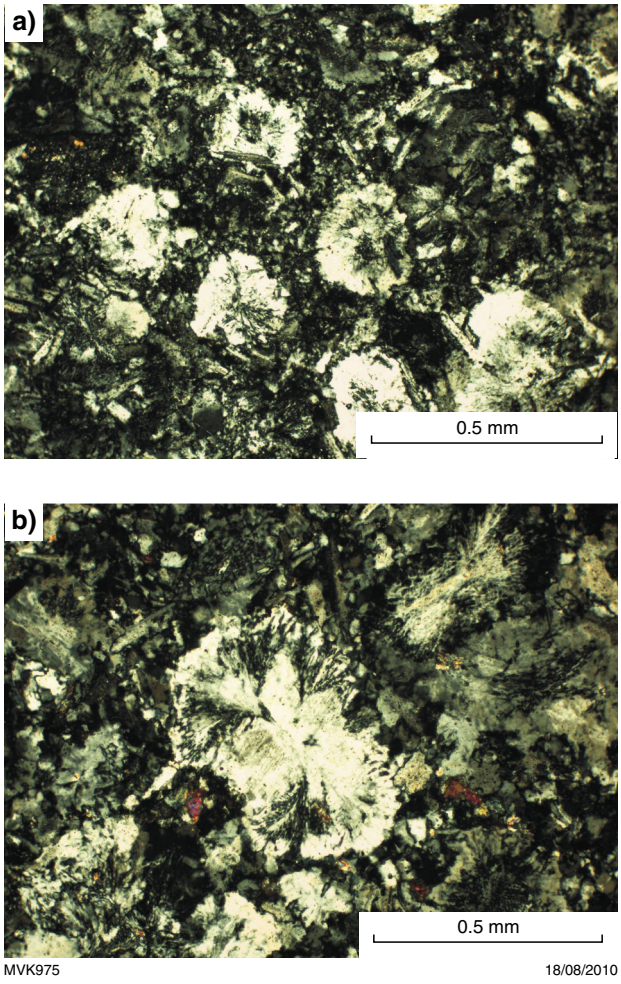


**Figure 23. Photomicrographs (cross-polarized light) of rhyolitic blocks from the volcaniclastic breccia at locality 2.1.10: a) radiating spherulites; b) spherulitic texture with plumose and bow-tie fibre sheafs**

The abundance of iron in the high-grade outcrops is considered to be vastly in excess of that present in adjacent outcrops of 'normal' banded iron-formation. Therefore the growth of hematite is considered to represent a low-temperature diagenetic or metasomatic event in which it has overgrown magnetite and displaced silica. This may have happened when the rocks were buried at as little as 500 m depth.

## Locality 2.3: Interbedded felsic volcaniclastic rocks and banded iron-formation

*Return to the Cue–Beringarra road and cross it, then head west (at MGA 557779E 7017724N). Go through gate onto a good dirt road. Drive for 5.6 km and turn left down good dirt track (MGA 552262E 7017711N). Drive 1.1 km and turn left (MGA 552731E 7016748N). Drive 0.5 km and park (MGA 553085E 7016714N). Walk south onto a hill (north of the main Weld Range) to locality 2.3.*


**Figure 24. Outcrop of banded iron-formation in the Weld Range (Wilgie Mia Formation, Polelle Group), showing apparent bedding defined by alternating layers of jaspilitic chert and magnetite**

At this locality (MGA 553092E 7016621N; Fig. 21), a 5 m-thick, bedded and foliated band of jaspilitic banded iron-formation lies within a fine-grained white felsic volcaniclastic rock with graded bedding showing way-up to south. Clasts grade from 5 cm to 2 mm. Several cycles of grading are seen, and some truncation of banded iron-formation layers by felsic volcaniclastic units may represent a cannibalization process. Pillow-like structures (Fig. 26) represent either load casting of dense ferruginous sediment on top of muddy volcaniclastic sediments or possibly a peperitic top layer of an intrusive rhyolitic sheet.

A fine-grained, yellow-weathering felsic volcaniclastic unit adjacent to this locality (about 100 m to the southeast at MGA 553155E 7016525N) is weakly bedded with occasional quartz pebbles (<1 cm) that show graded bedding with younging to the south (Fig. 27).

You may walk upsection (uphill, towards the Weld Range to the south) to observe the incoming of the significant banded iron-formation units (MGA 553183E 7016433N) where jaspilitic banded iron-formation can be seen to be in contact with felsic volcaniclastic sedimentary rock.

## Locality 2.4: Geochronology sample site of clasts in felsic volcanic breccia

*Go 500 m west-northwest from the parking spot at Locality 2.3.*

At this locality (MGA 552237E 7016611N), a felsic volcanic breccia is exposed on top of a small knoll.

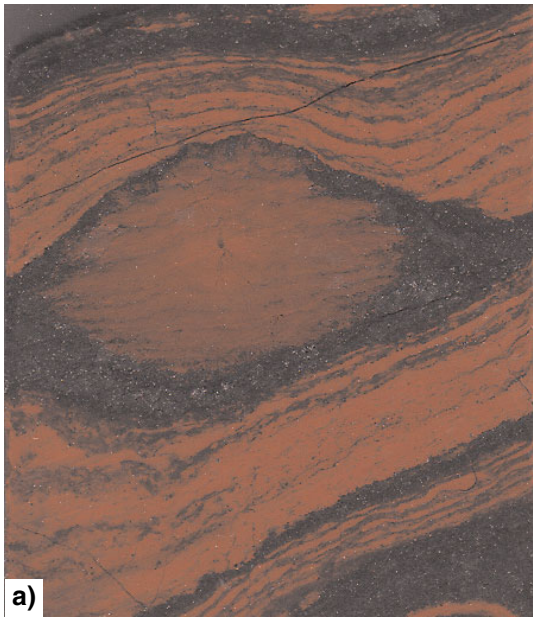


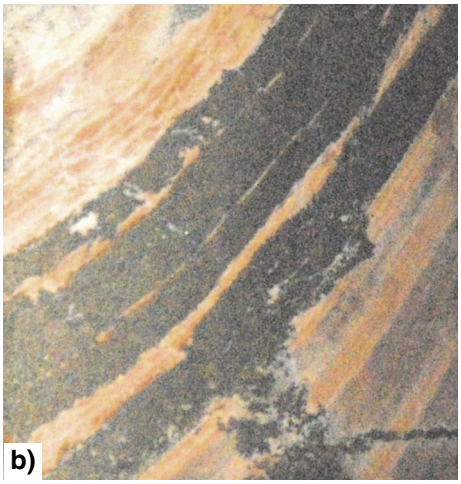


MVK974 13/10/2010

**Figure 25. Textural evidence for the replacive origin of magnetite in Weld Range banded iron-formation: a) sample of fresh drillcore showing magnetite rind surrounding and cutting off bedded jaspilitic chert; b) sample of fresh drillcore showing remobilization of magnetite from a depleted layer of white (originally jaspilitic) chert into a vein and sill array within bedded jaspilitic chert**

MVK977 09/08/2010

**Figure 26. Unusual ball-and-pillow structure within felsic volcaniclastic rocks of the Greensleeves Formation, Polelle Group, north of the Weld Range at excursion locality 2.3**

MVK978 09/08/2010

**Figure 27. Example of graded bedding in felsic volcaniclastic rocks of the Greensleeves Formation, Polelle Group, north of the Weld Range at locality 2.3**

MVK973 09/08/2010

**Figure 28. Felsic volcanic breccia of the Greensleeves Formation, Polelle Group, north of the Weld Range at locality 2.4**

Euhedral quartz phenocrysts are visible in rhyolite clasts (GSWA geochronology sample 193971) in a fine-grained matrix (GSWA geochronology sample 193972). The clasts are angular to rounded and 5 mm to 30 cm in diameter (Fig. 28). Scattered clasts of jaspilitic iron-formation are also present.

## Locality 2.5: Drillcore through the Weld Range banded iron-formation

### (Leader: Rob Walker, Sinosteel)

*Return to the main road and turn left. Continue south for 4.4 km to the turnoff into the Sinosteel Midwest main camp and proceed to the outdoor core yard.*

Two diamond drillcores are laid out for inspection:

1. WRRC 1227D was drilled 55°→150° from the base of the stratigraphically lowermost banded iron-formation horizon, just east of Locality **2.1** of this fieldtrip;

2. WRRD 1128 was drilled 60°→340° on the south side of the stratigraphically lowermost banded iron-formation horizon to the north-northwest (Fig. 21).

Simplified drill logs are presented in Table 1. Drillcore WRRD 1128 intersects black shale with pyrite (192–198 m depth) in the stratigraphically higher part of the hole, and layered jaspilitic chert–magnetite banded iron-formation (227–238 m depth) deeper down. The layered jaspilitic chert–magnetite rock is particularly interesting. In particular, note that the magnetite is everywhere of secondary origin, despite its broadly layer-parallel occurrence (e.g. Fig. 25a,b). This can be seen in greater detail through investigation of thin sections (Fig. 29). The most significant observations are that layered jaspilitic chert and clear chert (actually microquartz) show evidence for the 'most primary' type of bedding, perhaps described anywhere in the world (Fig. 29a,b). Throughout most

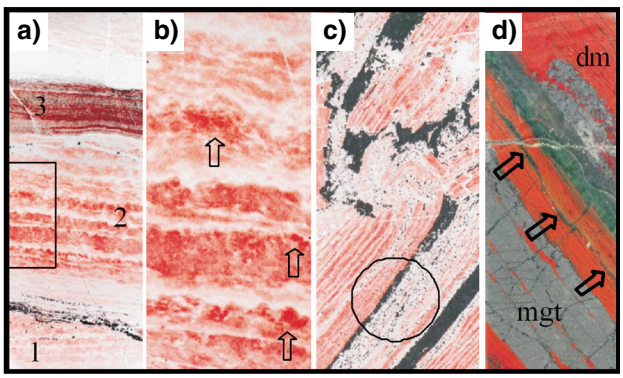


MVK985 18/08/2010

**Figure 29. Thin section features of Weld Range banded iron-formation: a) primary banded jaspilitic chert, with minor secondary magnetite. Note the presence of three disconformity-bound bedding packages (labelled 1–3), each characterized by distinct bedding features. Rectangle outlines area of part b). Width of view about 1 cm; b) detail of primary bedding between jaspilitic chert layers and layers of clear chert (actually microquartz), with 'thundercloud'-like, irregular contacts. Note that jaspilitic beds become increasingly red (more hematitic) upsection (arrows). This is interpreted as the 'most primary' type of bedding preserved in the banded iron-formation. Width of view about 0.3 cm; c) finely bedded jaspilitic and clear chert affected by faulting and crystallization of secondary magnetite along fault margins. Note the development of secondary magnetite from dissolution of hematite in the circled area. Width of view about 1 cm); d) layered jasper–magnetite banded iron-formation, showing veins of pure magnetite emplaced parallel to bedding defined by jaspilitic chert (mgt) and another area of more dispersed secondary magnetite (dm) cutting across bedding in the top right of the section. Note the more transposed appearance of the jaspilitic chert in this sample compared with a) and b). Arrows point to stylolite within the jaspilitic chert, which is lined with grains of pyrite and carbonate. Greenish band in upper part of section is of microquartz with ?chlorite and carbonate. Width of view about 1 cm. a) and b) from WRRD 1228, 231.25–231.5 m depth; c) from WRRD 1228, 231.65–231.95 m depth; d) from WRRD 1228, 227.57–227.87 m depth**

of the core, however, this primary bedding has been transposed to variable degrees and replaced and/or intruded by secondary magnetite (Fig. 29c,d). Magnetite itself is then cut by pyrite during a second period of hydrothermal alteration (Fig. 30), possibly during folding of Polelle Group rocks prior to deposition of the Glen Group (see Locality **2.13**).

Drillcore WRRC 1227D intersects a thick unit of green shales, characterized by minnesotaite, stilpnomelane, chamosite–greenalite, and minor siderite (151–208 m). Downhole the green shales pass (upsection) into layered magnetite-rich rocks with quartz, siderite, and minnesotaite cut by secondary pyrite (Table 1). Towards the bottom of the hole, layered magnetite is strongly oxidized (278–300 m depth) and host-rock lithology is highly altered by clay–quartz alteration (300–310 m depth). Pyrite is

**Table 1. Logs of lithology and mineralogy from drillcores WRRC 1127D and WRRD 1128 across the Weld Range. Mineralogy determined by XRD of individual samples and Hylogger analysis of half-core pieces from selected intervals**

| *Depth (m)* | | *Hylogger* | *magnetite* | *pyrite* | *carbonate* |
|---|---|---|---|---|---|
| **WRRC 1127D** | 55 degrees towards 150 (i.e. shales below magnetite banded iron-formation, but folded) | | | | |
| 151–161 | layered, variegated green shales (minnesotaite, trace stilpnomelane) and finely layered magnetite | ankerite, calcite | | | |
| 161–172 | dark green shales; chlorite–minnesotaite–septechlorite(chamosite–greenalite), minor stilpnomelane | ankerite, calcite | | | |
| 172–176.7 | dark green shales cut by pyrite (secondary); minnesotaite–septechlorite(chamosite–greenalite), minor stilpnomelane and siderite | | | | |
| 176.7–177.2 | chlorite, cut by carbonate veins | calcite Mg-clay | | | |
| 177.2–186.8 | green shales; stilpnomelane–minnesotaite–septechlorite(chamosite–greenalite), minor siderite | calcite, ankerite | | | |
| | stilpnomelane–minnesotaite–septechlorite(chamosite–greenalite), minor siderite | siderite | | | |
| 186.8–196 | magnetite and chlorite | | | | |
| 196–208.2 | magnetite–quartz–siderite; minor minnesotaite–septechlorite–stilpnomelane–pyrite | | | | |
| 208.2–210 | Fe-chlorite and magnetite | | | | |
| 210–219 | magnetite and yellowish mineral bands | dolomite, siderite | | | |
| 219–222 | magnetite–pyrite–chlorite | ankerite, dolomite, siderite | | | |
| 223–229 | magnetite and white layering (?chert or carbonate) | calcite | | | |
| 229–240 | magnetite–quartz–siderite–minnesotaite | ankerite, calcite | | | |
| 240–260 | finely layered quartz–magnetite–siderite and pyrite (secondary) | | | | |
| 260–278 | magnetite–quartz–siderite, minor minnesotaite | | | | |
| 278–282 | Fe-oxide alteration of magnetite, with carbonate and pyrite veins | | | | |
| 282–289 | banded magnetite, white ?chert | | | | |
| 289–297 | banded magnetite, partly oxidized and cut by pyrite veins | | | | |
| 297–300 | altered banded magnetite–quartz | | | | |
| 300–310.6 | banded pyrite and white (?clay/quartz) alteration | | | | |
| End of Hole | | | | | |
| **WRRD 1128** | 60 degrees towards 340 (i.e. shale above banded iron-formation, unfolded) | | | | |
| 192.0–192.3 | black shale with pyrite | | | | |
| 196.5–196.7 | black shale with pyrite | | | | |
| 197.75–197.8 | black shale with pyrite | | | | |
| 227.57–227.87 | jaspilite–magnetite banded iron-formation | | | | |
| 231.25–231.5 | jaspilite–magnetite banded iron-formation | | | | |
| 231.65–231.95 | banded jaspilite–quartz–magnetite (secondary) | | | | |
| 236.4–236.7 | jaspilite–magnetite banded iron-formation | | | | |
| 238.3–238.4 | vein quartz with banded jaspilite–magnetite | | | | |

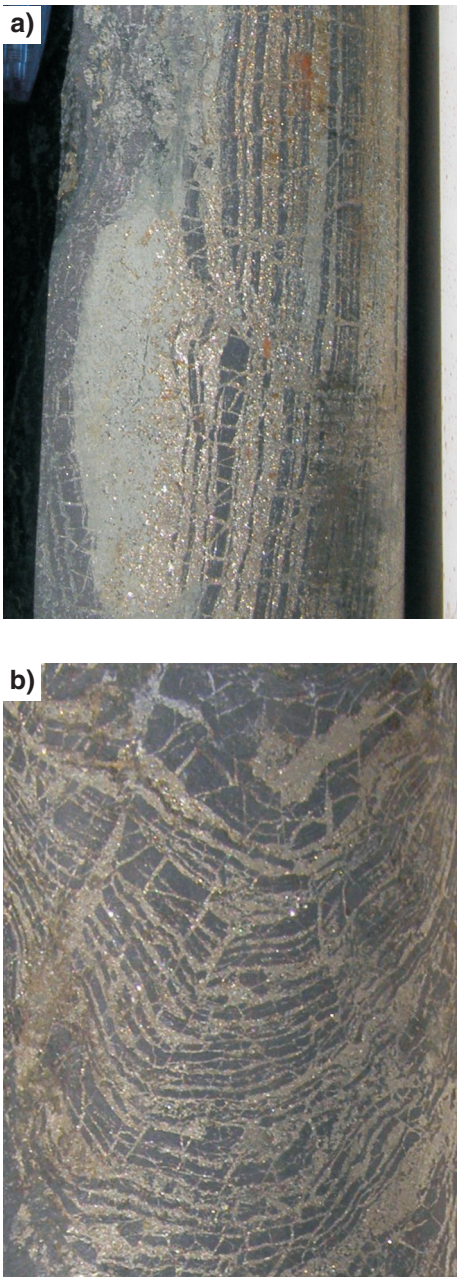


**Figure 30. Drillcore samples showing relationship between magnetite and pyrite: a) layered green shale and magnetite rock, cut by secondary pyrite (from 219–222 m depth in WRRC 1227D); b) layered magnetite cut by secondary pyrite veinlets oriented along the axial plane of folded magnetite, suggesting pyrite emplacement and/or remobilization during folding (from 240–260 m depth in WRRC 1227D)**

common in the lower parts of this hole and, together with the clay and oxide alteration assemblages, suggests formation during the circulation of acidic hydrothermal fluids during a secondary alteration stage after magnetite alteration of the primary jaspilitic chert.

The low-Fe contents (1–7 wt%) and $\delta^{56}$Fe values (0.54 – 0.72‰) of fine-grained hematite in jaspilitic chert are consistent with incomplete oxidation of $Fe^{2+}_{aq}$ and Fe oxide precipitation (Czaja et al., 2010). Secondary magnetite has similar, but slightly lower, $\delta^{56}$Fe values (0.37 – 0.60‰), reflecting net addition of $Fe^{2+}$-rich fluids. High $\delta^{56}$Fe values for pyrite (0.81 – 0.94‰) probably reflect interaction between dissolved sulfide in reducing hydrothermal fluids and excess $Fe^{2+}_{aq}$. That the relative $\delta^{56}$Fe values of hematite–magnetite–pyrite follows that expected for Fe isotope equilibrium, suggests formation of banded iron-formation by entirely abiologic pathways from a major, probably common, reservoir of $Fe^{2+}_{aq}$.

Petrographic and sulfur isotope data from pyrite indicate two sources of sulfur in these rocks. First phase sulfur in the cores of some grains in banded iron-formation and in carbonaceous shales have a range of $\delta^{34}$S values (+5 to -15‰), interpreted to reflect the effects of bacterial sulfate reduction. Pyrite overgrowths and vein pyrites have a much narrower range of $\delta^{34}$S values (0 to -5‰), interpreted to reflect the effects of sulfur remobilization and averaging of first phase sulfides during hydrothermal processes.

Thus, a three-stage process for the formation of Weld Range banded iron-formation is inferred. In the first stage, primary hematite and chert is precipitated from seawater enriched in iron as a result of low-temperature hydrothermal processes associated with waning felsic volcanism. This resulted in deposition of jaspilitic chert precursors to the banded iron-formation, but with only between 1 and 5 wt% Fe. In stage 2, hydrothermal circulation within an enclosed basin (collapsed volcanic caldera) caused reduction of primary hematite to magnetite and enrichment in total Fe. Stage 3 involved a further period of hydrothermal alteration, but this time from hot, acidic, sulfur-rich fluids that most likely derived from fluid flow through the organic-rich shales interbedded with the jaspilitic chert precursors in the lower part of the Wilgie Mia Formation. This stage of alteration may have accompanied folding of the rocks, possibly associated with emplacement of the Gnanagooragoo Igneous Complex (see Locality **2.13**), but certainly prior to deposition of the Glen Group at c. 2735 Ma. None of the post-Wilgie Mia rocks (e.g. c. 2745 Ma Gnanagooragoo Igneous Complex, c. 2740 Ma granites, or the c. 2735 Ma Glen Group) show evidence of having been affected by either magnetite or pyrite alteration.

## Locality 2.6: Glen Homestead monzogranite and syn-plutonic mafic dykes

*From the Sinosteel camp, return to main road and turn left. Continue south along sealed road for 7 km and turn left into Glen homestead, just at the end of the airport*

*runway on the left (east) side of the road. Continue past the house, and head southeast over the small dirt barrier and follow the track past the old car dump. Then follow the fence line for 4.2 km and pass through the gate (at MGA 568387E 7006782N). Follow the track to the left for a further 0.6 km to MGA 568786E 7006770N. Here turn hard right (switchback) just before the windmill and follow the track to south and southeast for 300 m, through a small creek and continue for about 4.0 km along the track to MGA 572419E 7005658N. At this point, turn right off track and head due south for about 400 m to the foot of a large granite outcrop rising to the south. Walk up the granite platform to a thin mafic dyke at MGA 572492E 7005085N.*

This large granite outcrop is a heterogeneous, leucocratic metamonzogranite that varies from medium grained to pegmatitic in an irregular way across the outcrop. This 2748 ± 5 Ma metamonzogranite is contemporaneous with widespread intermediate to felsic volcanism of the Greensleeves Formation throughout the Murchison Domain. Clots of mafic material can be seen scattered throughout the outcrop, but this texture is much better developed in the next outcrop.

The main feature at this outcrop is the presence of at least four syn-plutonic mafic dykes. These fairly thin (<40 cm), but long, sinuous dykes are characteristically discontinuous along strike, with evidence of both their intrusion into the metagranitic host, but also of intrusion of granite into the dykes without any textural evidence that the granite represents a distinctly different phase from the host (Fig. 31a–c). The dykes are more leucocratic than normal tholeiitic dolerites and contain hornblende–biotite–titanite–plagioclase (Fig. 31d).

The presence of synplutonic mafic dykes in granitic rocks of this age is significant in that it demonstrates continued input of mantle melts during a period of dominantly felsic magmatism across the Murchison Domain, and raises the question as to the origin of intermediate magma compositions that occur generally at the transition from mafic–ultramafic volcanism to felsic magmatism (volcanics + granites) during this time period, as discussed in more detail at the next locality.

## Locality 2.7: Mafic clotty-textured granite and syn-plutonic mafic dykes

*Drive west along the foot of the granite outcrops for about 850 m until you reach a creek (trees). Follow the creek bed southwest for 600 m and merge onto a sandy track. Continue southwest for a further 600 m, then head left (due south) along open ground for about 800 m. Swing left and head southwest for 1.5 km, heading to MGA 571950E 7003230N. Park the vehicle at the fence and climb over it, heading south to a large flat granite outcrop.*

This wonderful exposure shows a variety of textures that are characteristic of a distinctive type of granite emplaced into the Murchison Domain at c. 2750 Ma, contemporaneous with regional intermediate–felsic volcanism of the Greensleeves Formation (Polelle Group). These mafic clotty-textured granites are typically tonalitic to granodioritic in composition and contain about 1–2% scattered, irregularly sized mafic clots that are now strung out parallel to the regional foliation, but which were originally (sub)spherical (Fig. 32a). These clots are typically hornblendite, but show a variety of textures, including more typically basaltic type with plagioclase phenocrysts (Fig. 32b). However, the beauty of this particular outcrop is the transition from dispersed, small to medium mafic clots to rare, larger xenoliths with ragged textures and evidence for in situ breakup within the granitic magma (Fig. 32c), to syn-plutonic mafic dykes (Fig. 32d; MGA 571816E 7003179N), similar to those observed at the last outcrop. Note also the presence of sheets of granite with slightly more melanocratic composition than the main part of the body, and that the granite is typically sheeted at metre to decimetre scale (Fig. 32e).

The irregular size and even distribution of the mafic clots throughout this outcrop and in other exposures of this and other granites, together with the evidence here for an association with syn-plutonic mafic dykes, suggest that the mafic clots represent the product of mixing or mingling between a small volume of mafic melt and contemporaneous, much more voluminous, tonalitic melt. The end product is represented by an evenly distributed mixture of mafic droplets within the felsic host, much the same as oil droplets are dispersed within a vigorously shaken vinaigrette salad dressing. However, note that the extreme elongation of the mafic clots is not matched by the fabric defined by quartz and feldspar in the granites, suggesting that the elongation of mafic droplets occurred in the magma, prior to crystallization of the granite (Fig. 32f).

This observation is significant in the context of the formation of intermediate volcanic rocks within the Murchison Domain at this time and, perhaps, to many Archean greenstone belts around the world.

In the Murchison Domain, andesitic volcanism commenced at c. 2760 Ma, and evolves into dacitic and rhyolitic volcanics through to 2740 Ma (Fig. 19), as we will see, upsection, at the next locality. These intermediate to felsic volcanic rocks were erupted at the same time as emplacement of the widespread Annean Supersuite of TTG. Annean Supersuite granites fall into three distinct compositional groups (Fig. 33a): 1) those with highly fractionated REE and no Eu anomaly, similar to average Archean TTG (Fig. 33b); 2) those with slightly flatter REE than group 1, and with no, or only small, negative Eu anomalies; 3) a group with significantly higher HREE and a large negative Eu anomaly, with high concentrations of HFSE. Group 2 represents the Cullculli Suite of mafic clotty-textured granites, which are compositionally similar to Greensleeves Formation andesites (Fig. 33c).

The smooth, relatively shallow REE profile of Cullculli Suite granites, when combined with evidence for contemporaneous emplacement of average Archean TTG and ongoing mafic magmatism (e.g. syn-plutonic dykes), suggests that Cullculli Suite granites (and compositionally

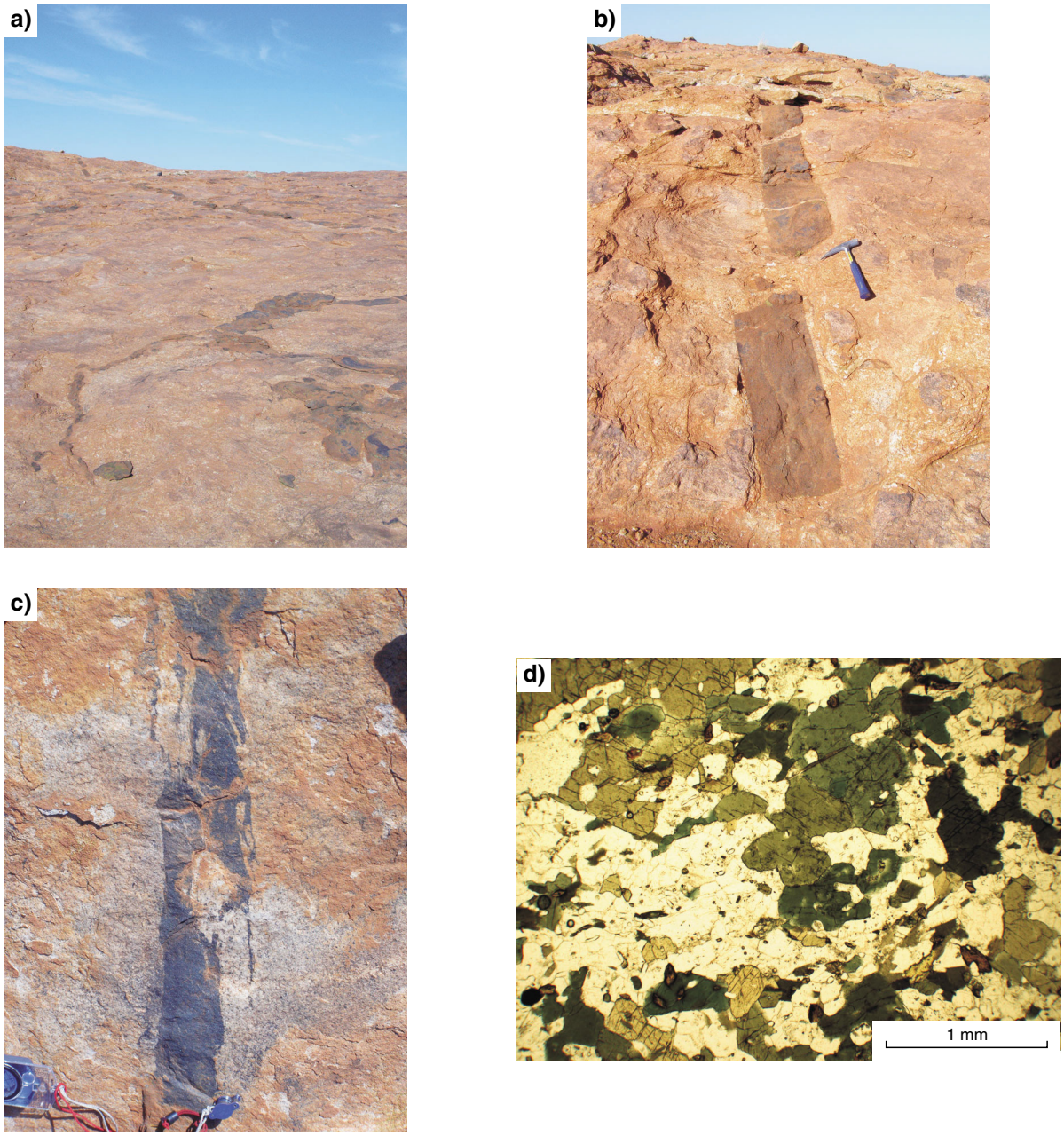


**Figure 31. Synplutonic dykes in the domal granite south of Glen Homestead at excursion locality 2.6: a) overview of sinuous mafic dyke cutting through granite; b) detail of synplutonic mafic dyke, showing offset and rotation of dyke segments by granite; c) detail of a synplutonic dyke, showing complex mutual intrusive relationships with granite; d) photomicrograph of synplutonic mafic dyke showing medium-grained texture of hornblende–biotite–titanate–plagioclase**

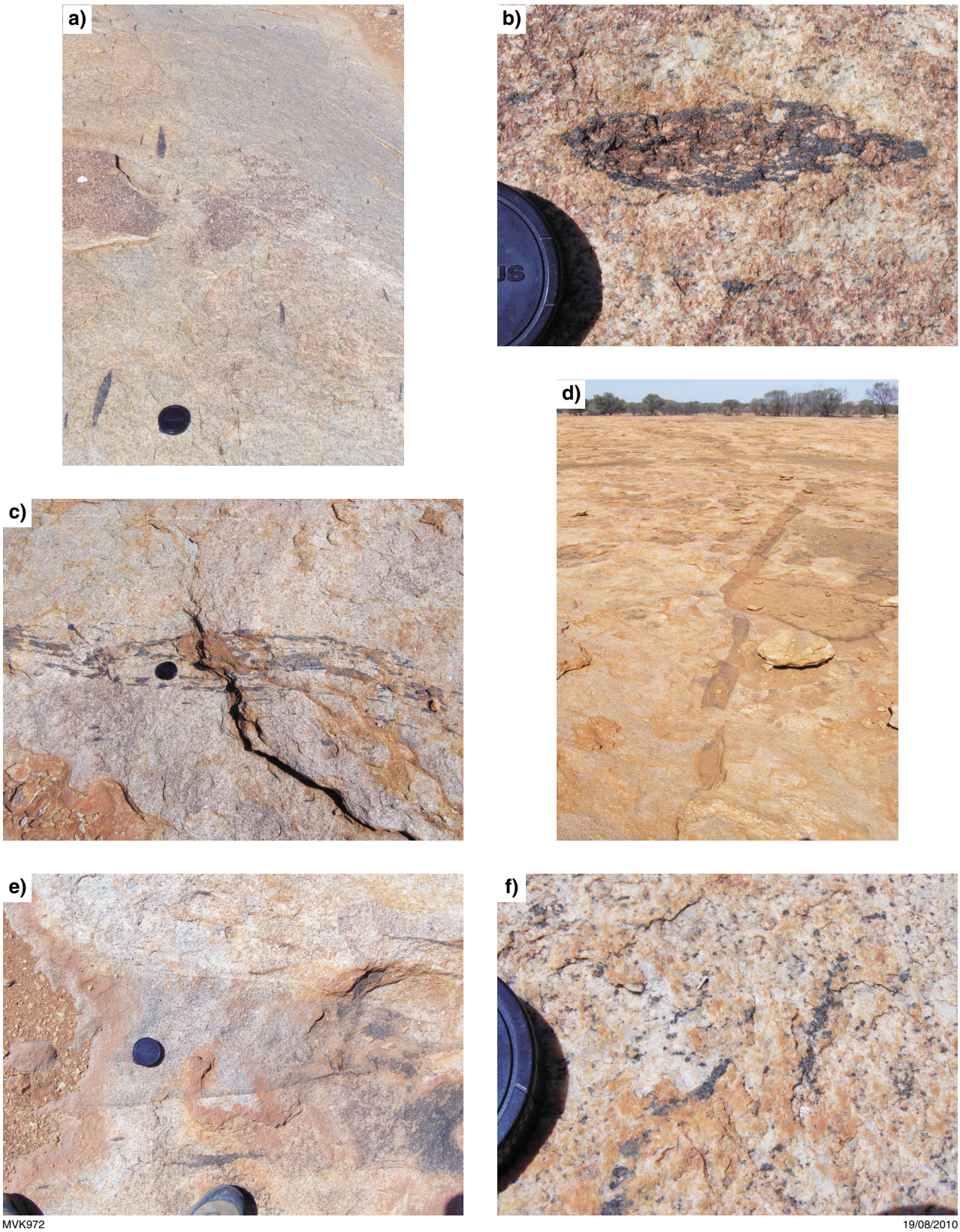


**Figure 32. Outcrop features of c. 2750 Ma mafic clotty-textured metatonalite (Cullculli Suite, Annean Supersuite) at locality 2.7: a) overview of foliated, elliptical mafic clots, showing their varable size; b) close-up of foliated mafic clot, showing ragged outline against granite and internal feldspar phenocrysts; c) disaggregated mafic enclave, commencing dispersal into mafic clots; d) synplutonic mafic dyke; e) intermediate composition granitic sheet within clotty-textured granite; f) close-up of granitic matrix, showing low internal strain contrasting with the strongly foliated nature of the mafic clots, suggesting syn-plutonic flow**

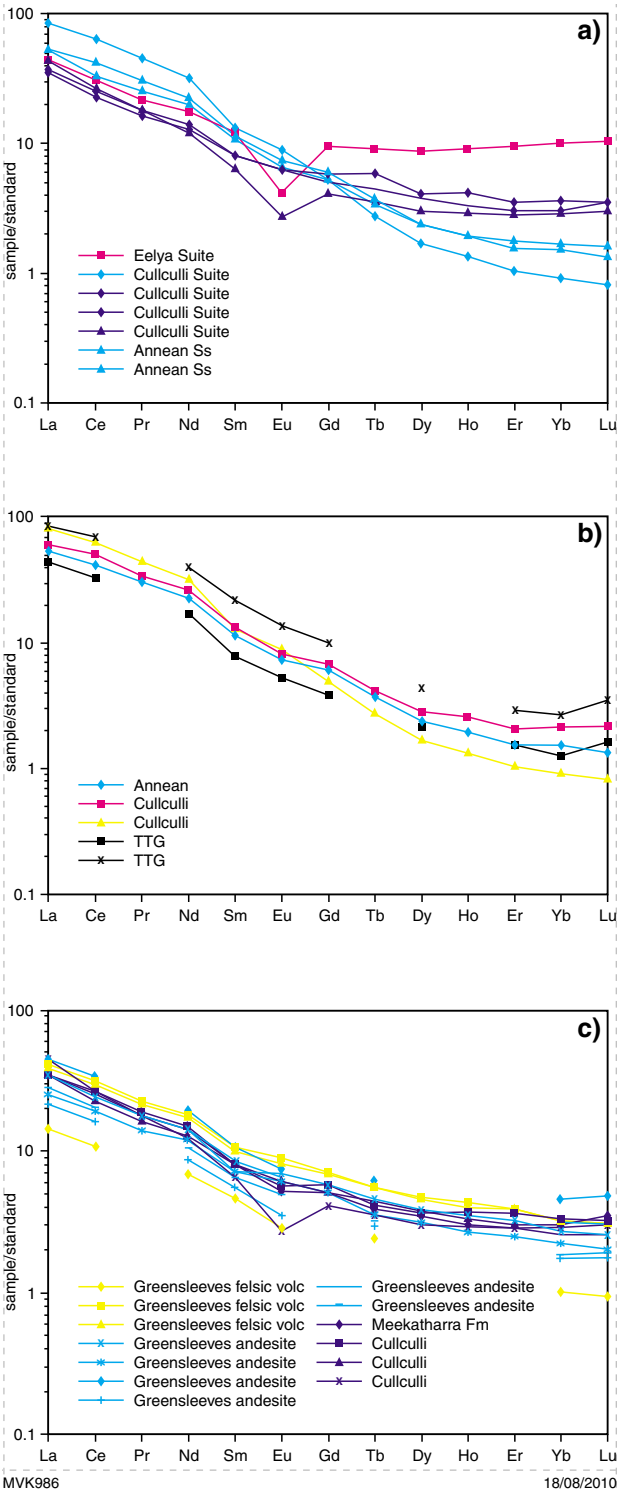


**Figure 33. Geochemical traits of Annean Supersuite granites, normalized to primitive mantle (Sun and McDonough, 1989): a) plot of rare earth elements (REE), for Annean Supersuite granites, showing derivation from three distinct sources. Mafic clotty Cullculli Suite granites have shallow REE profiles and small negative Eu anomalies; b) REE plot showing the good general comparison of mafic clotty-textured Cullculli Suite granites with average Archean TTG (data from Martin et al., 2005); c) REE plot comparing mafic clotty-textured Cullculli Suite granites with contemporaneous Greensleeves Formation andesites, showing their similar composition**

similar Greensleeves Formation andesites) may represent a mixture of average Archean TTG and basaltic melts. This was tested through simple geochemical modelling of a 50:50 mix of an average Meekatharra Formation tholeiitic basalt and a representative Annean Supersuite TTG. Results show a very good match with Cullculli Suite mafic clotty granites (and Greensleeves Formation andesites), including not only the REE, but a suite of 37 elements (Fig. 34a,b).

Recent petrogenetic studies of Archean TTG have shown that they derive primarily from infracrustal melting processes, rather than from melting of a subducted oceanic slab, as was formerly widely assumed. Studies of Murchison Domain (indeed Yilgarn-wide) TTG have confirmed an infracrustal origin for these rocks. Thus, it seems likely that Murchison Domain mafic clotty granites and compositionally similar andesites may represent the products of mixing between a crustal source (TTG) and a mantle-derived (mafic) source, following on from mantle-derived mafic–ultramafic magmatism. Significantly in this regard, the onset of Cullculli Suite magmatism and Greensleeves Formation intermediate–acid volcanism commenced c. 30 Ma after the onset of mafic–ultramafic volcanism in the Meekatharra Formation (c. 2790 Ma), equivalent to the duration required for plume-related mantle heat to conduct through average thickness continental lithosphere (Campbell and Hill, 1988). The presence of true komatiites in the Meekatharra Formation, and of two distinct sources for Meekatharra Formation basalts deriving from shallower and deeper mantle source regions (Watkins and Hickman, 1990), strongly suggests that the onset of Polelle Group magmatism was related to the melting of a mantle plume. The 30 Ma time lag between the onset of this plume-related magmatism and the transition to intermediate and then widespread acidic magmatism of the Polelle Group and Annean Supersuite, in combination with the field and geochemical evidence for magma mixing, suggests that andesitic–rhyolitic magmatism reflects the onset of widespread crustal melting resulting from plume heating of pre-existing continental lithosphere.

A dominantly infracrustal origin for intermediate to acid melts is supported by Hf in zircon data, which show a dramatic increase (10 εHf units) in the amount of recycled crustal material in Murchison Domain magmas at 2760 Ma, following 30 Ma after a peak in emplacement of juvenile material at 2790 Ma (Fig. 35). These data strongly suggest that the intermediate composition melts (andesites, mafic granites) in the Murchison Domain are mixtures of mantle- and crust-derived magmas that show no influence of subduction. It is interesting to contemplate what this might mean for the interpretation of many other Archean greenstone belts where a sharp, and often repeated, transition from mafic–ultramafic volcanism to intermediate and felsic volcanism is commonly observed.

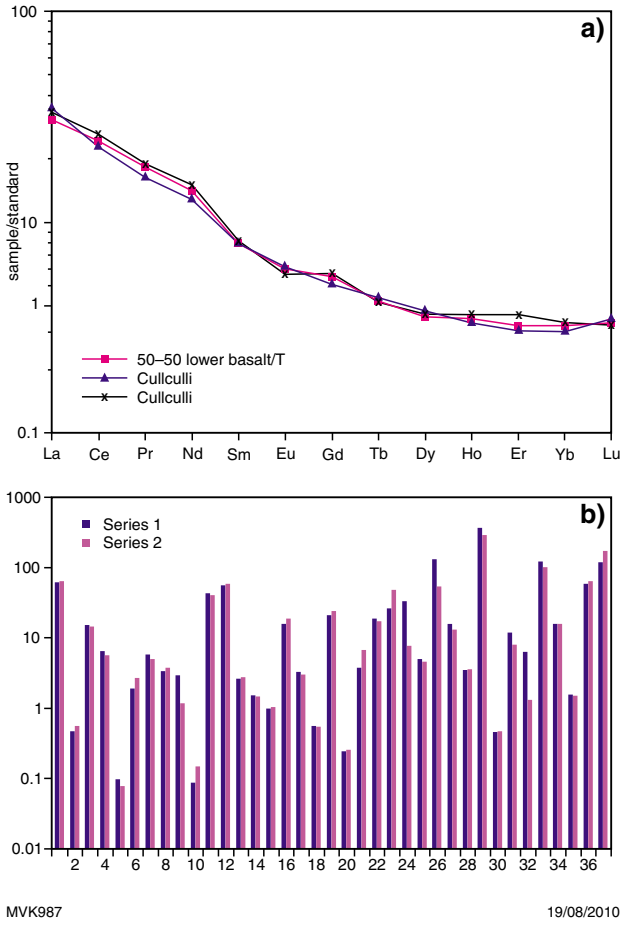


**Figure 34. Geochemical modelling of Cullculli Suite mafic clotty-textured granites, normalized to primitive mantle (Sun and McDonough, 1989): a) plot of REE, showing the good comparison between Cullculli Suite mafic granites and a simple binary mixture of 50% average Meekatharra Formation basalt and 50% average Annean Supersuite tonalite; b) histogram plot of the same comparison between Cullculli Suite mafic granites (light purple) and a simple binary mixture of 50% average Meekatharra Formation basalt and 50% average Annean Supersuite tonalite (dark purple) for 37 different elements**

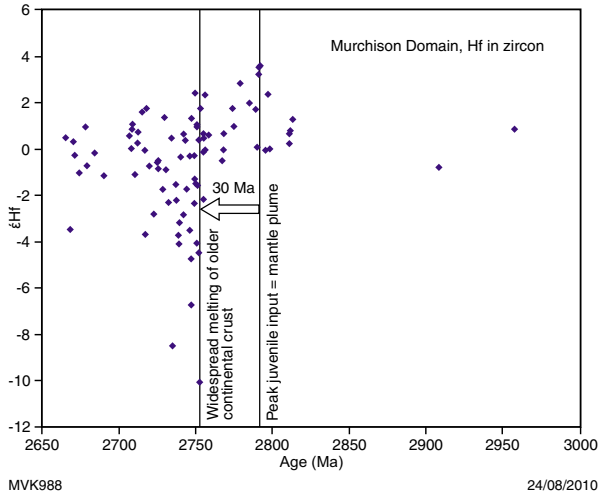


**Figure 35. Hf vs age diagram of dated zircons from selected Murchison Domain rocks, showing the sharp involvement of significantly older crust at c. 2755 Ma, some 30 Ma after the peak onset of mantle heat input, as represented by Meekatharra Formation basaltic eruptions**

# Locality 2.8: Polelle Group andesitic to dacitic volcaniclastic rocks and differentiated gabbroic sills of the Yalgowra Suite (Wattagee Hill)

*Return to the track and head back to Glen Homestead. Turn left onto the sealed road and drive south for about 32 km to a small track and gate at MGA 578480E 6982233N. Turn left onto the track and pass through the gate. Continue northeast along the track for 3.2 km to a bend at MGA 581125E 6984241N and go straight ahead for 600 m to MGA 581657N 6984492E. Follow the track as it bends east and proceed for about 300 m, keeping left. At MGA 581793E 6984571N, turn left through the gate, proceed north-northeast along the track for 4.9 km to MGA 584482E 6988350N, and then continue straight ahead (on right fork) for 1.7 km to MGA 585852E 6989393N. Turn right onto a faint track and head along about100° for 600 m. Park the vehicle at MGA 586457E 6989233N and walk to the low outcrops on the left (north) of the track at MGA 586570E 6989303N.*

This locality lies within the Greensleeves Formation of the Polelle Group in a well-constrained (stratigraphically and geochronologically) stratigraphic section (Fig. 36). The rocks here consist of foliated (along 190°/75°*), but well-preserved, coarse-grained (boulder to pebble), andesitic volcaniclastic rocks. Clasts are mainly intermediate (andesitic) to porphyritic dacite in composition and fine to medium grained, but well-rounded boulders of coarsely vesicular basalt (?basaltic andesite) are also present.

From here, walk towards 300° across strike, and note the gradual change to finer grained and more felsic compositions, including porphyritic dacite.

Continue walking northwest across the felsic volcaniclastic rocks to a flat area of low outcrop and poor exposure at MGA 586483E 6989331N. Here, we are at the ultramafic base of a thick, differentiated gabbroic sill of the Yalgowra Suite, emplaced into the c. 2750 Ma felsic volcaniclastic rocks between 2735 and 2710 Ma. Walking farther northwest across strike (to MGA 586451E 6989386N) brings you to low outcrops of dun-coloured, medium-grained metadunite in which relict cumulate texture of olivines is locally preserved.

Continue walking towards 290° across strike, to MGA 586324E 6989390N, where you encounter a low

* All foliation and bedding measurements are quoted according to the 'right-hand rule' unless otherwise stated

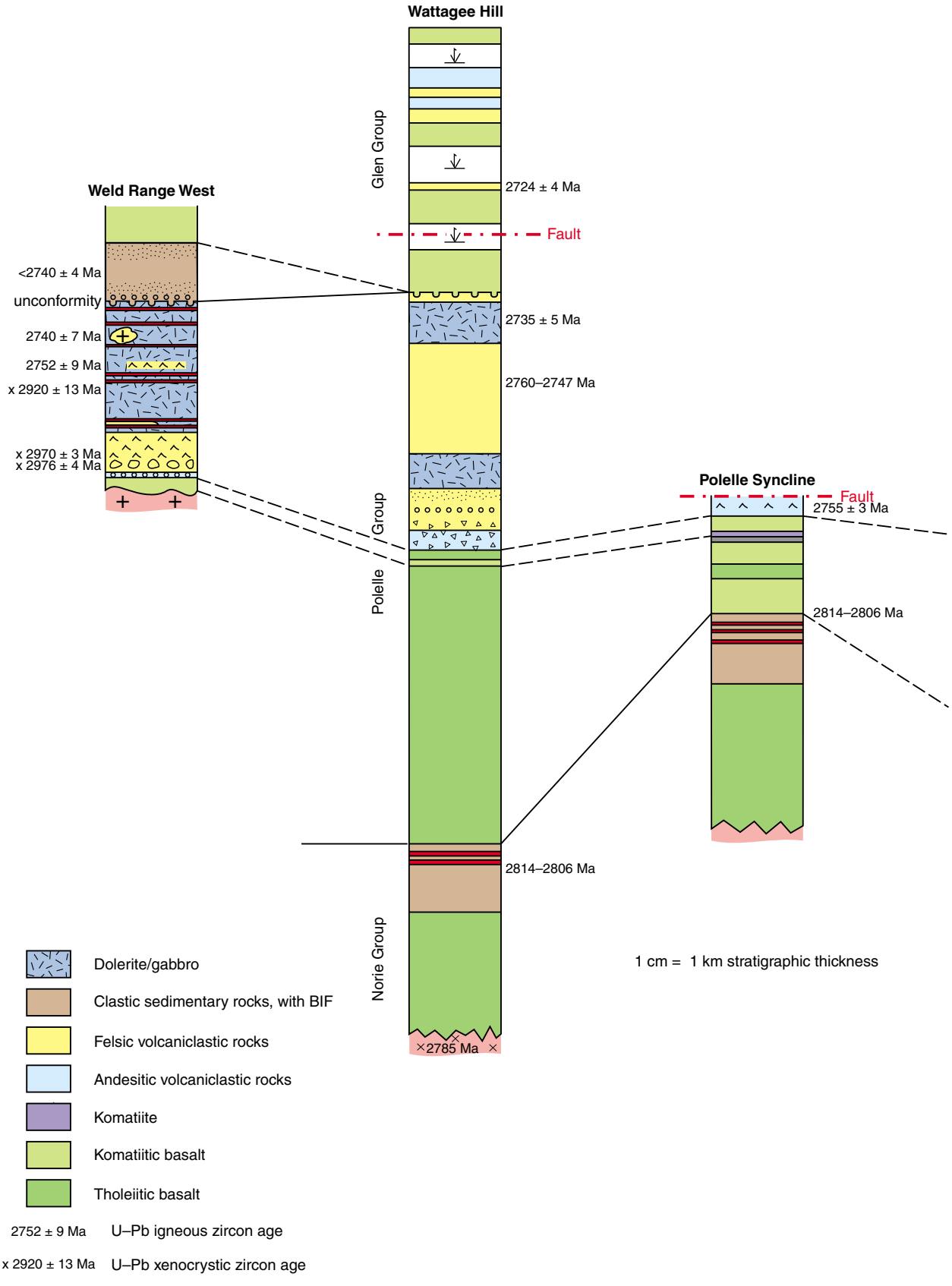


**Figure 36. Comparative stratigraphic sections across the northeastern Murchison Domain, showing correlations and available age data**

ridge of weakly layered igneous pyroxenite, composed of stubby clinopyroxene crystals up to 5 mm in a light green matrix. Note the old drill collars in the low area immediately east of this ridge, where exploration for nickel–copper mineralization was undertaken in the 1980s, with poor results. To the northwest of here is gabbro, which we will see at the next locality.

## Locality 2.9: Yalgowra Suite gabbro, Polelle Group volcaniclastic sedimentary rocks, and Glen Group komatiitic basalts (Wattagee Hill)

*Return to the main track (600 m). Turn left (south), travel for 400 m and then turn right towards the west (no track). Proceed for 400 m and then swing to the northwest and then north across a low saddle, skirting the base of the hill on your right, for 300 m, to MGA 585197E 6989379N.*

Walk up onto the low hill to the right (east). Here you at the top of the same Yalgowra Suite sill we saw the base of at the end of the last locality. The sill is about 900 m thick, although this includes screens of host-rock volcaniclastic rocks. Here, the rock is a leucogabbro, characterized by long, feathery pyroxene needles, indicative of its slightly elevated magnesian composition (Fig. 37a). If you scour hard at the foot of the slope, you may be able to find a few small (in situ to very slightly displaced) pieces of the top, anorthositic contact of the sill (MGA 585209E 6989390N), which show faint layering and scattered centimetre-long pyroxene needles (Fig. 37b).

The sill has an intrusive contact with strongly foliated, very fine grained, grey (yellow-weathering) metasedimentary rocks (shale) at the uppermost part of the Polelle Group in the low valley to the west.

Walk west across this small valley and up the low slope of the flanking hill to the west. As you proceed upslope, you will pass through some low outcrops of well-bedded sandstone (1–5 cm-scale beds), including graded bedding (MGA 584935E 6989480N and MGA 584924E 6989478N). Farther uphill, is the basal unit of komatiitic basalt of the unconformably overlying Glen Group, the contact of which we will see in better detail at Locality **2.13**. Here, it appears that the Glen Group komatiitic basalts are deposited across a low-angle unconformity that is marked by a thin unit of poorly exposed, baked sedimentary conglomerate (go to MGA 584842E 6989364N). Note that bedding in the underlying metasedimentary rocks is overturned along 020°/77° (i.e. dipping east, but facing west), whereas bedding in the overlying basalts is vertical along a variable strike between 000–011°. The contact zone contains the following rock types along strike for 60 m to the south: coarse-grained quartz fragments lined with Fe-oxides (most common in outcrop); local grit and sandstone; locally silicified sandstone; leucocratic, hybridized pyroxene spinifex-textured komatiitic basalt containing fragments of quartz-rich, very finely laminated sedimentary rock; pyroxene spinifex-textured basalt with backveins of quartz and remobilized sandstone. The

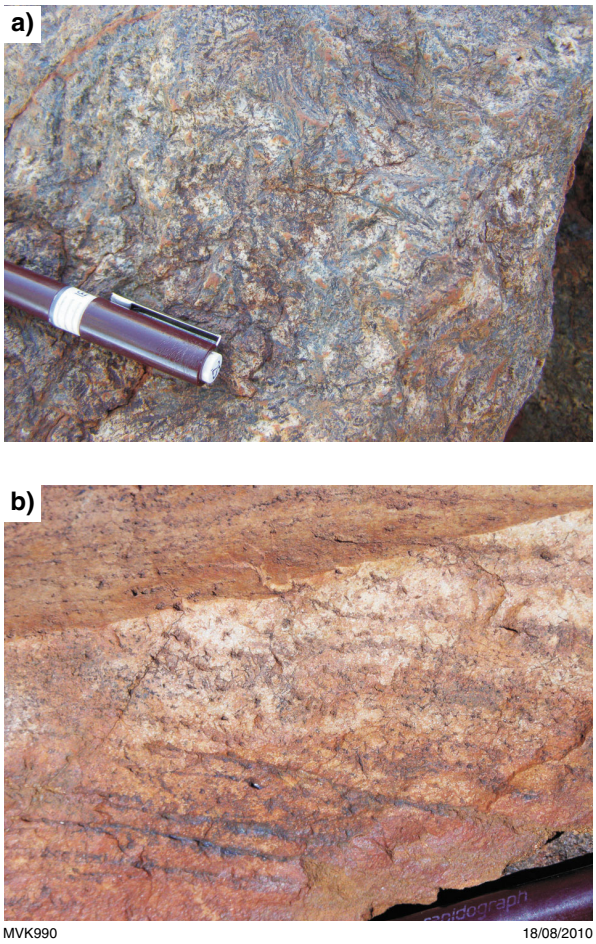


**Figure 37. Outcrop features of a Yalgowra Suite differentiated mafic–ultramafic sill at locality 2.9: a) feathery, long pyroxene phenocrysts in leucogabbro near the top of a of the Yalgowra Suite; b) fine pyroxene needles in the anorthositic top of the sill**

leucocratic, hybridized komatiitic basalt has sharp contacts with the partly melted and recrystallized metasedimentary rock (Fig. 38a,b), but retains well-developed pyroxene-spinifex texture, despite widespread growth of epidote and white mica (Fig. 38c). The recrystallized metasedimentary rock contains abundant, coarse euhedral epidote and white mica and quartz that, together with similar assemblages in the basalt, indicate high volumes of fluid alteration resulting in the complete disintegration of feldspars, loss of sodium, and calcium metasomatism (Fig. 38d). This is interpreted to have occurred during the eruption of lavas onto a wet-sediment substrate.

## Locality 2.10: Coodardy Formation quartzite (basal Polelle Group) and intrusive granite sheets

*Return to the sealed Cue–Weld Range road and turn right. Proceed for 9.42 km to where the old rabbit-proof fence crosses the road, and turn left onto a small drive (at MGA 573640E 6989200N). Park the vehicles and walk up through both gates onto the rocky outcrops.*

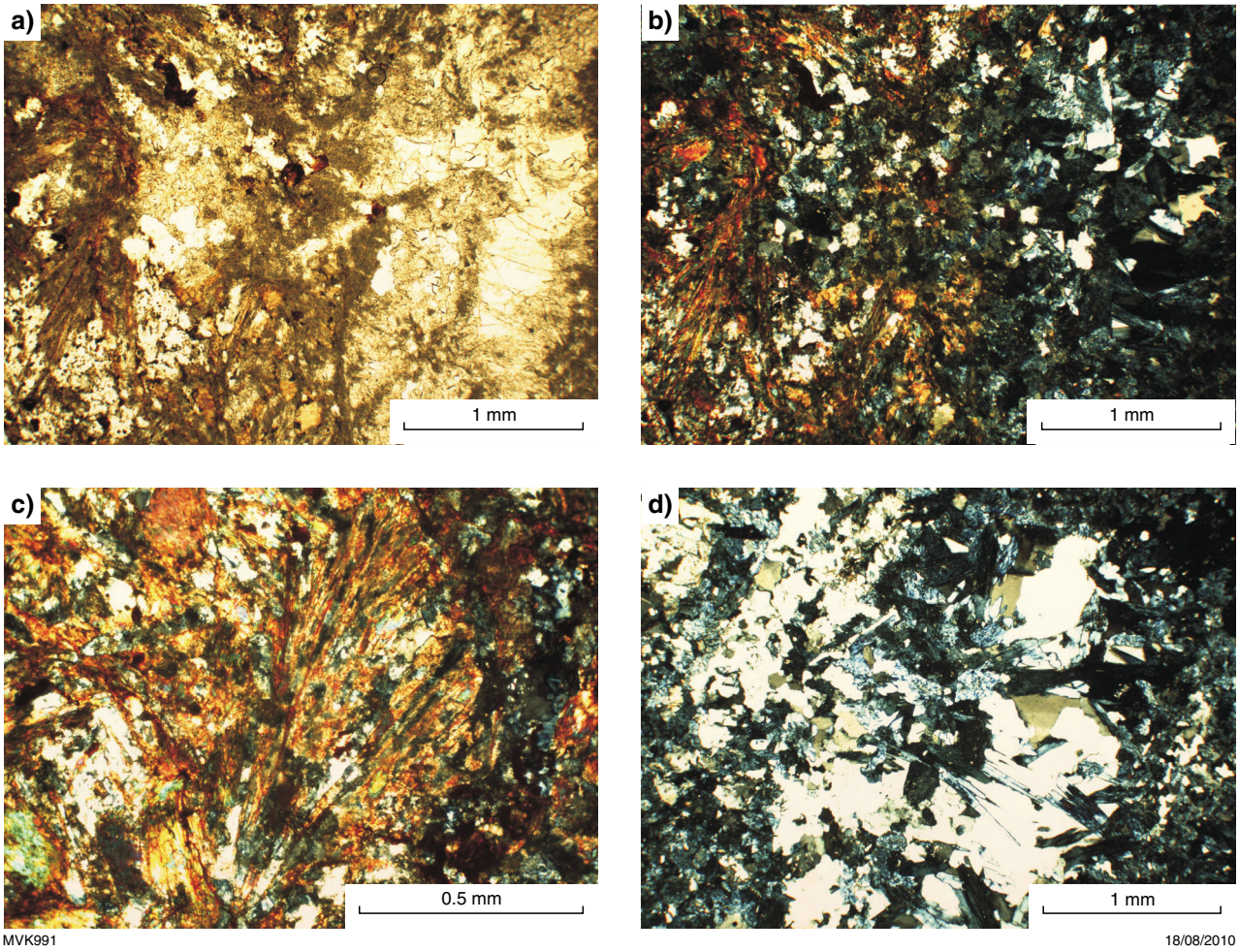


**Figure 38. Thin section features along a komatiitic basalt – wet sediment interface at locality 2.9: a) and b) plane- and cross-polarized light photomicrograph pair, showing contact (diagonal, from upper right to middle bottom) between leucocratic pyroxene spinifex-textured basalt (left) and metasedimentary rocks (right) characterized by white mica–epidote alteration; c) cross-polarized light photomicrograph, showing detail of contaminated pyroxene spinifex-textured metabasalt, showing fine pyroxene needles (altered to very fine grained brown material) intergrown with abundant quartz (white and grey) and white mica (green, blue, and yellow); d) cross-polarized light photomicrograph of coarsely recrystallized metasedimentary rock, with abundant epidote (light blue)**

From the roadside to the outcrops inside the two gates, you will notice a mixture of quartzite and foliated muscovite (and/or biotite) metagranite. Quartzite is an unusual lithology in Archean rocks and thus is always worth a closer look, as it may indicate the presence of a prolonged period of weathering and sediment recycling, and thus possibly an unconformity. Quartzite in the Cue region is associated with an overlying unit of banded iron-formation and together these are referred to as the Coodardy Formation at the base of the Polelle Group.

At this locality, the contact of the quartzite with underlying greenstones is not preserved, and the relationship of the quartzite to the granite is an intrusive one (Fig. 39). As you walk around these outcrops, you will see thin slivers and larger blocks of quartzite interlayered with strongly foliated and lineated metagranite. Lineations are parallel to fold axes and plunge gently to the north, the result of the late east–west compressional deformation across the Murchison Domain at c. 2660 to 2640 Ma. The best locality to observe a convincing intrusive relationship of the granites in the quartzite is at MGA 573582E 6989182N, but there are many other localities (MGA 573528E 6989205N; MGA 573525E 6989200N; MGA 573537E 6989171N).

## Locality 2.11: Glen Group komatiitic basalt, with north–south foliation

*Return onto the sealed road, turn left, proceed north for 17.4 km and turn left onto the Kalli road (MGA 566903E 7003495N). Follow the Kalli road west for 15.5 km to a minor track on your right (MGA 551900E 7006180N). Turn right and follow the track north for 3.9 km to MGA 552720E 7009869N). Walk 25 m to a low brown outcrop (at MGA 552693E 7009904N).*

MVK992 08/09/2010

**Figure 39. Outcrop photograph showing contact relationship between intrusive, foliated muscovite-bearing metagranite and a thin peel (xenolith) of quartzite belonging to the Coodardy Formation (basal Polelle Group)**

Komatiitic basalt of the Glen Group (Wattagee Formation) at this locality lies within the hinge of a tight easterly trending, steeply plunging fold (Fig. 40). These lower greenschist-facies rocks display a moderately well-developed foliation oriented at 000°/75°, subparallel to bedding as defined by regional aeromagnetic patterns and local way-up structures defined by pillows. The foliation at this outcrop shows that folding was not a result of normal buckling. The significance of this at a larger scale will be discussed at the next locality.

## Locality 2.12: Bedding and cleavage relationships in the Ryansville Formation

*Continue north along the track for 300 m, just past a right-hand bend ,and turn left onto a small track (MGA 552827E 7010134N). Follow the track northwest for about 500 m (to MGA 552487E 7010479N), then head right for about 100 m and turn left before the costean (MGA 552654E 7010520N). Head north through the bush, following open country for about 700 m and proceed up onto a low, brown, sloping hill of laterite. Pass over this low rise and down over the north side to a low, open plain. Park the vehicle on the flats (at MGA 552470E 7011513N) and walk to a small, low outcrop (at MGA 552362E 7011478N).*

This outcrop, and others nearby (e.g. at MGA 552381E 7011473N and MGA 552540E 7011463N) of the lower Ryansville Formation of the Glen Group show an anticlockwise angular relationship between bedding ($S_0$ = 053°/80°) and a spaced fracture cleavage ($S_1$ = 040°/90°) (Fig. 41). The orientation of the cleavage is unexpected at this locality, given its position on the northern limb of a tight regional east-trending fold (Fig. 40). As with the last locality, the cleavage is not axial planar to this tight fold and, furthermore, is at an angle to bedding in the *opposite direction* (anticlockwise) to that anticipated (clockwise) for cleavage refraction of an axial planar fabric developed during buckling.

These structural relationships suggest that the tight east-trending fold in this area formed through an unusual style of folding, possibly related to greenstone sinking into

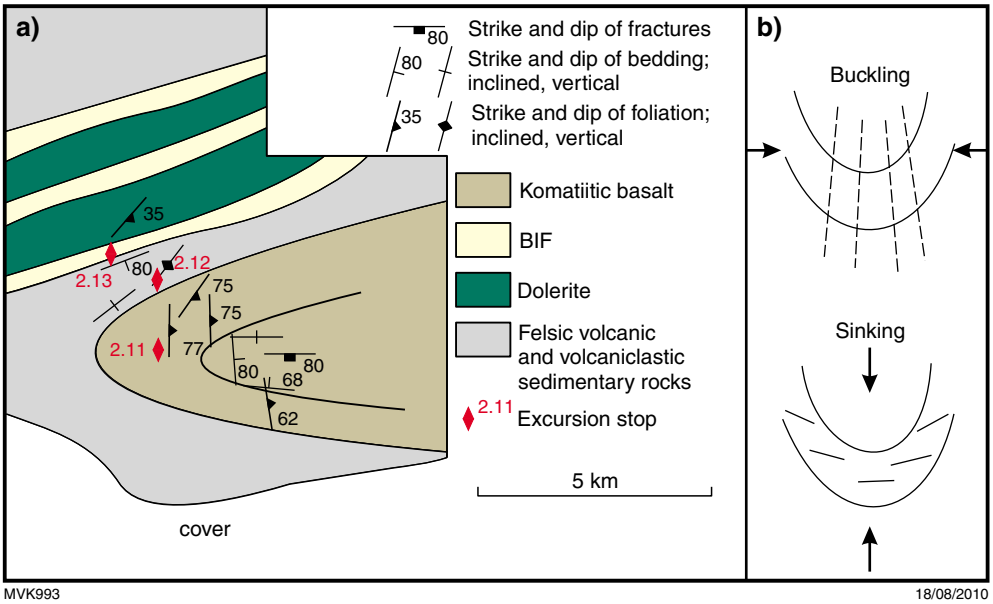


MVK993 18/08/2010

**Figure 40. Details of the tight easterly trending fold visited at localities 2.11 and 2.12: a) simplified geological map of the fold, showing bedding–cleavage relationships and location of excursion localities; b) schematic development of contrasting fold styles and associated cleavage through buckling (upper) and greenstone sinking (lower). Arrows represent orientation of maximum compressive stress**

MVK994 09/08/2010

**Figure 41. Outcrop photograph, looking north, showing relationship between irregular, spaced fracture cleavage striking 050° and easterly striking bedding at excursion locality 2.12**

partially molten granitic middle crust at c. 2675 Ma. In this model, a subhorizontal foliation is developed in the greenstones as they commence downward flexure into partially molten granites, as a result of vertical stress associated with sinking (Fig. 40, lower panel of part b). Subsequent re-orientation of the greenstones during progressive folding and asymmetrical sinking resulted in the preservation of the structures.

# Locality 2.13: Unconformity between the Glen and Polelle groups

*Proceed west-southwest along a track for about 400 m to MGA 552021E 7011419N. Here, the track heads north, but ignore this and continue straight ahead (west-southwest) along the fainter track for about 600 m (to MGA 551831E 7011419N) and turn right onto a weakly preserved track heading towards 030° and then to the north, passing an outcrop on the left (at MGA 551778E 7011779N). Continue on the track for about 50 m and turn left (west), past a marked tree, and head towards 240° for about 100 m to MGA 551603E 7011761N.*

This ridge of small outcrops (Fig. 40) straddles the angular unconformity between a lower package of irregularly folded jaspilitic cherts of the c. 2790–2740 Ma Polelle Group (Wilgie Mia Formation) and weakly strained dolerite–gabbro of the c. 2745 Ma Gnanagooragoo Igneous Complex, and an upper package of dominantly coarse clastic sedimentary rocks of the c. 2735–2710 Ma Glen Group (Ryansville Formation; Fig. 42). The unconformity was recognized first from outcrop relationships (see point **2.13.5** below) and subsequently from the differential strain state of the rocks (folded and tilted Polelle Group versus only tilted Glen Group; Fig. 43).

## Locality 2.13.1

*Walk about 10 m due south to a low outcrop (at MGA 551606E 7011741N).*

This locality preserves a low outcrop of layered red (jaspilitic) and white chert at the top of the Wilgie Mia Formation (Polelle Group). Bedding in this unit trends at 252°/73°. Note the low rubbly outcrops about 10 m due south, which are of the basal conglomerate of the unconformably overlying Glen Group (Ryansville Formation).

## Locality 2.13.2

*Walk about 12 m towards 110°, east-southeast (to MGA 551619E 7011730N).*

This low outcrop of dolerite is representative of the subsurface lithology since the last locality, and onward to the next locality. The dolerite is the upper part of the Gnanagooragoo Igneous Complex, which splits apart the Wilgie Mia Formation in the Weld Range for more than 70 km along strike. This large, layered igneous complex includes a lower, funnel-shaped basal part lying to the northeast of the Weld Range, which is composed of layered peridotite and peridotite with PGE, gold, nickel, and cobalt mineralization (Fig. 21).

## Locality 2.13.3

*Walk towards 074° (east-northeast) for about 35 m (to MGA 551655E 7011736N).*

This small outcrop of boulder conglomerate (Fig. 44a) represents the lowest unit of the unconformably overlying Glen Group (Ryansville Formation).

Note the low percent of matrix in the conglomerate and the presence of jaspilitic chert cobbles (i.e. at the base of the dead tree). Note also that the layered jaspilitic chert unit just to the north of this locality is now much closer to this basal conglomerate than at locality **2.13.1** (Fig. 42).

## Locality 2.13.4

*Walk about 35 m east-northeast from locality 2.13.4 (to MGA 551690N 7011759E).*

This outcrop (as well as outcrops along strike to the east) of the layered jaspilitic chert shows contorted bedding resulting from either soft-sediment deformation or from the effects of heat and emplacement of the dolerite of the Gnanagooragoo Igneous Complex (Fig. 44b). These highly non-cylindrical folds plunge moderately to steeply across the southern hemisphere of a stereonet plot (Fig. 43), indicating they are probably not part of a regional post-depositional deformation event as the rocks themselves are planar-bedded over long distances in this area. Regardless of their specific origin, the folds are absent from unconformably overlying clastic sedimentary rocks of the Ryansville Formation (Glen Group) and thus indicate a period of deformation unique to the older rocks, as well as a hiatus between the deposition of these two groups of rocks.

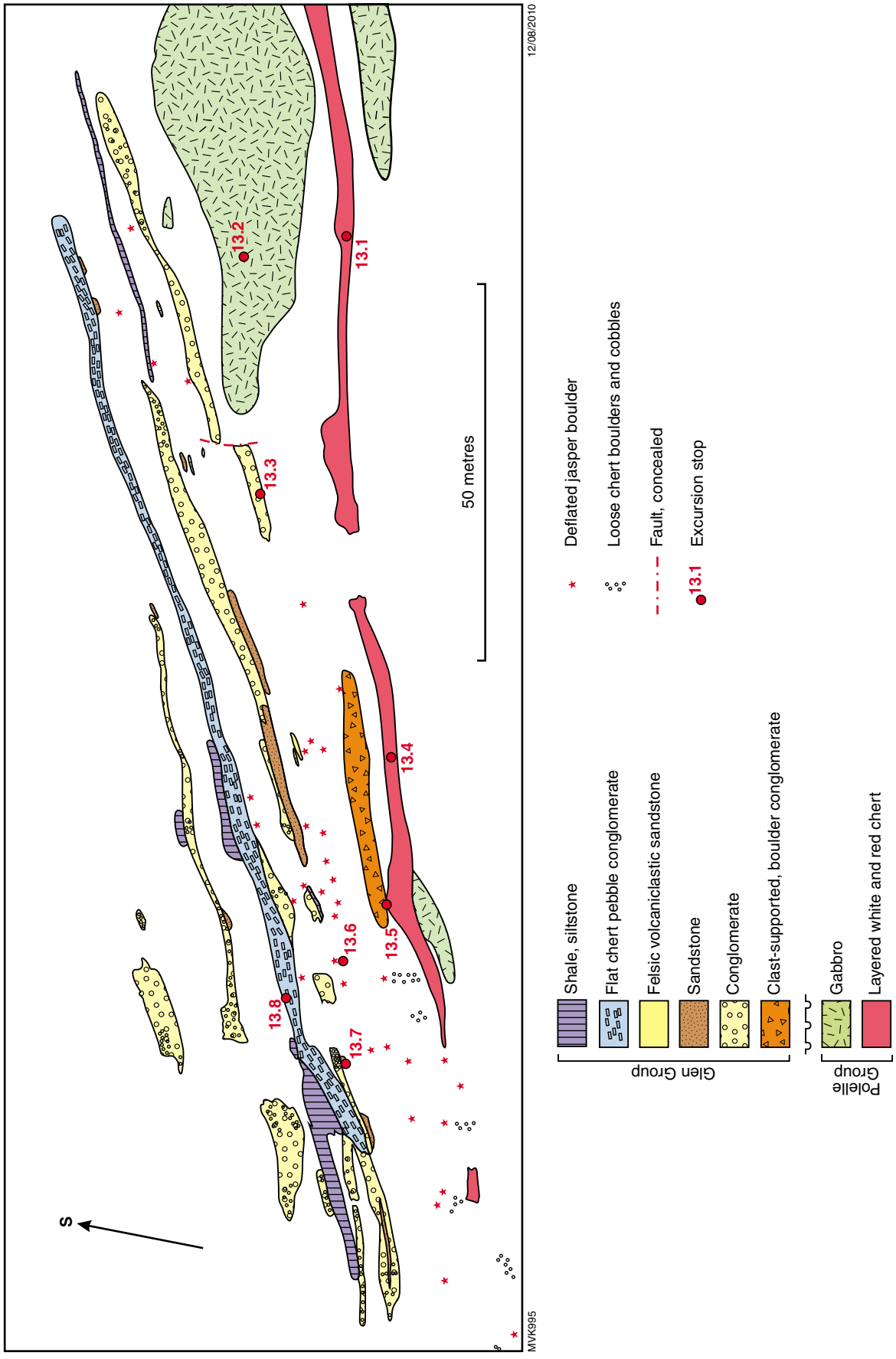


**Figure 42. Simplified geological map of the unconformity at the base of the Glen Group, as exposed at locality 2.13. Note the difference in angle between bedding in the Glen and Polelle Groups. Specific excursion stops for locality 2.13 are indicated as 13.1–13.8. Note that the orientation of the diagram is with top to the south**

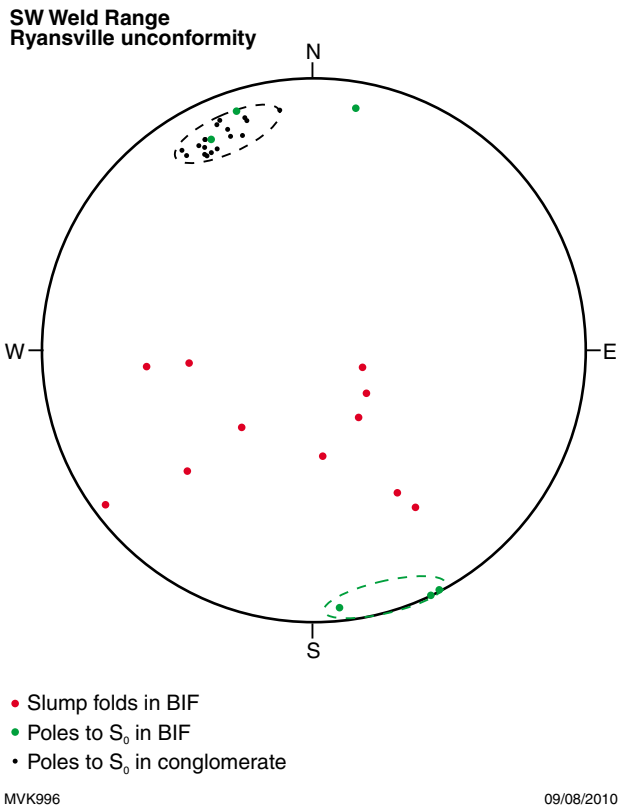


**Figure 43. Equal area stereonet plot of structures measured at the unconformity at locality 2.13, including poles to bedding and the axes of slump folds in Polelle Group banded cherts**

## Locality 2.13.5

*Walk about 15 m along strike to the east-northeast (075°) to MGA 551705E 7011760N.*

A small (30-cm wide), low outcrop 30 cm north of the rock cairn preserves the unconformity between the overlying basal conglomerate of the Glen Group (Ryansville Formation) and the underlying layered chert of the Polelle Group (Wilgie Mia Formation; Fig. 44c). Outcrops along strike show boulders of isoclinally folded jaspilitic chert within the conglomerate (Fig. 44d), confirming the existence of a pre-Glen Group folding episode.

## Locality 2.13.6

*Walk about 9 m southeast (to MGA 551714E 7011757N).*

Here, you see one example of a train of deflated, but largely in situ, jasper boulders that are aligned parallel to the strike of other units within the Ryansville Formation (Figs 42, 45a). These form part of an otherwise unexposed boulder conglomerate unit. Note that the textures of these boulders differ from the underlying layered jaspilitic unit of the Wilgie Mia Formation and must originate from an eroded unit not exposed at this locality.

## Locality 2.13.7

*Walk about 20 m east (to MGA 551735E 7011759N).*

Continuing upsection within the Ryansville Formation, this outcrop shows well-preserved cross-bedding within a sandstone to pebbly conglomerate unit (Fig. 45b), indicating the right way up (although steeply dipping) orientation of the Ryansville Formation (bedding at 067°/72°). This unit probably represents deposition under fluvial conditions.

## Locality 2.13.8

*Walk about 40 m west-southwest (to MGA 551698E 7011740N).*

This distinctive unit of tabular chert-pebble conglomerate is characterized by well-sorted, angular to subrounded, tabular clasts of dominantly blue-grey laminated chert (Fig. 45c). However, a few layered jaspilitic chert clasts that locally show zoning from red cores grading out to blue-grey edges indicate some sort of in situ, post-depositional alteration (Fig. 45d). The flat-pebble nature of the conglomerates suggests deposition on a low-angle talus slope under arid conditions — conditions quite similar to the present day. However, the alteration of jasper to blue-grey material suggests the effects of reducing fluids and, given the subaerial nature of the deposition of the pebbles, may be used to support a reducing late Archean atmosphere. An unusual feature of the rock in thin section is the presence of abundant stylolites along the margins of laminated clasts (Fig. 46). Stylolites are common in carbonate rocks, but not so in siliceous rocks, suggesting that the clasts were originally carbonates that have been extensively silicified. If this is the case, then the jaspilitic colouring may be due to alteration of siderite or ankerite, as found for similar-looking jaspilitic cherts in the Pilbara Craton (e.g. Van Kranendonk et al., 2008). What might this infer for the origin of banded iron-formations? Comments, ideas welcome …

# Locality 2.14: Dated Coodardy granites

*Turn around and follow route out to the east for about 200 m to a small track heading south (at MGA 551753E 7011807N). Turn right onto this track, heading south for about 200 m and then continue south-southeast for another 200 m. At this point (MGA 551819E 7011394N), follow the track south-southeast (straight ahead) along the side of a small gully on your left, until you reach a low, yellow-weathering mesa (about 1.6 km, at MGA 552373E 7010470N) and swing left across the creek, heading east to join a small track. Turn right onto this track (at MGA 552488E 7010477N) and head south for a short distance until you reach another track and once more turn right (at MGA 552838E 7010137N). Head south and take this track back out to the Kalli road (about 4.2 km) and turn left, heading east. Continue for 15.5 km to the sealed road to Cue and turn right. Head south for 7.4 km. Just past the Afghan Rock turnoff on your left, take the dirt road to the right (at MGA 571458E 6997895N), heading south. Continue south for 12.6 km and turn right off the track (at MGA 566306E 6987178N). Head northwest for 200 m and park at the fence (at MGA 566179E 6987402N). Cross*

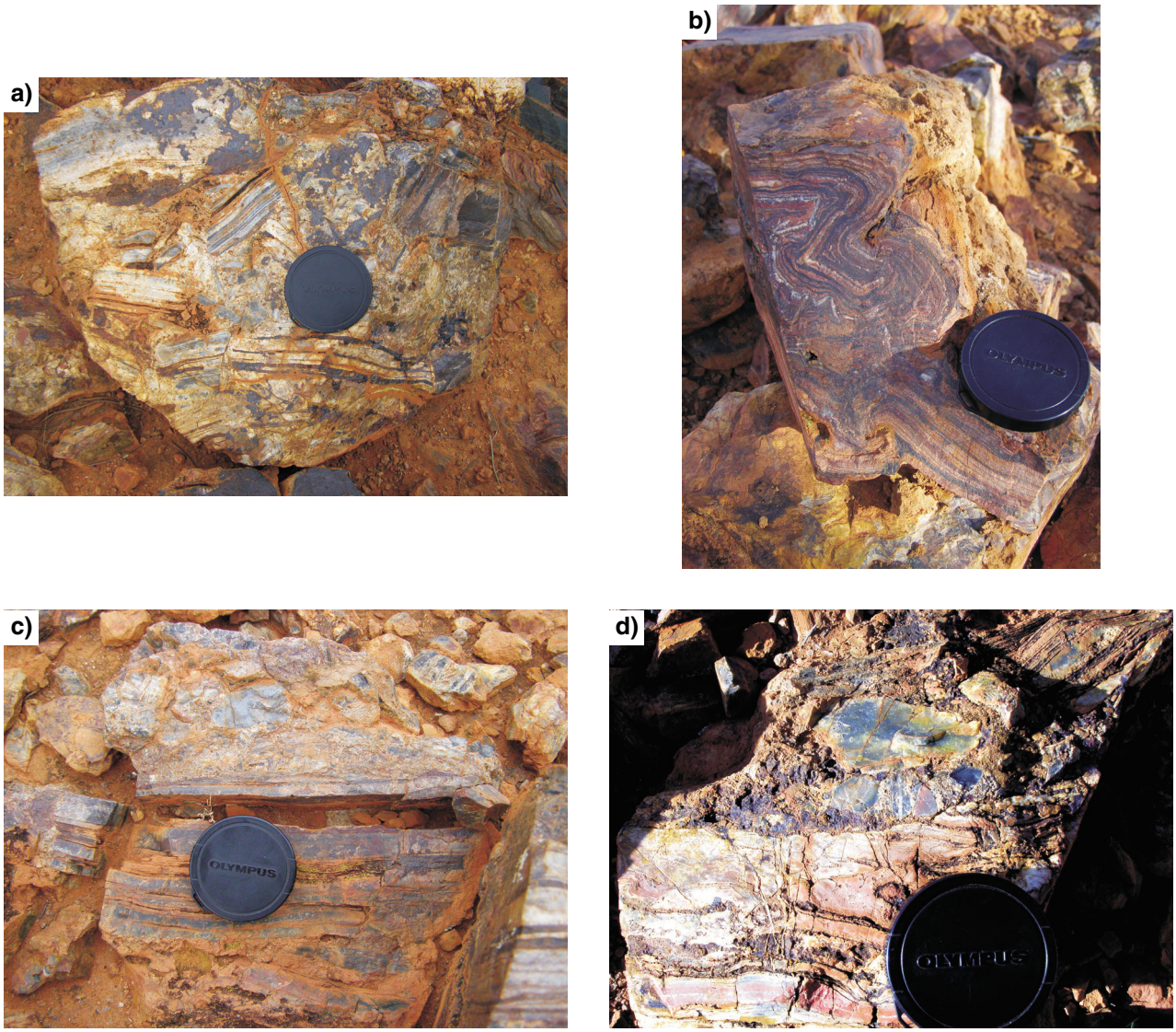


**Figure 44. Outcrop photographs of the unconformity at locality 2.13: a) angular cobble conglomerate of the basal Glen Group (locality 2.13.3); b) contorted bedding in layered jaspilitic chert of the Wilgie Mia Formation, topmost Polelle Group (locality 2.13.4); c) outcrop of the unconformity between conglomerate of the overlying Glen Group and layered chert of the Polelle Group at locality 13.5; d) another view of the unconformity along strike to the east of locality 2.13.5, showing contorted bedding in Polelle Group cherts that is absent from overlying Glen Group conglomerates**

*the fence and walk 200 m northwest to a fresh blast site in a low, prominent outcrop of granite (at MGA 566026E 6987540N).*

This outcrop of strongly foliated tonalitic orthogneiss consists of a mafic clotty-textured tonalitic precursor (mafic clots are now just very thin lenses), dated at 2744 ± 4 Ma, and several centimetre- to decimentre-thick veins of pegmatitic granite, dated at 2678 ± 6 Ma. The rocks have been affected by a strong foliation along 206°/75°, with weak, subhorizontal mineral elongation lineations. Dextral shear-sense indicators on horizontal outcrop surfaces include rotated feldspar porphyroclasts in the tonalitic gneiss, S–C–C' relationships in the gneiss, and S–C and well-developed C' extensional shear bands in the pegmatites (Fig. 47a,b).

An interesting feature of this outcrop is that some of the pegmatites are zoned and contain abundant garnet in the central portions, with garnet-free, medium-grained, equigranular granitic rinds that show no, or very little, strain compared with the main part of the pegmatite veins and the host (Fig. 47c,d). Indeed, these marginal phases — particularly well developed in the 10 cm-thick vein at MGA 566023E 6987541N — may represent a late component of melt that crystallized along the margins of the more strongly deformed pegmatite veins during the latest episode of strain in this rock.

The pegmatite veins are clearly derived through injection from a melt source lower in the crust, but represent the onset of widespread crustal melting or deformation in this area, at c. 2678 Ma. Significantly, this same date has also been obtained from a series of plutons emplaced

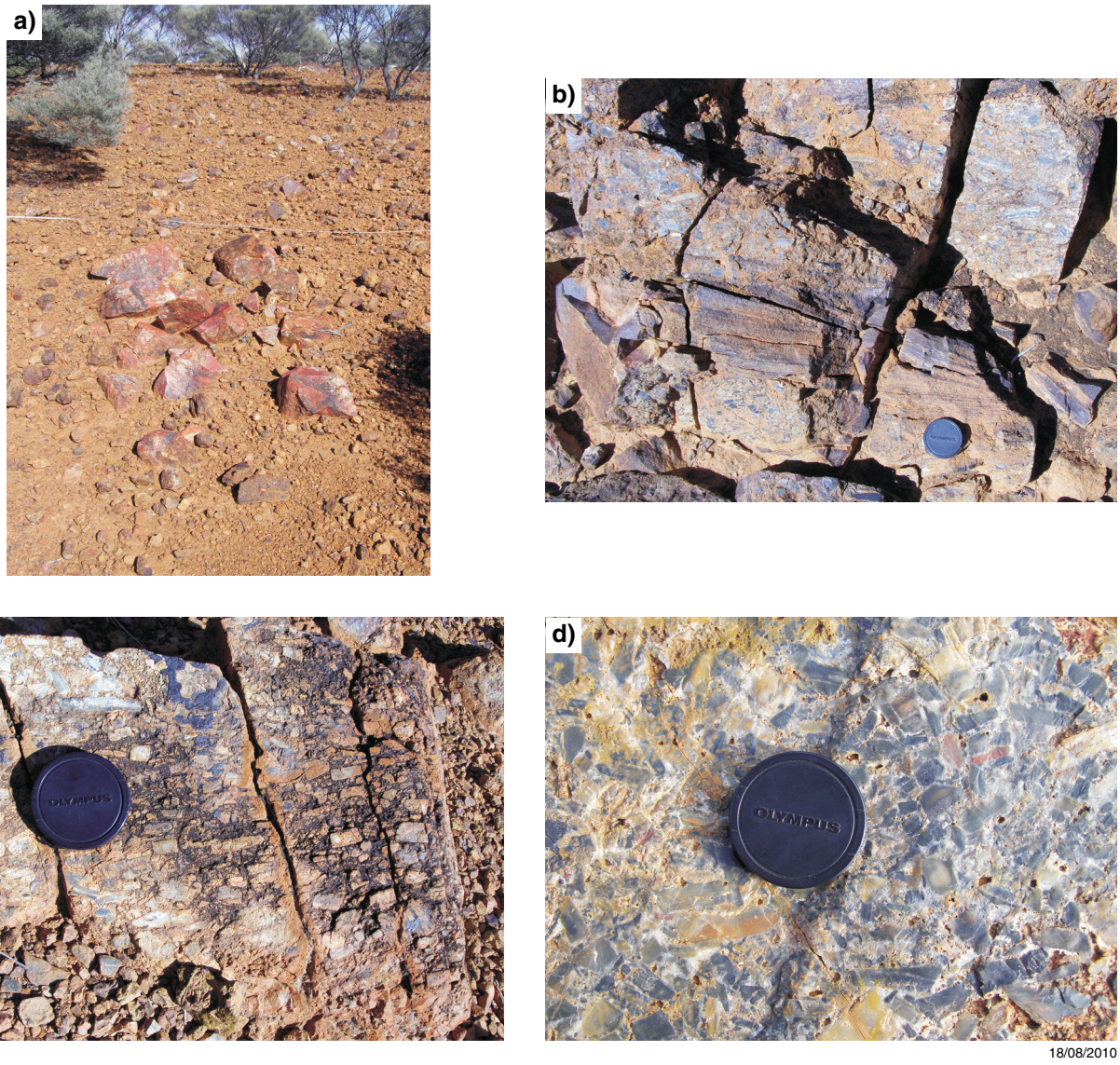


MVK998 18/08/2010

**Figure 45.** **(above) Outcrop photographs of the Glen Group at locality 2.13: a) view looking west-southwest, of deflated boulder of jaspilitic chert (locality 2.13.6); b) outcrop view, looking down, at cross-bedding in sandstone and conglomerate, suggestive of fluvial deposition (locality 2.13.7); c) outcrop view, looking down, of flat-pebble chert conglomerate (locality 2.13.8); d) close-up view of flat-pebble chert conglomerate, showing faint jasper cores of some clasts**

MVK999 09/08/2010

**Figure 46.** **(left) Whole thin section view (plane light) of flat-pebble chert conglomerate of the Glen Group from locality 2.13, showing common stylolitic contacts around chert pebbles**

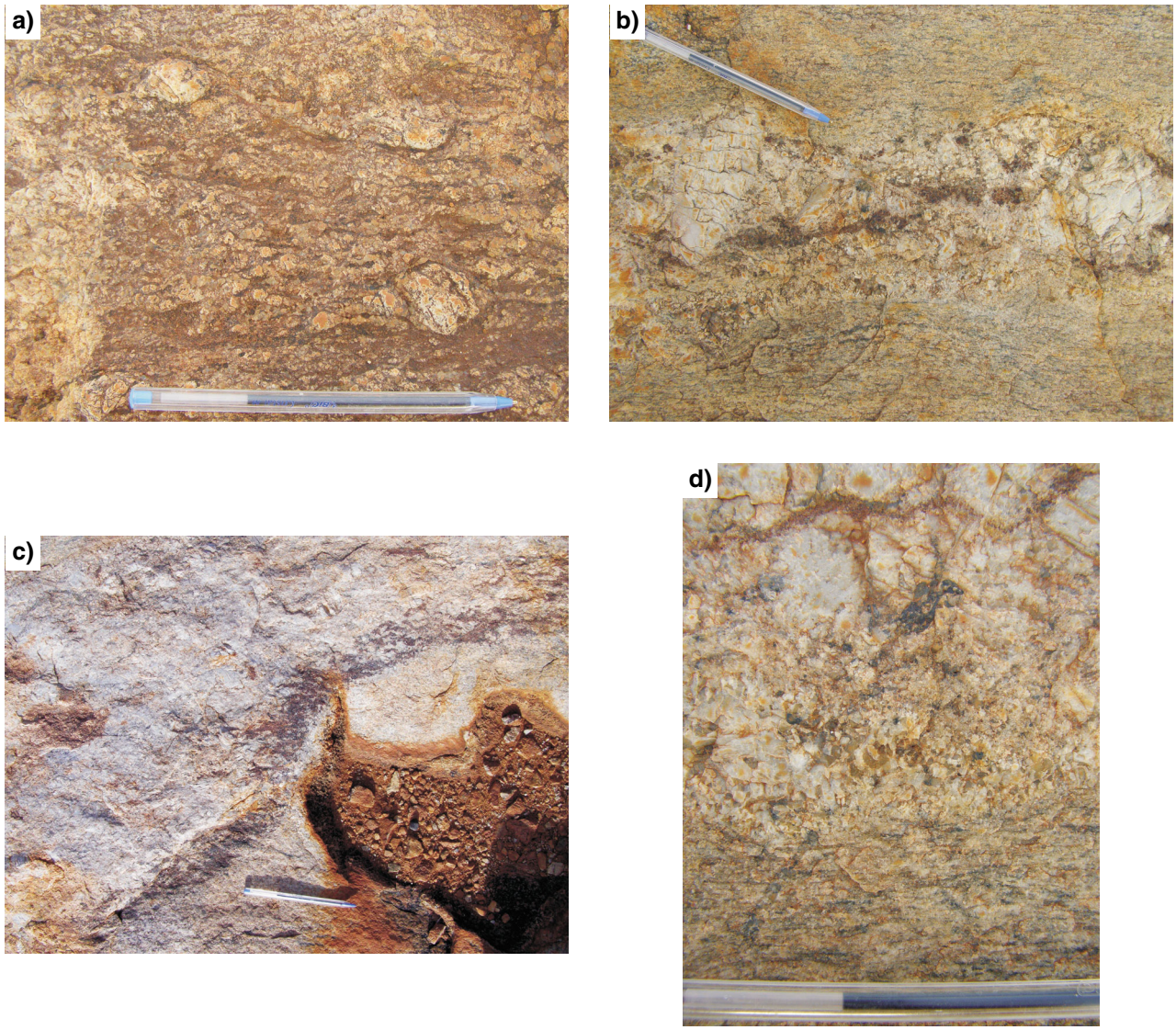


**Figure 47. Strain and shear-sense indicators in Coodardy granites and associated pegmatites at locality 2.14: a) dextral C (parallel to pen)–S–C' fabric with well-developed extensional shear bands in strongly foliated porphyritic metamonzogranite; b) sheared garnet-bearing pegmatite, transected by dextral extensional shear band (parallel to pen); c) close-up view, looking down, of garnet-rich margin of pegmatite, showing strong foliation defined by aligned garnets (parallel to pen); d) close-up view, looking down, of the undeformed margin of a strongly foliated pegmatite, suggesting syn-kinematic emplacement of the pegmatite**

within greenstones located structurally higher in the crust, indicating the presence here of a melt transfer zone from a deeper source to more shallow plutons emplaced into greenstones.

## Locality 2.15: Big Bell: sheared mafic volcanic rock

*Return to road and proceed 2.5 km southwest to Coodardy Homestead and turn left, following the sign towards Big Bell. After 1.4 km, turn right, heading southwest and then south. Follow the main road as it swings left and stop at the top of a small rise, after a total distance of 5.6 km (MGA 565327E 6979686N).*

The outcrops on either side of the road here represent strongly sheared and metamorphosed tholeiitic pillow basalts (actinolite–epidote–chlorite). The shearing has produced a strong schistosity on 024°/72°, and metamorphic mineral elongation lineation of 63°→082°. Note the presence of thin, boudinaged quartz veins on the outcrop facing the road.

The strongly deformed rocks here are part of one of the largest shear zones in the Murchison Domain, which extends along strike to the northeast for more than 100 km, past the eastern margin of the Weld Range. The zone continues along strike to the southwest for about 10 km, but is cut out by post-tectonic granites farther to the south.

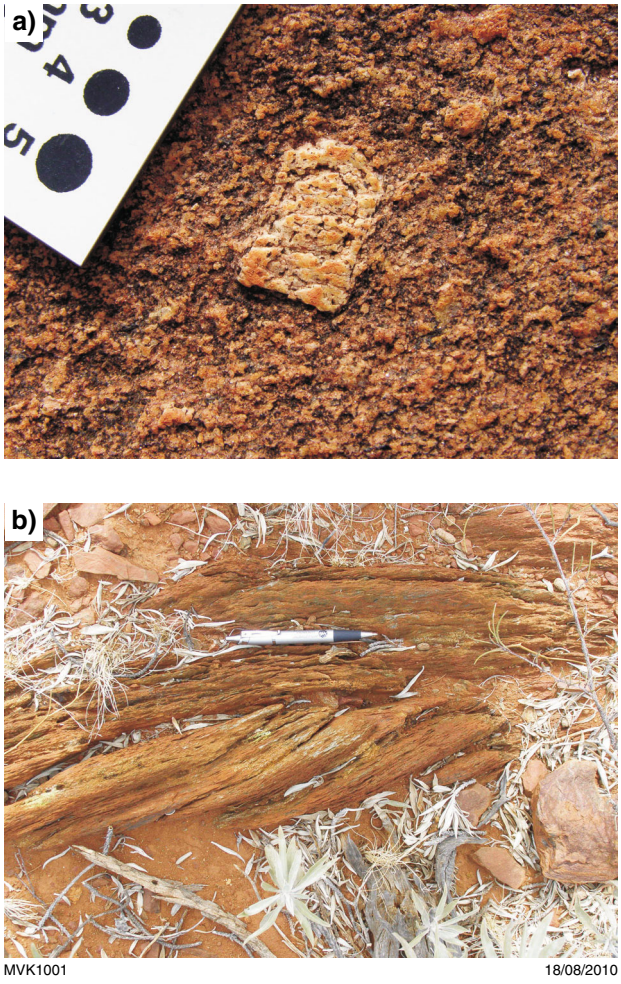


**Figure 48. Dextral shear-sense indicators of late shear deformation: a) rotated K-feldspar porphyroclast in weakly foliated metamonzogranite; b) S–C (parallel to pen) fabric in mafic metavolcanic schists**

For most of its strike length to the north, the shear zone is characterized by lineations plunging shallow to moderately to the northeast and southwest, and by foliations that show abundant evidence of dextral shear (e.g. Fig. 48). However, this part of the shear zone is unique, in that it is characterized by steep metamorphic mineral elongation lineations and high metamorphic grade (lower amphibolite facies), with no obvious kinematic asymmetry.

## Locality 2.16: Big Bell sheared granite–greenstone contact

*Continue along the track for 500 m and turn left. Follow main road for about 10 km, keeping the tailings piles on your right. Turn right onto a 'No access' track and head west, turning left after a short way into a small quarry with a well-exposed cut rock surface (MGA 564538 6976161N).*

This very nice little exposure shows the strongly sheared and faulted contact between greenstones to the west and granitic rocks to the east, including a very wide white quartz vein (8 m) in the middle that displays evidence for several episodes of crack-seal emplacement (Fig. 49). At the far eastern (left-hand) side of the rock face are strongly foliated granitic rocks, dated nearby at 2702 ± 6 Ma (Mueller et al., 1996). These lie in fault contact with a sliver of greenschist-facies mafic schist and quartz-phyric felsic schist, both of which are in fault contact with the wide quartz vein. The western side of the quartz vein is in fault contact with a tight fold within felsic schist. Tension gashes in the fault zone are filled by minor grey quartz veins that indicate a west-side-down sense of displacement. The folded felsic schist contains an axial planar quartz vein and is in fault contact with mafic schist farther west.

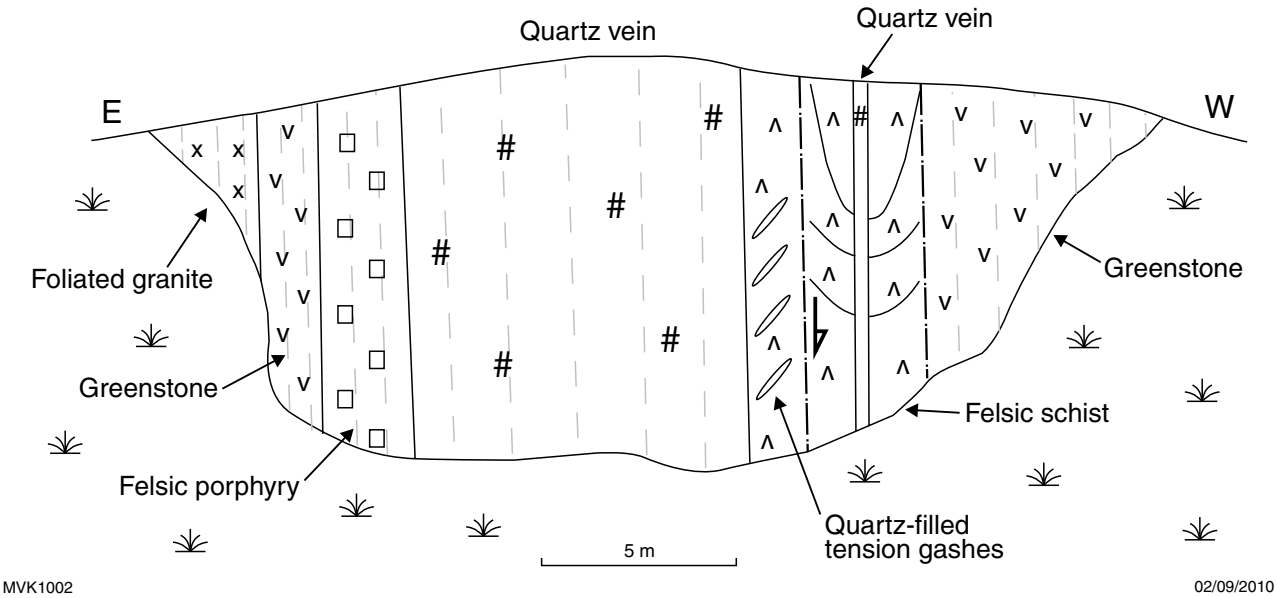


**Figure 49. Sketch, looking south, of the rock face at locality 2.16, showing the features associated with a strongly sheared granite–greenstone contact**

## Locality 2.17: Big Bell quartz porphyry and mine pit

*Continue about 500 m north along road to a rock barrier. Walk over the barrier to the first outcrops on the right of the track.*

Just behind you, near the barrier, are low outcrops of dark-brown-weathering mafic schist, the same as seen at Locality **2.15**. From this point to the mine itself, the rocks consist of strongly foliated quartz-phyric felsic rocks with 2 to 4 mm quartz phenocrysts. Mueller et al. (1996) obtained a date of 2737 ± 4 Ma from this unit, which falls in the younger range of ages for the Polelle Group and Annean Supersuite.

Within the mine, strongly sheared metabasaltic rocks are now represented by strongly foliated and lineated hornblende–epidote–plagioclase–quartz mafic schists (Fig. 50a,b). Folded quartz veins with retrograde greenschist-facies margins attest to a late increment of strain (Fig. 50c).

Gold mineralization at Big Bell forms a planar unit along the contact between strongly sheared mafic metavolcanic rocks and a felsic unit that was interpreted by Mueller et al. (1996) to represent an altered granodiorite gneiss, but which may also represent a felsic volcanic unit. A graphitic marker horizon (interflow sediment) bounds the western side of the mineralization. The timing of main gold–sulfide–scheelite mineralization is constrained by a concordant U–Pb almandine date of 2662 ± 5 Ma from a low-grade cummingtonite–hornblende zone of alteration (contact skarn of Mueller et al., 1996). Muscovite from the strongly foliated felsic unit yielded an Ar–Ar plateau date of 2639 ± 16 Ma, close in age to that of the post-tectonic granite (2627 ± 8 Ma) that forms part of the western boundary of the greenstone belt, but slightly older than the 2614 ± 2 Ma date of titanite from a scheelite and sulfide-bearing andradite–diopside replacement vein (Mueller et al., 1996).

## Locality 2.18: Walganna (Walga) Rock: post-tectonic granite and Aboriginal art

*Drive back out to the east, past the old town of Big Bell (peak activity in 1954, with 850 people and two churches). At the end of town, turn right and take the track south for about 7.5 km to a T-junction. Turn right, heading west, and continue for about 24.6 km to the sign for Walganna (Walga) Rock. Turn left into the designated parking area.*

The Aboriginal art gallery at this site is famous for its array of paintings, but particularly for one of a two-masted boat. This image, which is more than 300 km from the coast, has been quoted as evidence of early contact between Aboriginal people and Dutch sailors. However, more recently, archaeologists have noted the similarity between the ship depicted in the painting and the coastal steamer SS Xantho, which operated along the Western Australian coast in the 19th century (Bigourdan, 2006). The gallery

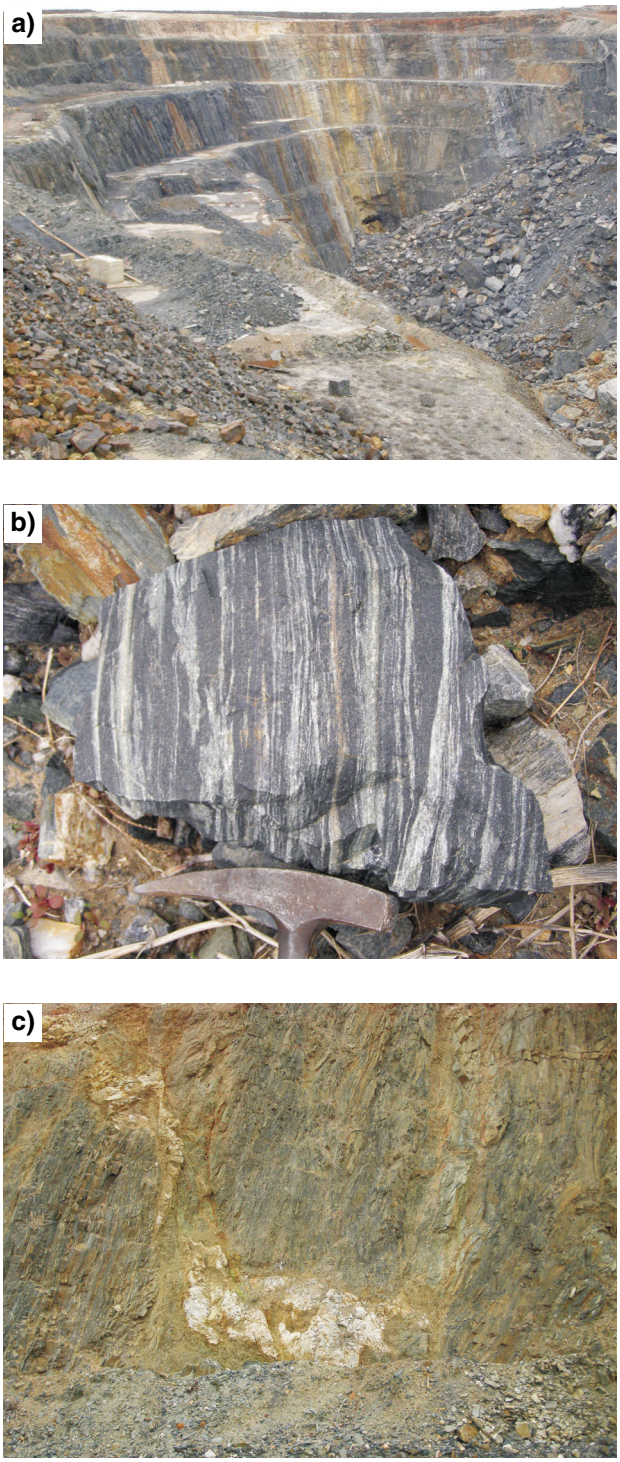


MVK1003 18/08/2010

**Figure 50. Big Bell: a) view looking northeast into the mine pit, from the northwestern side of the mine, showing the strongly sheared nature of the rocks here and the contact between mafic metavolcanic rocks and felsic schists down the centre of the mine pit wall; b) hand-sample view of strongly altered and deformed hornblende–epidote–carbonate schist derived from metabasalt, from the western pit wall of the Big Bell Mine; c) view, looking south, on a vertical surface along the western side of the pit, showing a folded late-stage quartz vein cutting across steeply dipping, mylonitic mafic schists**

site owes its preservation to the interaction between geology and weathering. The outcrop is one of many large granite whalebacks scattered throughout the whole of the Yilgarn Craton. The rock is a coarse K-feldspar porphyritic monzogranite that forms the type area for the post-tectonic Walganna Suite (2640 to 2600 Ma). Many of these granites contain well-developed igneous flow banding defined by aligned, tabular K-feldspar phenocrysts. Above the gallery, you can observe large slabs of the granite in the process of being spalled-off the main outcrop. This process reflects expansion and contraction of the surface of the outcrop under the extreme temperatures of this arid climate. The recessed lower part of this outcrop results from dominantly wind erosion of granite, altered by rainwater collected at its base. The overhang here has protected the paintings from further erosion and probably provided shelter to Aboriginal people in the past. The paintings have not been dated but there is archaeological evidence of human activity in the area dating back 10 000 years (Bindon, 1997).

# Mid-Murchison Domain

**by I Zibra**

## Introduction

The following three localities present a cross section through a sheared granite–greenstone contact. The area is located along the Great Northern Highway, some 40 km south of the town of Cue in the central Murchison Domain. This area includes a granitic body, broadly elongate north–south, bounded to the east and west by narrow greenstone belts (Figs 51, 52).

The granitic body consists mainly of medium-grained, biotite-bearing monzogranite associated with porphyritic monzogranite characterized by 2 to 5 cm K-feldspar phenocrysts. These rocks are intruded by muscovite-bearing leucocratic microgranite and pegmatitic to aplitic veins. Leucocratic veins may contain muscovite and, less commonly, garnet. Contacts between different granitic types are commonly lobate and irregular, suggesting that they could represent different magma pulses within the same granitic suite. The emplacement age of the granitic suite has been constrained at between 2650 and 2685 Ma (Schiøtte and Campbell, 1996).

This granitic suite shows several types of fabric, acquired during magmatic flow and subsequent solid-state flow at high to moderate temperatures. Magmatic features are better preserved in the southern half, and in the core of the body, away from the sheared contacts with greenstone belts. Magmatic features mainly include a northerly trending, steep pronounced foliation that is typically associated with a shallow-dipping lineation. Schlieren fabric is commonly observable in monzogranite. Local, small-scale, melt-filled shear zones suggest that magma crystallization likely occurred in a dynamic tectonic setting. Solid-state fabrics are better developed near the boundaries with greenstone belts. Here, a steep northerly trending mylonitic foliation is associated with a subhorizontal stretching lineation and displays a dextral shear sense. Metamorphic conditions, estimated by microstructural means, range from the upper amphibolite facies to the mid-greenschist facies. Higher temperature fabrics are locally preserved in the southern Wynyangoo Hill area, whereas the lower temperature fabrics dominate in the central and northern portions of the body. As a whole, the sheared granites in this region testify to the occurrence of a regional-scale, dextral strike-slip shear zone forming part of the 'Meekatharra structural zone' defined by Spaggiari (2006).

In this area, the two greenstone belts flanking the granitic suite are unrelated, suggesting that the displacement along the strike-slip shear zones is probably in the order of some tens of kilometres. In the west, the granitic suite is in contact with the Murrouli Basalt (Watkins and Hickman, 1990), which is dated at about 2820 to 2800 Ma (Van Kranendonk and Ivanic, 2009, and references therein) and mainly composed of tholeiitic and subordinate komatiitic basalts, associated with mafic to ultramafic sills. The eastern boundary of the granitic suite is marked by an association of tholeiitic and komatiitic basalts interlayered with thin mafic sills, banded iron-formation units, and mica-schist layers. The western end of this greenstone belt is marked by a distinctive unit of foliated amphibolites, likely derived from amygdaloidal basalts. As a whole, this unit could belong to the Meekatharra Formation, which has an estimated age of about 2760 to 2800 Ma (Van Kranendonk and Ivanic, 2009, and references therein).

The strike-slip event described above is not visible in the greenstone belts flanking the granitic suite. Indeed, both the eastern and the western belts show a northerly trending sub-vertical foliation associated with a mineral and stretching lineation that is vertical or steeply plunging to the north. Kinematic indicators consistently point to 'western side up' shear sense (i.e. shearing with a sinistral component on north-plunging lineations). Microstructures suggest that the main metamorphic foliation developed under mid-amphibolite facies conditions (syn-kinematic hornblende and staurolite porphyroblasts in metabasalts and mica schists, respectively).

These structural observations suggest that, in this area, greenstone belts preserve evidence of a tectonic event pre-dating the development of the 'Meekatharra structural zone', consistent with observations along strike to the north (Van Kranendonk, 2008). The older tectonic episode has distinctive kinematics and a higher metamorphic grade than the younger strike-slip event.

The two-step tectonic evolution is also confirmed by aeromagnetic data (Fig. 53) which show that, at the southern end of the eastern greenstone belt, the metamorphic foliation is bent by kilometre-scale drag folds related to dextral shearing. Also, within the western greenstone belt, an undeformed pegmatite–aplite vein cuts the metamorphic fabric in amphibolites, whereas, a few hundreds of metres to the east, the same vein is sheared along the granite–greenstone boundary. Geochronological investigation of this vein is currently in progress to better constrain the age of the two shearing events.

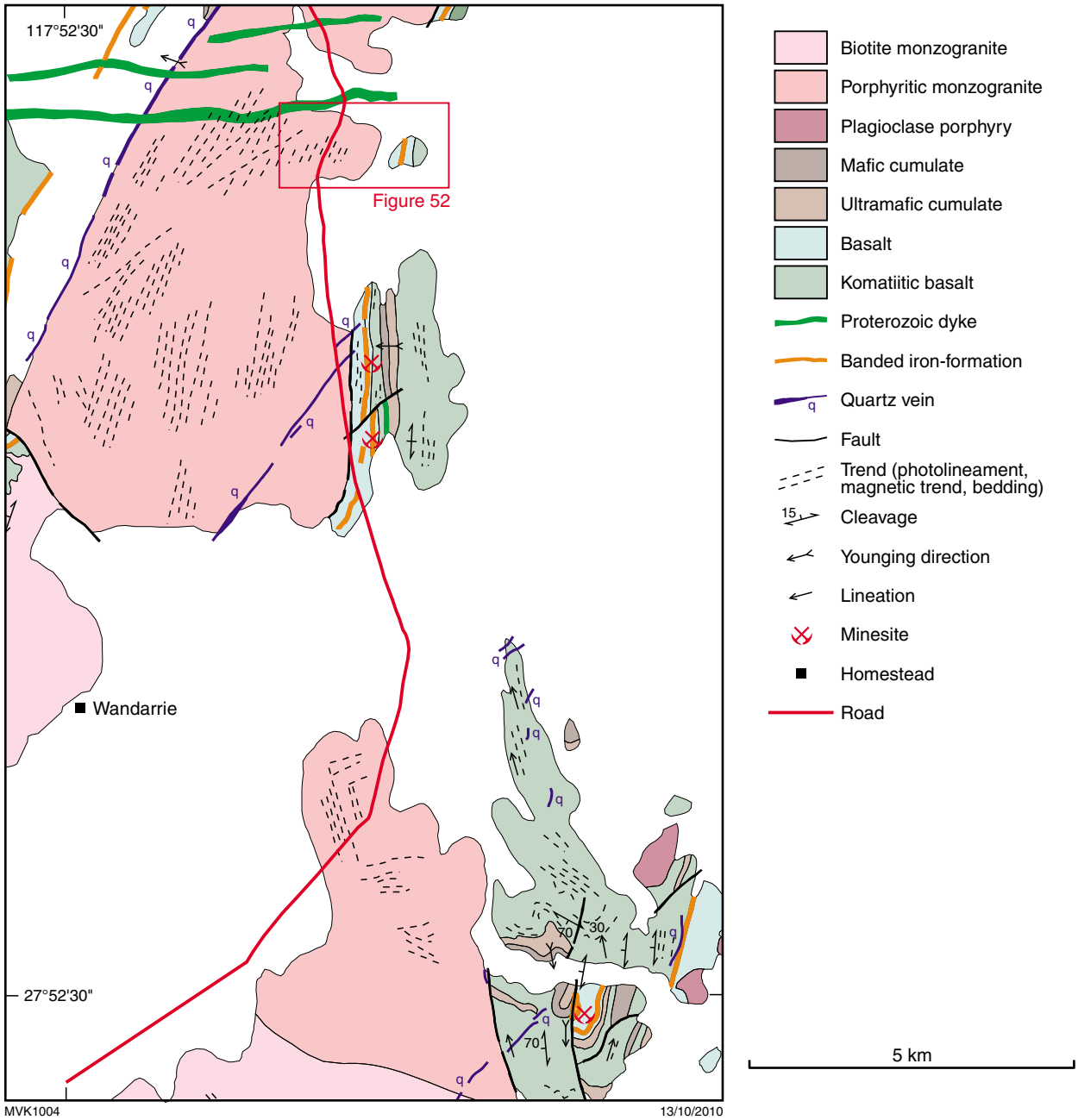


**Figure 51. Map (modified after Hallberg, 1993) showing the geology in the vicinity of this locality. The area is characterized by a granitic suite (pink on the map) flanked by greenstone belts (green). The red rectangle highlights the area to be visited on this excursion**

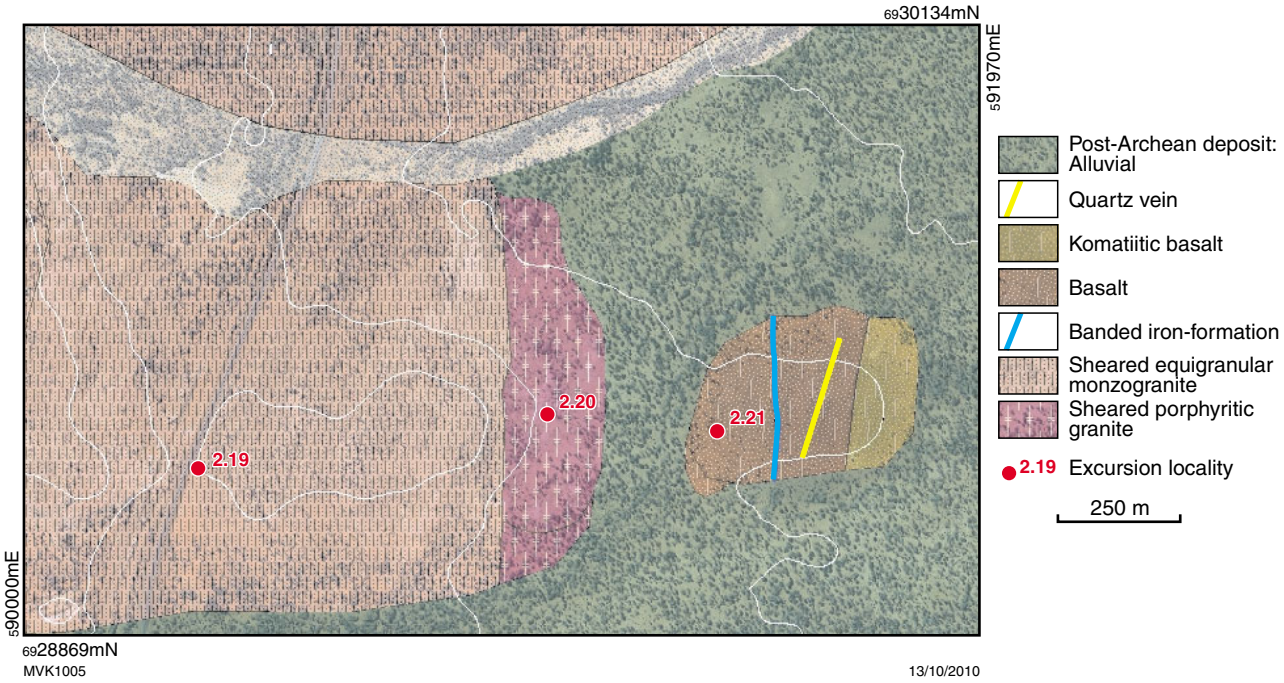


**Figure 52. Detailed map showing the location of the excursion localities (red circles).**

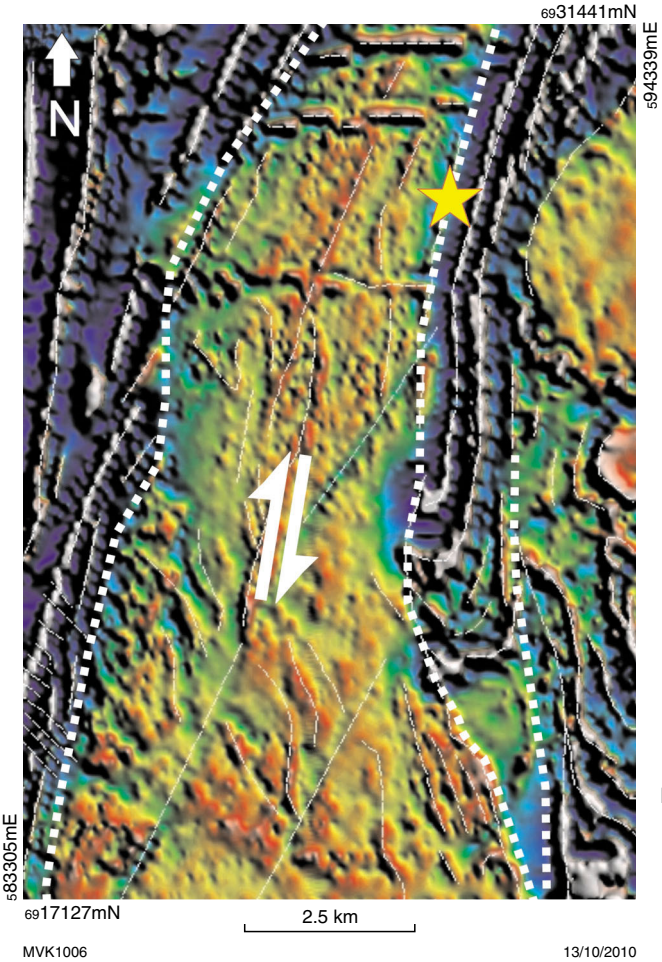


**Figure 53. Aeromagnetic map of the area showing the elongate granitic suite flanked by greenstone belts (compare with Figure 51). Thin, dashed white lines highlight the trend of the main structures; thick dashed lines mark the granite–greenstone boundaries. The star indicates the excursion localities, at the granite–greenstone boundary**

The geodynamic significance of the older tectonic fabric is not clear. It could result from an east-directed thrust (equivalent to the Carbar Fault), as described by Spaggiari (2006), possibly steepened during subsequent tectonic evolution. Alternatively, it could reflect vertical tectonic movements related to granite emplacement. Further P–T–t data are required to provide a well-constrained tectonic model.

## Locality 2.19: Mylonitic monzogranite

*From Walganna (Walga) rock, head back north to the main road, turn right and head about 37 km east towards the town of Cue. At the T-junction (MGA 578747E 6972698N), turn right and proceed for 12 km into Cue. At the Great Northern Highway, turn right and proceed south along the highway for 40.5 km (to MGA 590369E 6929236N).*

This locality has good exposure of the mylonitic, biotite-bearing monzogranite. On the western side of the highway, on a whaleback, the north-trending mylonitic foliation dips 290°/80°. On this surface, a subhorizontal stretching lineation (05°→200°) is defined by thin biotite trails wrapping around recrystallized aggregates of quartz and feldspar. The shear sense is visible on several low outcrops nearby. On these subhorizontal surfaces, dextral shearing is indicated by S–C fabric, C' shear bands, and asymmetric tails developed around feldspar porphyroclasts.

## Locality 2.20: Sheared monzogranite

*Drive for about 700 m eastward, flanking the southern end of the granitic outcrop (to MGA 591075E 6929346N).*

The easternmost end of the granitic outcrop at this locality is composed of sheared porphyritic granite. As with the previous locality, both horizontal and vertical outcrop surfaces offer the opportunity to observe the subvertical foliation and associated subhorizontal stretching lineation. Here, the foliation is 010°/80° and the lineation is 04°→190°. Dextral kinematic indicators are mainly represented by asymmetric K-feldspar porphyroclasts and C' shear bands on subhorizontal outcrop surfaces (Fig. 54).

MVK1007 09/08/2010

**Figure 54. Horizontal outcrop surface showing C' shear bands cutting mylonitic foliation in a sheared porphyritic granite. Dextral shear sense**

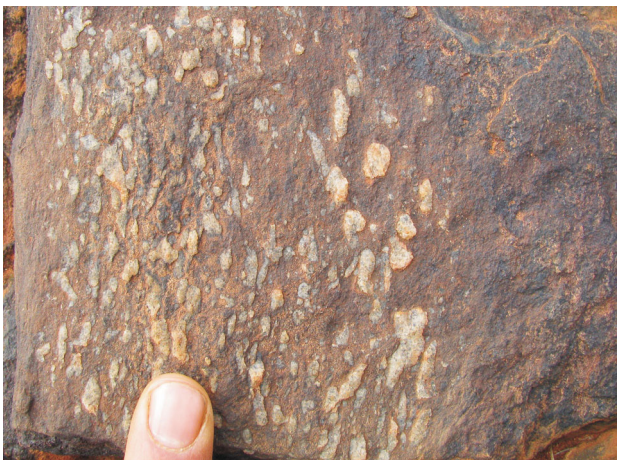

MVK1008 09/08/2010

**Figure 55. Subvertical foliation surface from sheared amygdaloidal basalt, displaying the subvertical stretching lineation, as highlighted by stretched quartz lenses**

## Locality 2.21: Sheared greenstones

*From Locality 2.20, proceed about 200 m east to a small outcrop of sheared tholeiitic and komatiitic basalt (at MGA 591418E 6929311N).*

This small outcrop is composed of sheared tholeiitic and komatiitic basalts, now represented by amphibolite and ultramafic schist, respectively. Here, the main tectonic fabric is readily observed in metabasalt as centimetre-sized, sheared quartz-filled amygdales. On subvertical foliation surfaces (010°/80°), quartz lenses highlight the steeply dipping stretching lineation (70°→020°; Fig. 55), which is associated with a hornblende and plagioclase mineral lineation. On outcrop surfaces parallel to the stretching lineation, the 'west-side-up' shear sense is provided by the sigmoidal shape of quartz lenses and C' shear bands that transect the main mylonitic foliation.

# Part 3: Windimurra and Narndee Igneous Complexes

by TJ Ivanic

## Introduction

Late Archean mafic–ultramafic rocks in layered intrusions comprise approximately 40% by volume of greenstones within the northern Murchison Domain (northwestern Youanmi Terrane) of the Yilgarn Craton in Western Australia. They cover an area of at least 250 × 400 km (Fig. 56), which is similar in extent to the Bushveld Igneous Complex in South Africa. The largest of these layered intrusions is the predominantly gabbroic Windimurra Igneous Complex, which outcrops over an area of about 2500 km$^2$. The nearby Narndee Igneous Complex covers an area of some 700 km$^2$. However, these mafic–ultramafic igneous complexes have been dissected by large-scale, strike-slip shear zones (Spaggiari, 2006) and intruded by Neoarchean granitic rocks, so that the full original extent of any single complex is unknown. Previous geochronology, as well as new results from precise ion microprobe (SHRIMP) U–Pb ages of zircon and baddeleyite help to confirm the stratigraphic context for these layered igneous complexes. Estimations of their original composition, stratigraphic setting, and volume have implications for the tectonic development of the craton.

## Regional geology

Recent mapping, petrography, and geochronology in the Murchison Domain have provided the basis for a new stratigraphic and structural framework for these large intrusions, as well as for the greenstones and granitic rocks (Fig. 19). Under this scheme, the layered mafic–ultramafic igneous complexes have been divided into four suites based upon lithological association, level of emplacement, relative age relationships, and geochronology. These are, from oldest to youngest: the Meeline, Boodanoo, Little Gap, and Yalgowra Suites. The Meeline Suite hosts significant vanadium mineralization (especially in the Windimurra and Barrambie Igneous Complexes), whereas chromium, nickel, copper, and PGE (platinum group elements) mineralization have also been noted in the intrusions of the Meeline, Boodanoo, and Yalgowra Suites. The volumetrically minor Little Gap Suite has not been extensively explored.

Supracrustal rocks that host the layered mafic–ultramafic complexes form part of the 2950–2700 Ma Murchison Supergroup (Van Kranendonk and Ivanic, 2009). Although c. 2950 Ma greenstones have been documented in the southern part of the Murchison Domain (Yeats et al., 1996; Wang et al., 1998), greenstones in the northern part of the domain were deposited in three groups, between 2825 and 2700 Ma — the Norie, Polelle, and Glen Groups (Figs 19, 20). The 2825–2800 Ma Norie Group is intruded at its base by synvolcanic and younger granitic rocks, but the younger 2800–2740 Ma Polelle and 2735–2700 Ma Glen Groups have disconformable to unconformable contacts on older greenstones. The groups are dominated by mafic and ultramafic volcanic rocks, but also include locally thick felsic volcanic units, as well as banded iron-formation and clastic sedimentary rocks (Van Kranendonk, 2008; Van Kranendonk and Ivanic, 2009).

The Norie and Polelle Groups host mafic–ultramafic complexes of different ages, emplaced as shallow-level subvolcanic sills during eruption of the overlying volcanic units (Van Kranendonk and Ivanic, 2009). The older, structurally lowermost sills include thick layered mafic–ultramafic igneous complexes (e.g. the Windimurra and Narndee Igneous Complexes) with evidence of multiple magma pulses and complex cyclical layering, whereas the younger sills (e.g. those in the Yalgowra Suite) are generally thinner and composed of a single magma pulse.

## Layered mafic–ultramafic igneous suites of the Murchison Domain

Mafic–ultramafic rocks in the Murchison Domain have been divided into four suites: the c. 2810 Ma Meeline Suite, which includes the large Windimurra Igneous Complex; the 2800 ± 6 Ma Boodanoo Suite (Fig. 57), which includes the Narndee Igneous Complex; the 2792 ± 5 Ma Little Gap Suite; and the 2735–2710 Ma Yalgowra Suite of layered gabbroic sills.

Outcrop patterns, aeromagnetic surveys, and gravity modelling (e.g. Ahmat, 1986) indicate that most intrusions of the mafic–ultramafic igneous suites form tabular bodies, i.e. sills, laccoliths, or lopoliths. The larger mafic–ultramafic layered intrusions of the Meeline and Boodanoo Suites — the Windimurra, Narndee, and Youanmi Igneous Complexes — preserve a large part of their original intrusion morphology, with relatively shallowly inward-dipping concentric layers. This contrasts with the majority of the other mafic–ultramafic intrusive rocks in the northern Murchison Domain, which are steeply dipping, parallel to greenstone bedding, and deformed into parallelism with major shear zones (Fig. 56). The margins of some of the larger igneous complexes are sheared and intruded by granitic rocks, so that information concerning

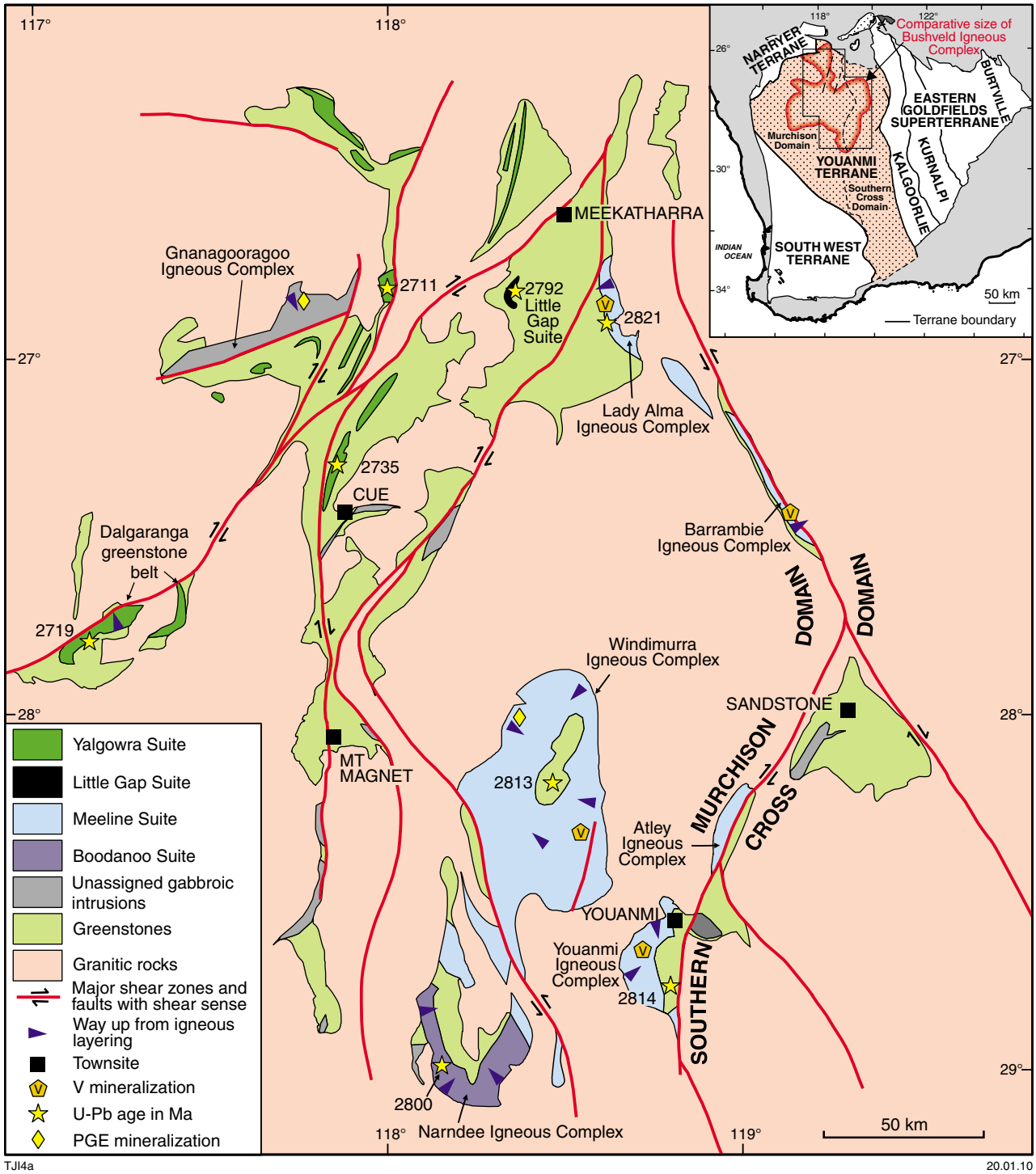


**Figure 56. Map of the mafic–ultramafic suites and igneous complexes of the northern Youanmi Terrane relative to greenstones and granites, modified from GSWA (2008)**

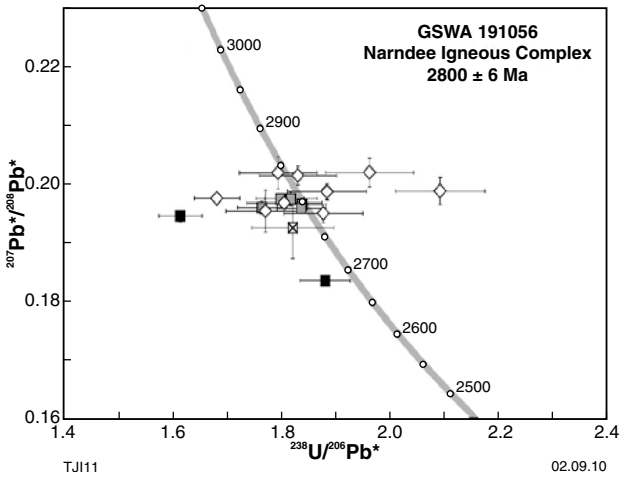


**Figure 57. U–Pb analytical data for zircon (diamonds) and baddeleyite (squares) from gabbronorite sample GSWA 191056 of the Narndee Igneous Complex (Wingate et al., 2010)**

the nature of the contact relationships with greenstones has been obscured.

Figure 58 shows the similarities within the internal stratigraphies of the Meeline Suite bodies. Correlation of the contacts in the upper zones illustrates how the ultramafic portions of many of these bodies are probably missing through dislocation. The distinctive characteristics of the Boodanoo and Yalgowra Suites are also evident, with widespread hornblende gabbro in the Narndee Igneous Complex and single-pulse fractionation in the Yalgowra Suite bodies.

The mafic igneous suites in the Murchison Domain represent a major addition to the crust over a 115 Ma period, contemporaneous with greenstone belt development. Combined volume estimates for the intrusions indicate they are second only to the c. 2060 Ma Bushveld Igneous Complex in South Africa. Currently, the distribution, ages, and compositions of rocks from the four mafic–ultramafic suites identified here are explained most readily by a modified version of a plume model of crustal development, such as that outlined in Campbell and Hill (1988). However, additional geochemistry is required to explain the presence of hydrous magmas in the Boodanoo Suite. Significantly, mafic–ultramafic magmatism in the northern Murchison Domain overlaps in time with that of the Burtville Terrane of the Eastern Goldfields Superterrane, now separated by more than 500 km. This suggests the possibility of a shared history over at least 100 Ma (c. 2820–2710 Ma), and possibly longer (Fig. 59).

# Geology of Windimurra and Narndee Igneous Complexes

## Windimurra Igneous Complex

The Windimurra Igneous Complex is the largest exposed, single mafic–ultramafic intrusion in Australia. The coherent main body of the complex extends for 85 km north–south and 37 km east–west, and covers an area of 2500 km$^2$. Additional parts of the intrusion form metamorphosed and sheared lenses to the south and east of the main body, east of the Challa Shear Zone (Fig. 60), with areas up to 25 km north–south and 5 km east–west as estimated from aeromagnetic images. Given the dismembered and sheared nature of a large proportion of this igneous complex, it is likely that the original form would have been similar in shape and size to one of the main lobes of the Bushveld Igneous Complex. The cumulative thickness of the layers of gabbroic and ultramafic rocks is 13 km where they exhibit lateral aggradation (offlap), representing a true thickness of 6 km (Ahmat, 1986, from gravity modelling). This interpretation is supported by observed shallower dips (as low as 10°) in the upper parts of the complex (Fig. 60). These features are probably due to emplacement into crust during significant extension. A significant magmatic discordant zone (the Shephards discordant zone), at least 20 km long, runs approximately north–south through the southern part of the complex (yellow line on Fig. 60). The maximum stratigraphic offset along this zone (from comparison of stratigraphic columns) is approximately 3 km in true thickness, suggesting a highly unstable substrate during magma emplacement. Ahmat (1986) divided the Windimurra Igneous Complex into an ultramafic zone, a lower zone, a middle zone, and an upper zone based on lithological association, mineralogy, and mineral chemistry (Fig. 61a). He also noted that there are many >100 m-thick megacyclic units that exhibit modal fractionation, with gabbroic rocks containing more-mafic minerals at their bases and more plagioclase at their tops. Ahmat (1986) also showed that there were at least 13 reversals of geochemical fractionation (to more primitive mineral chemistry, e.g. in Mg# and V/Ti). These reversals were interpreted as being representative of new magma pulses. Disregarding small-scale reversals, there is an overall progression from more-mafic rocks in the lower zone to large volumes of anorthositic and leucogabbroic rocks at the top of the Windimurra Igneous Complex (Fig. 61a). Figure 61b shows the generalized stratigraphy of the complex, corrected for vertical thickness estimates.

The exposed complex has an extremely felsic overall composition, which suggests the presence of a large volume of concealed ultramafic rocks below the currently outcropping units. The only exposure in the region that could represent part of the ultramafic zone is the detached series of rocks located to the southwest of the coherent body and bounded by shear zones (Fig. 60). A recent gravity survey over the central Murchison Domain (Fig. 62) indicates that there is a particularly dense zone beneath the central and western parts of the Windimurra Igneous Complex, which may be partly due to the presence of unexposed lower zone rocks as well as very dense, Fe-rich, upper zone rocks. Higher density regions in the centre of the main body of the complex could mean there is a concealed, funnel-shaped basal portion that contains a significant thickness of ultramafic rocks. Ahmat (1986) defined a border zone along the boundary between sheared supracrustal rocks and the lower zone gabbros. This is thought to represent the chilled original magma, although it is commonly metamorphosed and altered. Also, at the margins of the complex, examples of

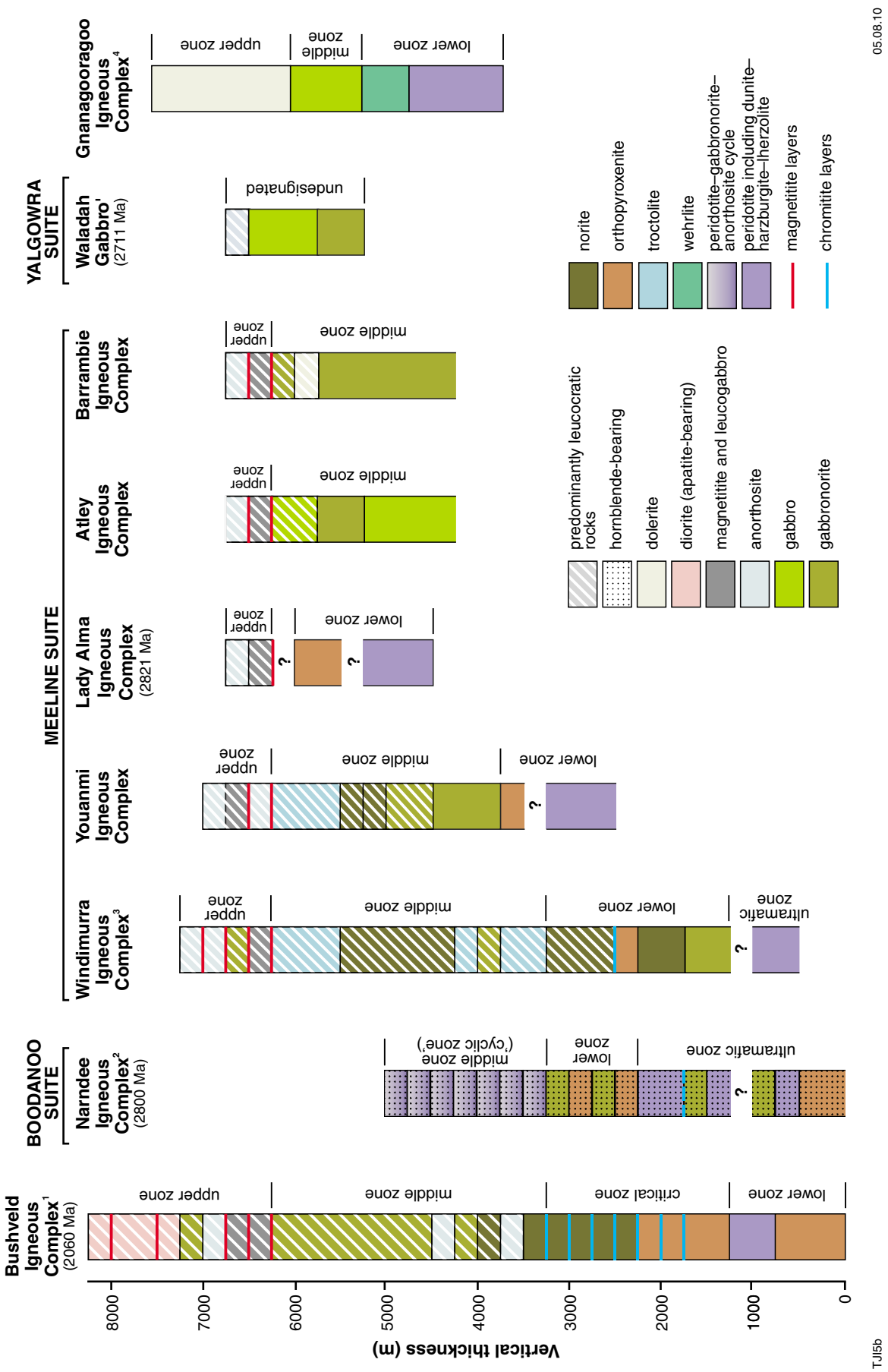


**Figure 58.** Comparative igneous stratigraphic columns for layered igneous complexes in the Murchison Domain compared to the Bushveld Igneous Complex, South Africa. [1]Adapted from Cawthorn and Walraven (1988); [2]adapted from Scowen (1991) and corrected to approximate true thickness; [3]adapted from Ahmat (1986) and corrected to approximate true thickness; [4]lower zone adapted from Parks (1998). Main and upper zone dimensions from Ivanic (2009)

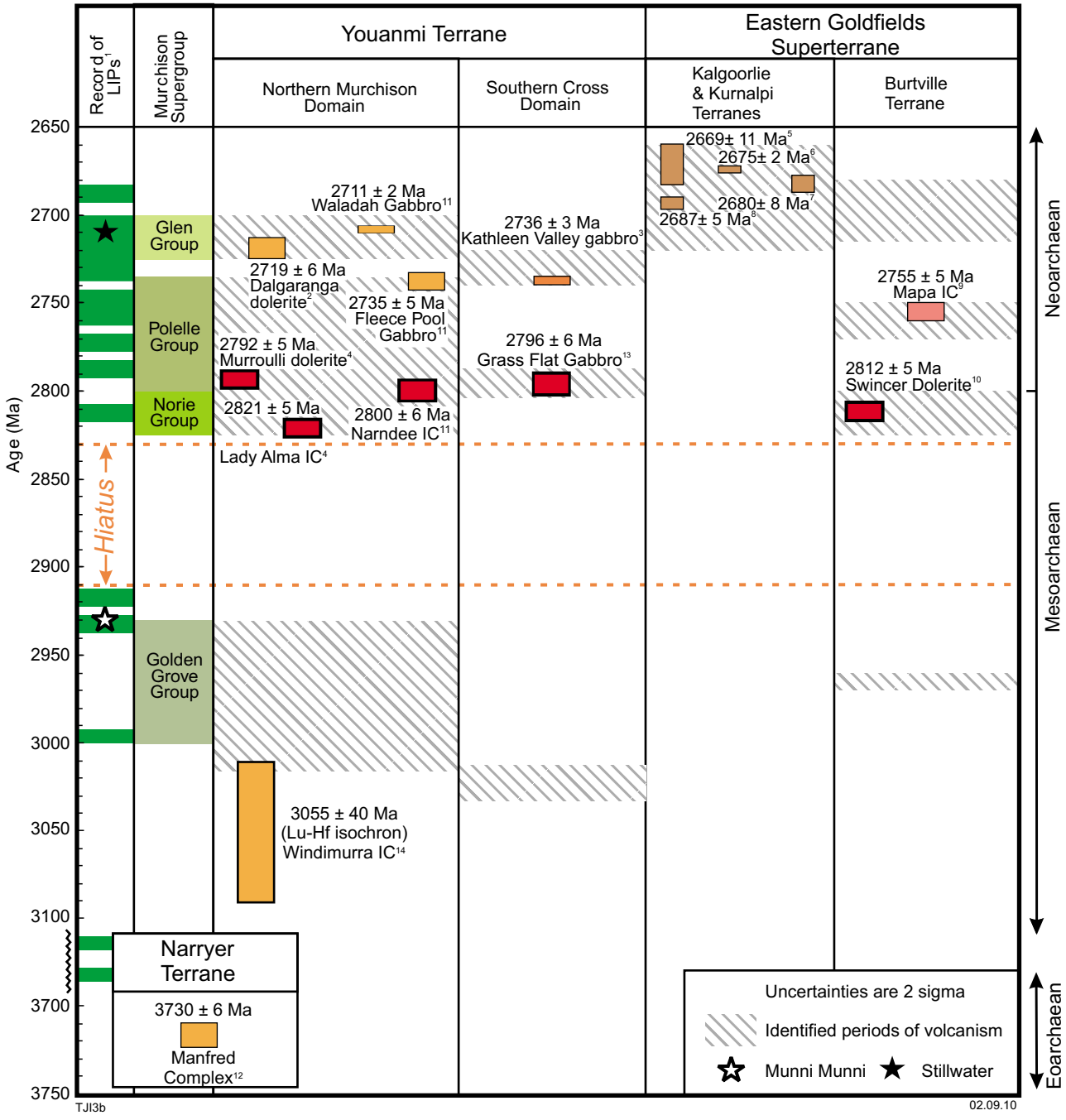


**Figure 59. Summary of age determinations for mafic intrusions in the Youanmi Terrane compared with those in the Kalgoorlie, Kurnalpi, and Burtville Terranes: [1]an extract from the global mafic magmatism 'bar code' (Ernst et al., 2005) is shown on the left. Ages: [2]Pidgeon and Hallberg (2000); [3]Liu et al. (2002); [4]Wang (1998); [5]Compston et al. (1986); [6]Woods (1997); [7]Carey (1994); [8]Kent and McDougall (1995); [9]GSWA 185976 (Wingate et al., in press a); [10]GSWA 185968 (Wingate et al., in press b); [11]GSWA 191056, 185922, 185927 (Ivanic et al., 2010); [12]Kinny (1988); [13]GSWA 184990 (Riganti et al., 2010); [14]Nebel et al. (unpublished data)**

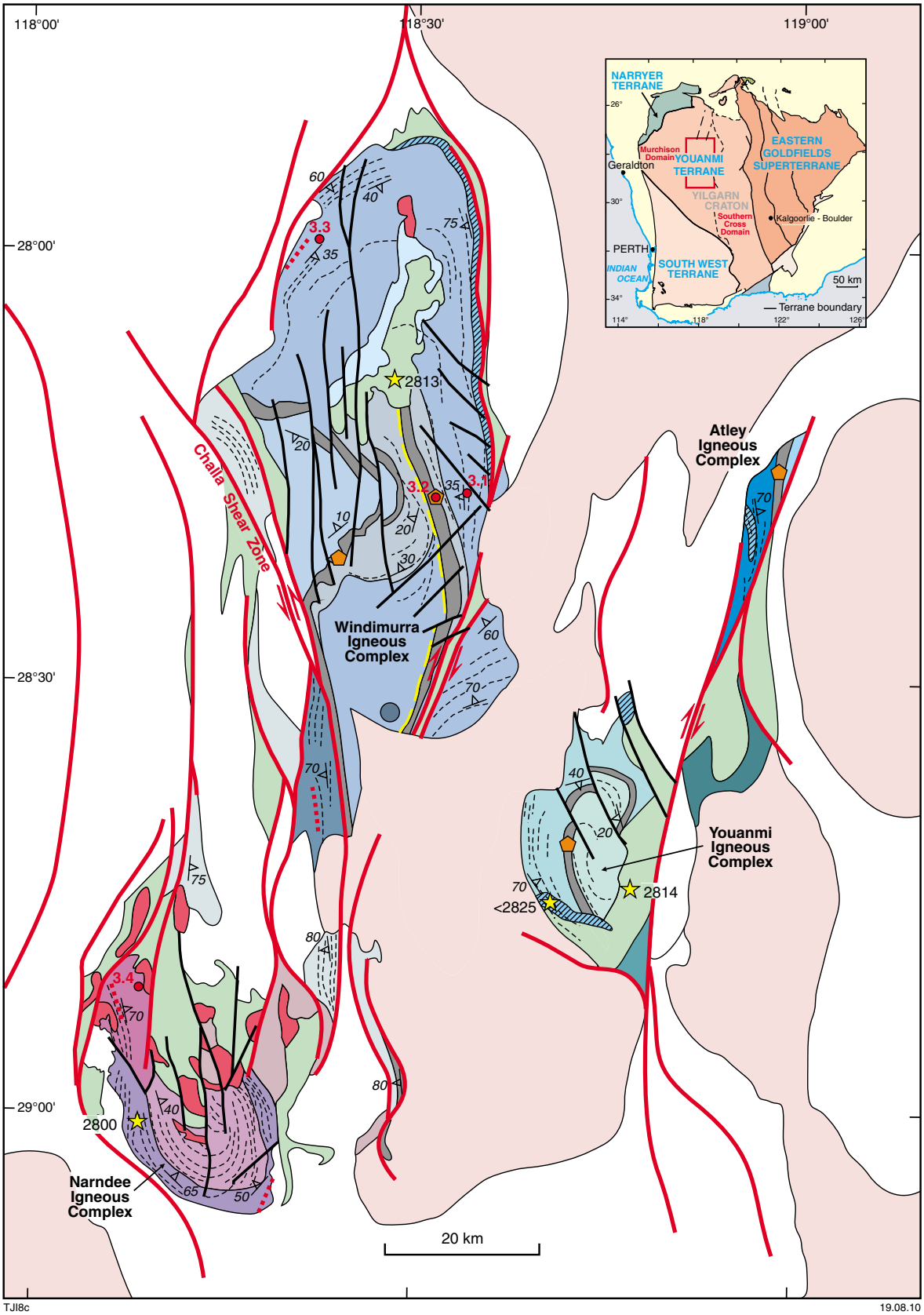


**Figure 60.** Interpreted geological map of Windimurra, Narndee, Youanmi, and Atley Igneous Complexes. Note that magnetitite east of Narndee Igneous Complex is thought to be related to the Windimurra Igneous Complex and would imply at least 80 km sinistral displacement along the major north-northwesterly trending shear zone. Similarly, dextral displacement of the Atley Igneous Complex of approximately 30 km is indicated along a north-northeasterly trending shear zone that marks the boundary of the Muchison Domain and the Southern Cross Domain of the Youanmi Terrane. Excursion localities shown in red

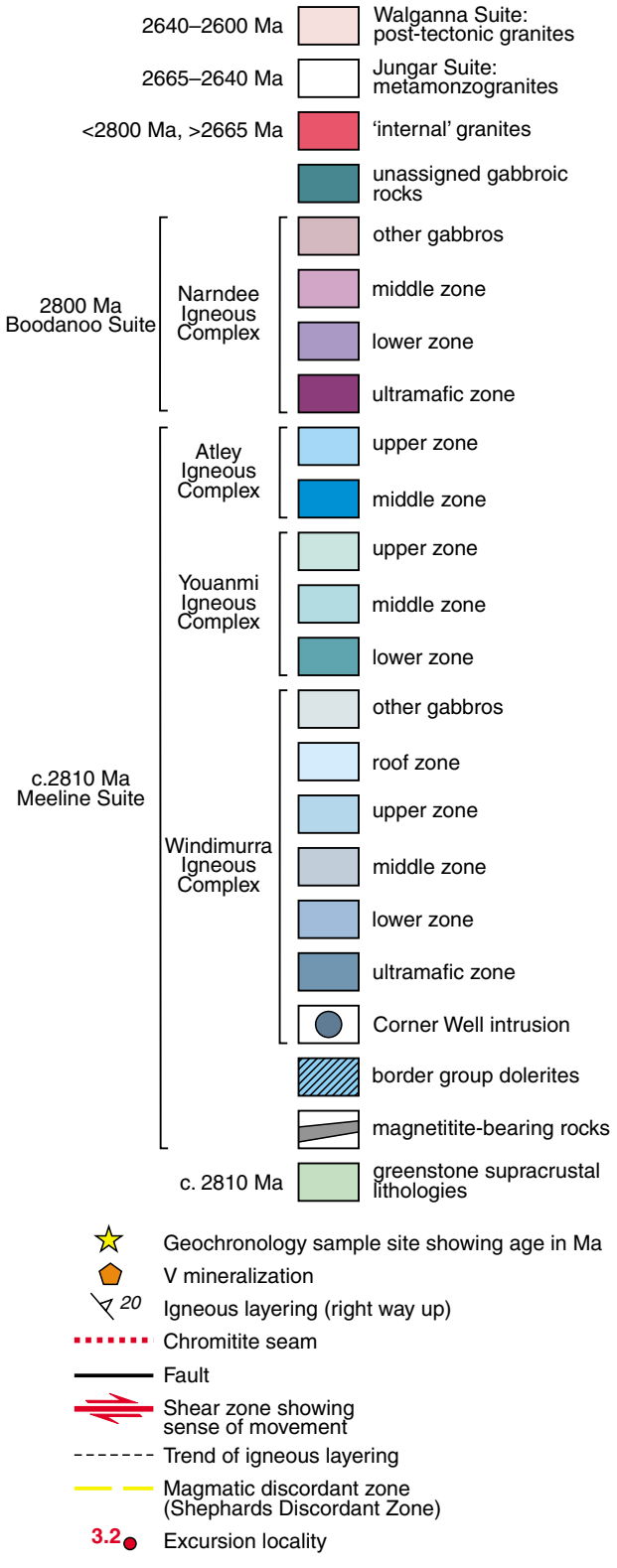


granulite facies contact metamorphism are preserved by pelitic xenoliths and wallrocks that belong to the Norie Group. Pyroxene mineral barometry from gabbros shows that the Windimurra Igneous Complex was emplaced at pressures of about 400 MPa (Ahmat 1986), at middle crustal depths.

## Narndee Igneous Complex

Located about 50 km south of the Windimurra complex, the Narndee Igneous Complex is exposed over 30 km north–south and 25 km east–west (about 700 km$^2$), and has a thickness of about 4.5 km. The sinistral Challa Shear Zone has displaced the complexes by a minimum of 80 km. This estimate is based on the dislocation of magnetitite units of the Windimurra Igneous Complex (Fig. 60). The Windimurra and Narndee Igneous Complexes may once have been in direct contact, but there is no preserved exposure of such a contact. The ultramafic zone of the Narndee Igneous Complex is mainly located in deformed rocks in a fault-bound segment to the northwest of the main body and so the true thickness of the complex is unknown. The upper parts of the Narndee Igneous Complex have only slightly shallower dips than those at the margins (Fig. 60). Consequently, the off-lap geometry seen in both the Windimurra and Youanmi Igneous Complexes is not so evident here. Crosscutting leucogabbro sheets in the northwestern part of the complex indicate at least two phases of magmatic activity, postulated to represent back intrusion of more-evolved middle zone material into the lower zone.

The Narndee Igneous Complex has been divided into three zones by Scowen (1991), essentially as shown in Figure 63. Figures 58 and 60 show how these zones have been incorporated into the overall interpretation with ultramafic through to lower and middle zones rather than 'Ultramafic' through to 'Gabbronorite' and 'Cyclic' zones as defined by Scowen (1991). The ultramafic zone at the base of the cumulate pile consists mainly of peridotite and pyroxenite, and is overlain by predominantly gabbronoritic rocks of the lower zone (Figs 58, 63). These are in turn overlain by at least seven megacycles of peridotite–gabbronorite–anorthosite, each more than 100 m thick in the middle zone (Figs 58, 63). All zones contain rocks bearing igneous hornblende, primarily as 1 cm-diameter oikocrysts (Fig. 64). In terms of major element chemistry, Scowen (1991) identified many instances of fractionation reversals upsection (e.g. Mg# in olivine and pyroxene), which were attributed to new pulses of magma. The composition of the Boodanoo Suite differs from the Meeline Suite in that the Narndee Igneous Complex contains a large volume of hornblende gabbro (Fig. 58) and a larger proportion of ultramafic rocks. It also has a finer grain size and a more persistent layering style, as seen in the middle zone (Fig. 58). It is thus considered to have been derived from a different parent magma than that of the Windimurra Igneous Complex (Scowen 1991). Scowen (1991) identified a tholeiitic affinity for the geochemistry of the Narndee Igneous Complex. However, the hydrous nature of the magma is not accounted for by a normal tholeiitic composition. As the average composition is relatively ultramafic, it is likely that a significant felsic upper portion of the original magma chamber has become eroded or detached from the currently exposed units. The stratigraphic setting for the Boodanoo Suite appears to be similar to that of the Meeline Suite (see above), intruding into similar parts of the stratigraphy (Norie Group). Pressure estimates of 100–300 MPa from pyroxene barometry indicate emplacement between approximately 3 and 10 km depth (Scowen 1991).

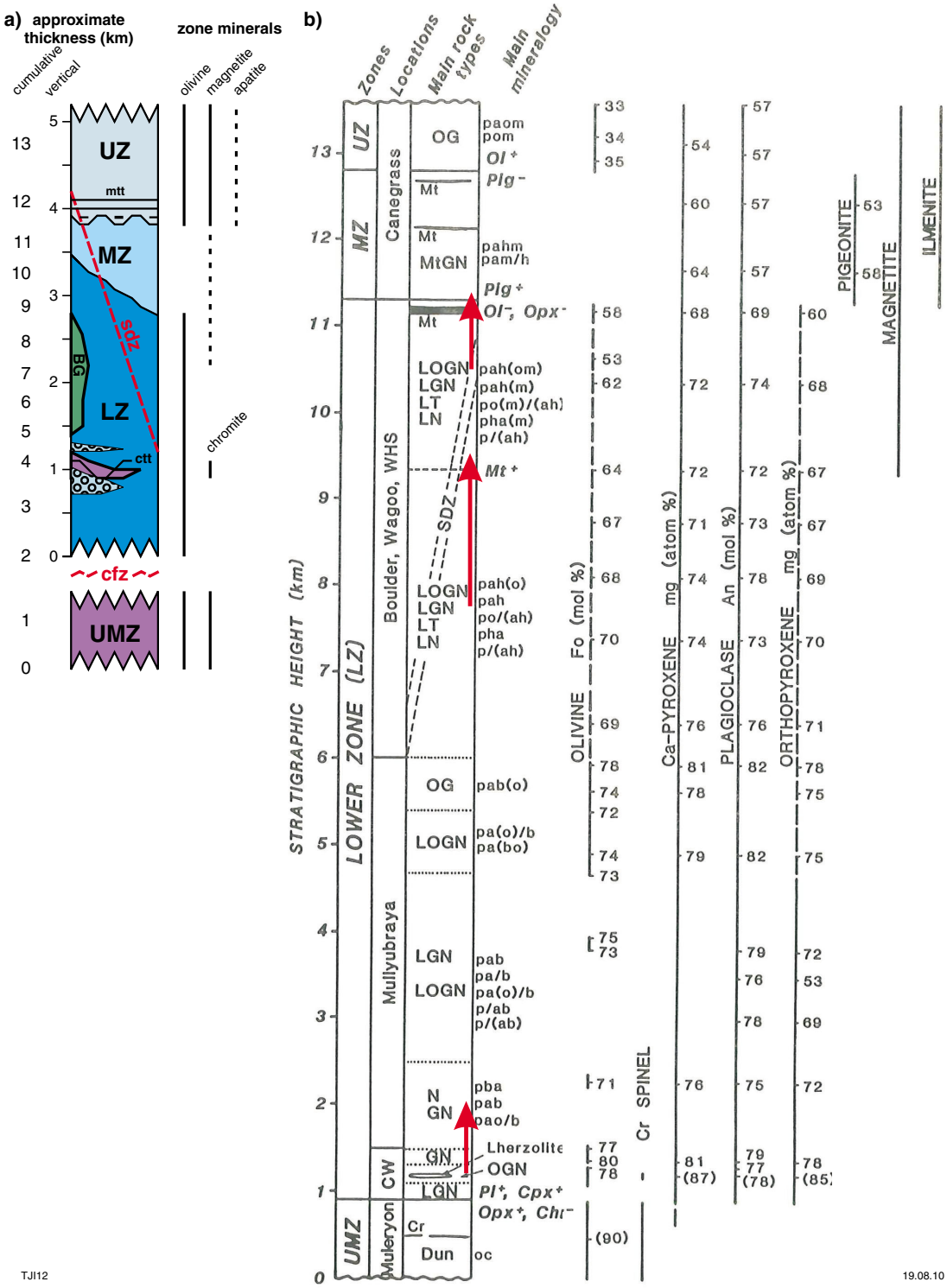


**Figure 61.** Stratigraphic column for the Windimurra Igneous Complex: a) simplified stratigraphy showing new zone classifications. UMZ = ultramafic zone, LZ = lower zone, MZ = middle zone, UZ = upper zone, ctt = chromitite, mtt = magnetitite, BG = Border Group, cfz = Challa Fault Zone, sdz = Shephards Discordant Zone, black circles on light blue are anorthosite boulder beds. Cumulus zone minerals are shown with thick vertical lines for cumulus phases and dashed for intercumulus; b) stratigraphy compiled from correlation of six main subareas (Mathison et al., 1991): Distribution of cumulus phases is shown by vertical lines, together with a summary of mineral composition data. SDZ = Shephards Discordant Zone, UMS = Ultramafic Series, CW = Corner Well. Rock type codes: Dun = dunite, Cr = chromitite seams, LGN = leucogabbronorite, GN = gabbronorite, N = norite, LN = leuconorite, LOGN = olivine leucogabbronorite, OG = olivine gabbronorite, LT = leucotroctolite, Mt = magnetite seams. Mineral codes: p = plagioclase, a = augite, o = olivine, b = bronzite, h = hypersthene, m = magnetite; e.g. po/ah indicates plagioclase–olivine cumulate with oikocrysts of augite and hypersthene. Arrows show approximate stratigraphic locations of traverses in localities 3.1–3.3

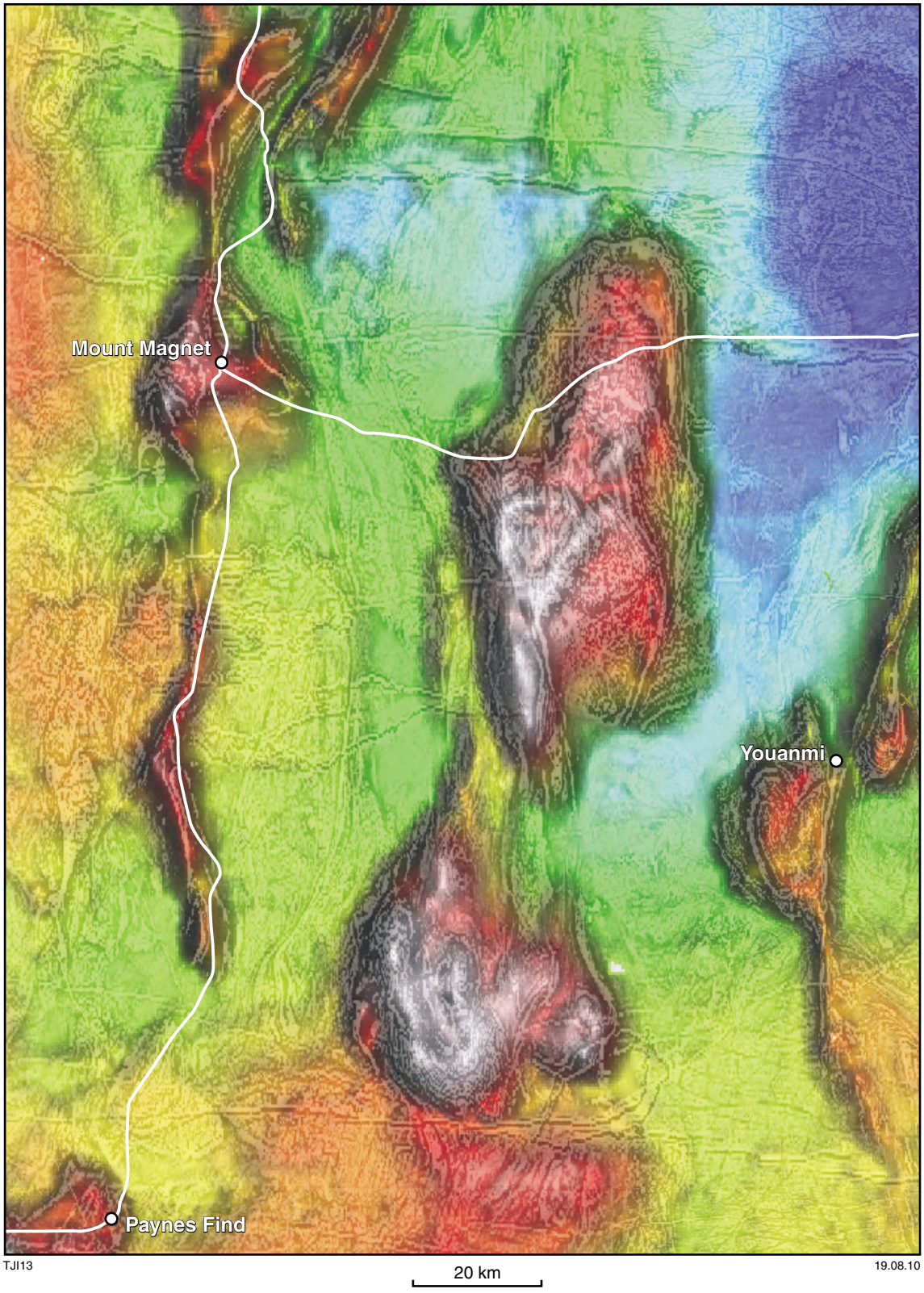


**Figure 62. Bouguer gravity anomaly image (colour) of the southern Youanmi Terrane with first vertical derivative magnetic overlay (grey-scale). Note gravity highs (white) correspond to the upper zone of the Windimurra Igneous Complex and the majority of the Narndee Igneous Complex. Also there is a dense region south of Narndee Igneous complex (red area) that is a granite at surface, possibly indicating a mafic intrusion at shallow depth**

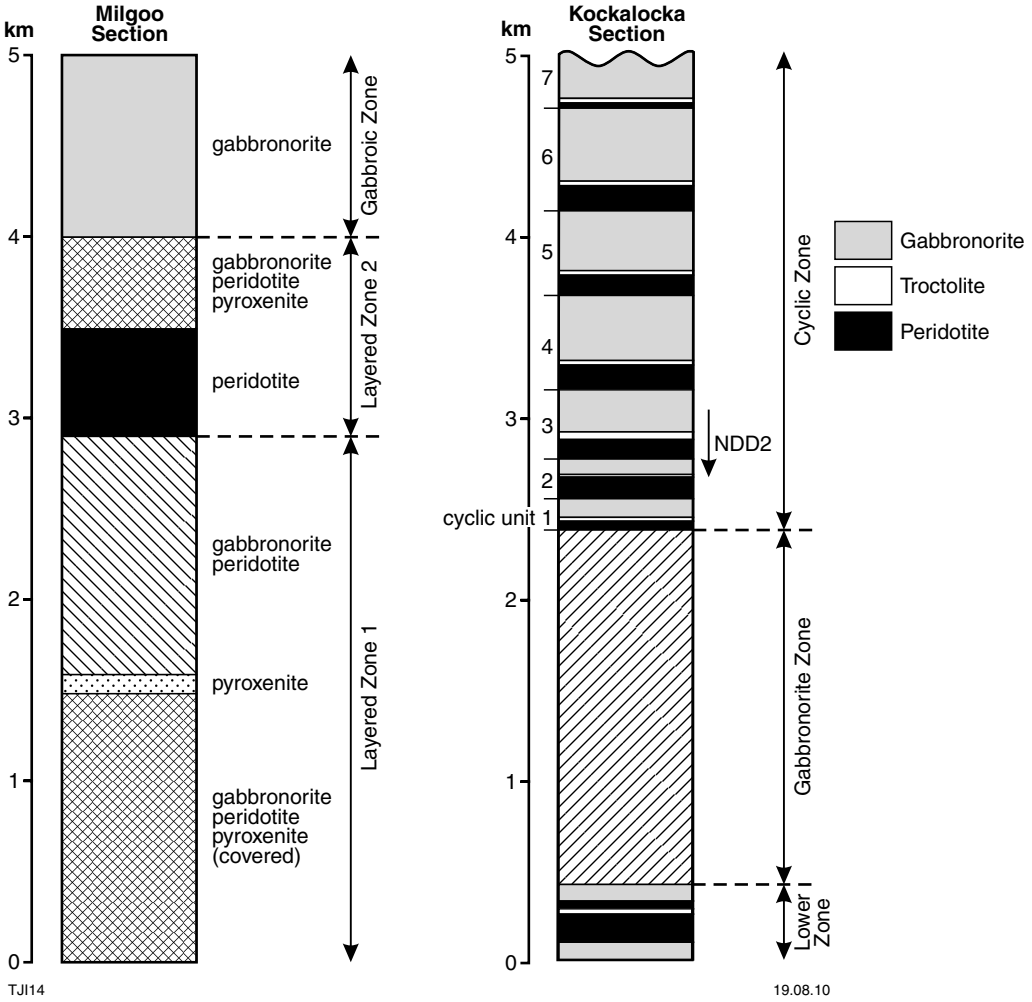


**Figure 63. Milgoo and Kockalocka sections (Scowen, 1991). Not true stratigraphic height**

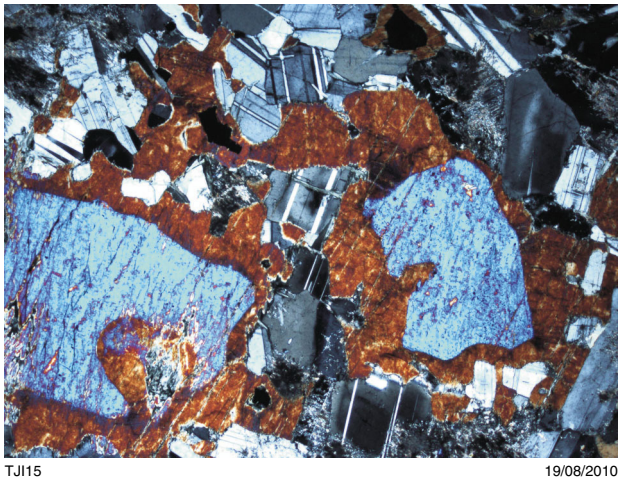


**Figure 64. Thin-section photomicrograph (crossed polars) of a hornblende gabbro (GSWA 191056, dated sample) from Narndee Igneous Complex showing igneous hornblende oikocrysts (brown) mantling augite cumulate crystals (blue) and interstitial to smaller plagioclase cumulate crystals. Field of view is 6 mm**

**Table 2. Known mineralized localities in the Windimurra and Narndee areas based upon recent exploration and mapping (sources include Bunting, 2004)**

| *Metals* | *Windimurra area* | *Narndee area* |
|---|---|---|
| Ni | – | Milgoo |
| Cu | Canegrass | Milgoo |
| PGEs | Wondinong | Milgoo |
| Au | Paynesville, Canegrass | Kiabye Shear |
| V | Shephards Hill, Canegrass | - |
| Cr | Wondinong, Muleryon Hill | Milgoo, Soak Bore |

## Mineralization

There are widespread indications of a variety of significant metal commodities in the Windimurra and Narndee areas (Table 2). Most significantly, the Windimurra Igneous Complex has been mined at the Windimurra vanadium mine from a typical occurrence of vanadiferous magnetitite units in the upper parts of Meeline Suite intrusions. This is likely a similar style of mineralization to that in the Barrambie Igneous Complex (Wyche, 2008).

Basal parts of the Meeline, Boodanoo, and Yalgowra Suites have been noted as hosting at least minor nickel–copper–PGE mineralization. Mineralization appears to be hosted primarily in sulfides and is most clearly demonstrated in the Milgoo area of the Narndee Igneous Complex (Bunting, 2004). Elevated copper in chalcopyrite and bornite has been noted in the Milgoo and Canegrass prospects.

Thin chromitite units are present in the Narndee and Windimurra Igneous Complexes, although, at Windimurra, they have been noted as containing relatively low chromium concentrations (Ahmat, 1986). Disseminated chromite also occurs in the Muleryon Hill region south of the Windimurra Igneous Complex. None of these occurrences has been shown to be economic.

## Locality 3.1: Windimurra Igneous Complex, Windimurra Hills Section

*Take the Sandstone road from Mount Magnet. After 45 km (MGA 626978E 6881693N) turn right onto the Youanmi road, which becomes unsealed after 2 km. At 76.6 km (MGA 654513E 6872722N) turn right onto the far side of a fence-line track (over a grid). Follow this until 79.2 km (MGA 654491E 6870085N) and cross the fence line at the well. Head southwest for 800 m and then south for 900 m to the base of large hill (MGA 653756E 6868900N).*

### Locality 3.1.1

The traverse begins in the stratigraphically lower part of the layered gabbroic rocks in the first gabbronorite zone (Figs 65, 66). Walking west for about 500 m across strike,

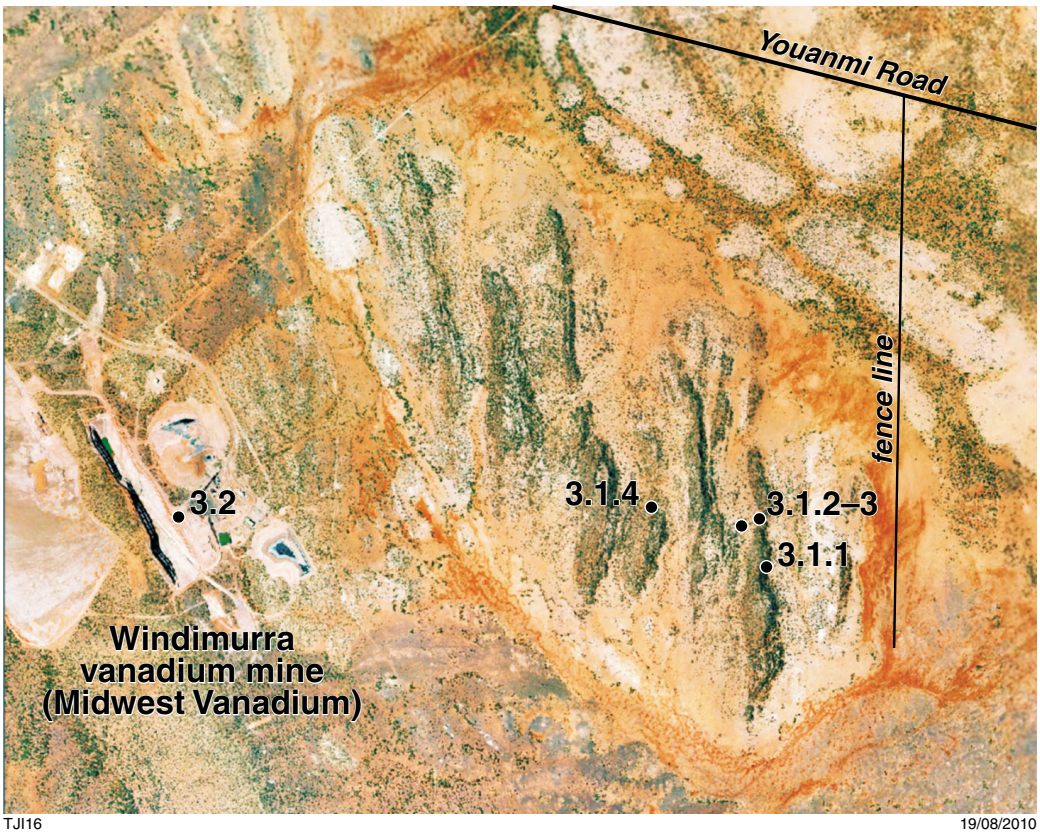


**Figure 65. Windimurra Hills area of the Windimurra Igneous Complex showing traverse localities**

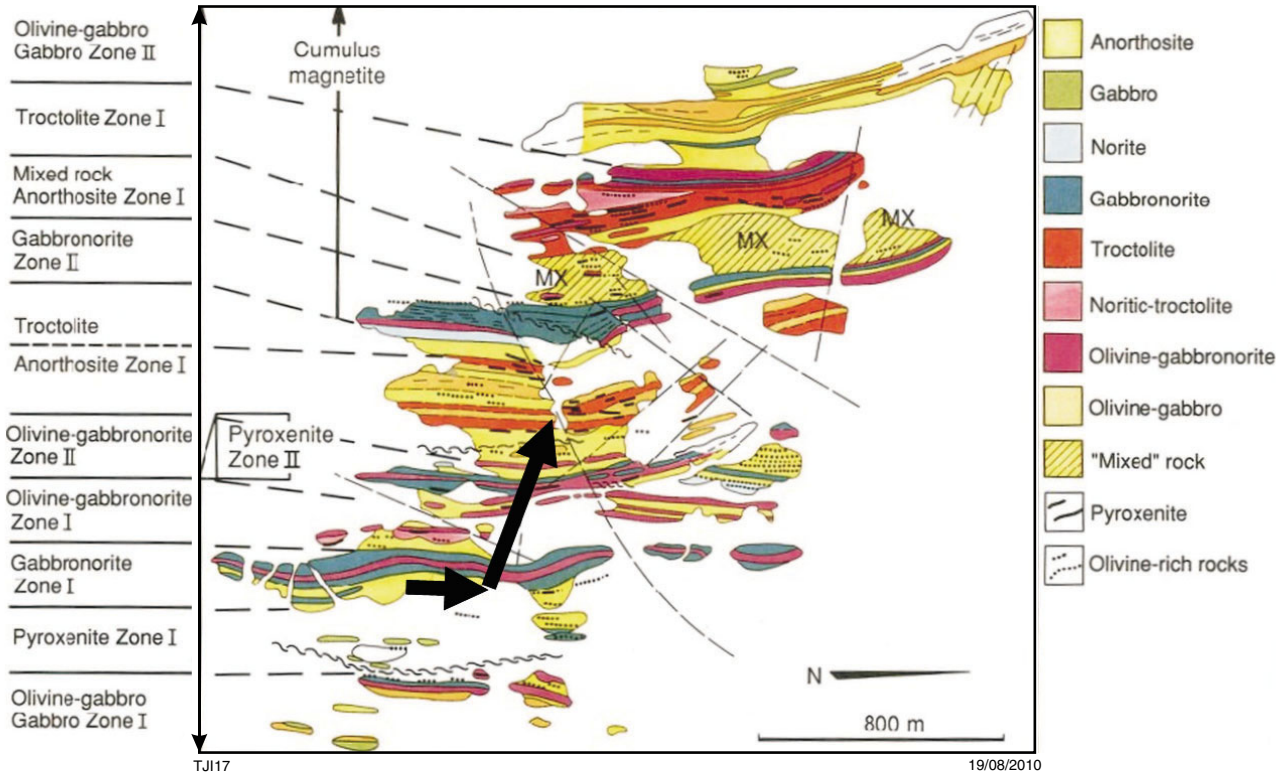


**Figure 66. Geological map of the Windimurra Hills (Parks, 1983). Black arrows indicate traverse 3.1**


**Figure 67. Modal layering of pyroxene and plagioclase in gabbro. The boulder is probably overturned, i.e. way up is to the bottom of the picture. Note also the truncation of a layer in the upper middle part of the boulder. The rock composition ranges from pyroxenite (in the most mafic layers) to leucogabbro in the most felsic layers. The scale is 10 cm**


**Figure 68. Pyroxene oikocrysts between 5 and 10 cm long surrounding 6 to 8 mm plagioclase cumulate crystals in leucogabbro**

we will progress upwards through approximately 300 m of igneous stratigraphy, through a second gabbronorite zone, and into a troctolite-rich zone where the incoming of magnetite is evident (Figs 65, 66). At the top of the first hill, the view across to the Windimurra vanadium mine gives an idea of the thickness of the intrusion. The hills of the Kantie Murdanna Volcanics are also visible to the northwest.

### Locality 3.1.2

There are plenty of examples of modal layering on the east side of the first hill of gabbronorite, with some of the most spectacular rocks being about halfway up the steep slope. Features such as simple modal layering, truncational discordance, channels, and some possible load structures can be seen (Fig. 67).

### Locality 3.1.3

In the valley past the first gabbronorite and before the second are good examples of mottled leucogabbro and anorthosite (Fig. 68).

### Locality 3.1.4

After a second ridge of mafic gabbronorites, troctolites become increasingly common. Lenses of pyroxenite are also present at the end of the traverse (Fig. 66).

## Locality 3.2: Windimurra Igneous Complex, Windimurra vanadium pit lookout

*Return to the Windimurra mine road, and drive in to the visitors' car park. The aim is to view the western pit wall from the eastern side of the pit, which is best done before 11 am.*

Three megacycles of magnetitite can be seen in the pit. The most vanadiferous magnetitites are in the east wall (megacycle 1). These magnetitites were the first significant quantities of magnetite crystals to precipitate and were able to scavenge the majority of vanadium from the magma. $TiO_2$ vs V ratios vary remarkably consistently through this section, with the highest ratios at the base in megacycle 1 (7–8). Megacycle 2 has ratios in the region 15–40 and megacycle 3 has ratios 40+. Megacycle 2 is at the base of the pit (Fig. 69), and megacycle 3 is at the top of the pit in the east (Fig 70). Each cycle represents approximately 10 m vertical section and contains multiple magnetitite bands (about 10 magnetitite layers, each about 0.5 m thick).

Many other features, such as possible slump structures, channels, and anorthosite drop stones, are visible in the western pit wall (Fig. 71). Up close, modally graded layers and a strong plagioclase lamination can be seen. Syn-magmatic normal faults truncate against lower units and offset magnetitite layers above. Good examples are directly across from the viewing platform. Ductile chloritic shear bands are subparallel to layering. Thin subvertical dykes crosscut the layering. The reverse faults that are plainly visible in the wall are thought to be post-magmatic features as they crosscut the normal faults. The interpreted magmatic shear zone ('Shephards discordant zone', Ahmat, 1986), which represents more than 3 km of offset

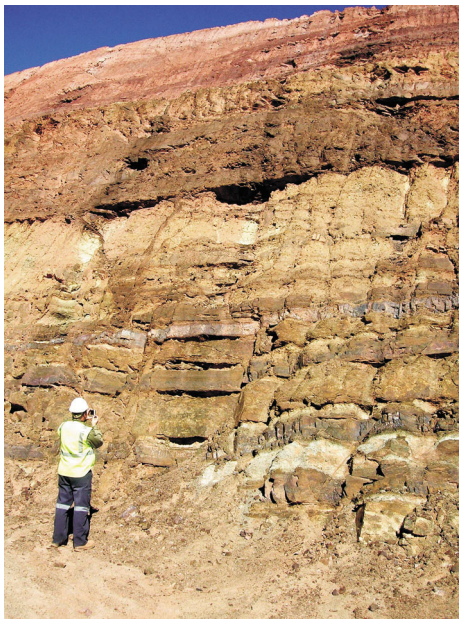

TJI20 19/08/2010

**Figure 69. Photo showing magnetitite layers in leucogabbro, looking west at the northern end of the pit**

TJI21 19/08/2010

**Figure 70. Photo looking south in Windimurra vanadium pit (40 m deep): magnetitite layers in leucogabbro dipping 40° to the west, Windimurra Igneous Complex**

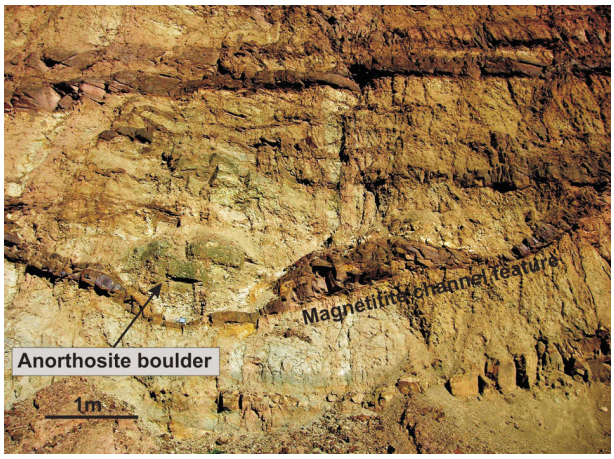


TJI22 19/08/2010

**Figure 71. Features in the Windimurra vanadium pit, looking west. A one m-wide anorthositic xenolith is present at the base of a magnetitite channel feature that has a truncated top contact with overlying magnetitite layers**

igneous stratigraphy (see stratigraphic column, Fig. 61a), is not exposed, but is mapped 500 m stratigraphically above the pit exposure.

## Locality 3.3: Windimurra Igneous Complex, Mingyngura Hill Section

*Go back to the Sandstone road and turn right. Drive 20.4 km and take a gravel road to the left (MGA 640047E 6894370N). Drive north for 3.0 km to where the track will turn to the left (north-northwest) and proceed for 1.46 km. The track will turn northwest for 4.1 km, crossing a one km-wide, dry creek bed. Keep on the track over a rocky rise and past one well for a further 2.7 km to another well (MGA 635580E 6903151N). Turn left and head east on a track for 1.7 km to a gate (MGA 633885E 6903160N). Go through the gate to the left and head southeast for 1.2 km across clear ground to the first locality (MGA 634144E 6901884N).*

At the start of this traverse (Fig. 60), there is an excavation into a 'boulder anorthosite' rock (Fig. 72). Coarse pegmatitic anorthosite with 5 cm grain size occurs as rounded spheroids up to 30 cm in diameter within a pegmatitic gabbro matrix. PGE sulfides have been found at this locality, possibly indicating a magma mixing event.

Walk south (to MGA 634032E 6901581N) to a 20 m-thick olivine gabbronorite layer outcrop. Note the distinctly pitted texture of weathered olivine-cumulate crystals. A serpentine–talc layer can be seen to the south on the way to a prominent ridge of clinopyroxenite (MGA 634165E 6901390N). The clinopyroxenite is overlain by a lherzolitic unit that contains disseminated chromite and may be the start of the PGE-bearing chromitite layer(s) of the next location.

Proceed west for about 250 m, across a low-lying area (to MGA 633955E 6901106N). Here a chromitite layer crosscuts pre-existing layering of pegmatitic anorthosite (Figs 73, 74) and gabbronorite with or without peridotite.

Walk north for about 500 m to outcrops of pyroxenite and gabbroic pegmatites (MGA 633643E 6901602N). They have undulating contacts but trend broadly parallel to layering, and have mafic bases and leucocratic tops. Crystal sizes may be up to 50 cm (Fig. 75).

## Locality 3.4: Narndee Igneous Complex, Milgoo Section

*Go south from Mount Magnet for 96.5 km along the Great Northern Highway. Turn left at Narndee West road and drive for 25.8 km (about 1.5 km past Kiabye bore). Turn left onto a track heading northeast. Proceed for 6.4 km*

TJI23 19/08/2010

**Figure 72 Rounded 'boulders' of pegmatitic anorthosite, 15–40 cm across, in a matrix of gabbro and pegmatitic gabbro. Minor sulfides are also present**

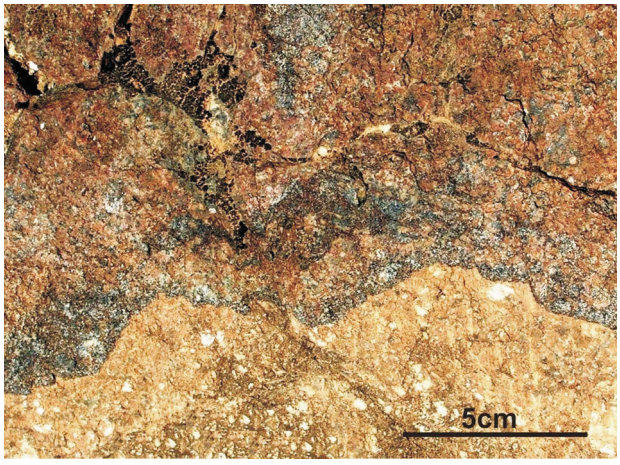


TJI24 19/08/2010

**Figure 73. Undulose chromitite layer overlying pegmatitic anorthosite. Disseminated chromite in norite above the chromitite layer is at the top of the photo**

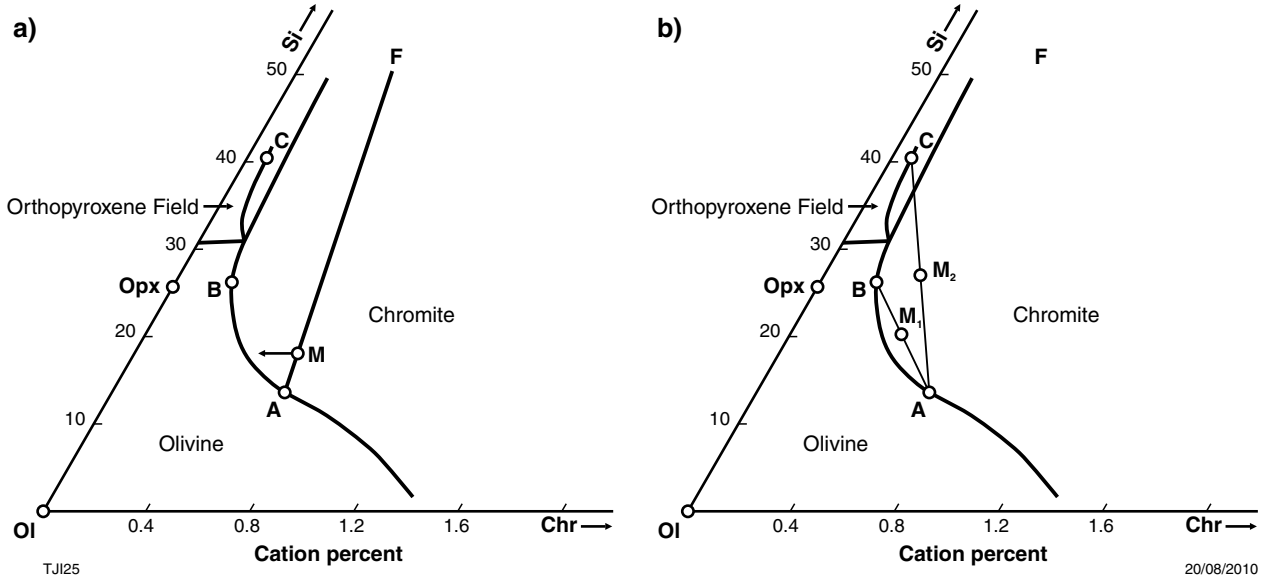


**Figure 74. Formation of chromitites (from Irvine, 1977): a) part of the system $SiO_2$ – $Mg_2SiO_4$ – $Cr_2FeO_4$ showing the fields of olivine, orthopyroxene, and chromite. Note the difference in scales between the Ol–Si and the Ol–Chr sides. Primitive magma of composition A differentiates along the curve A–B precipitating a dunite with 1.5 to 0.5% chromite Continued differentiation from B to C moves the magma into the orthopyroxene field where first olivine and then chromite cease to crystallize. The magma path leaves the pyroxene–chromite peritectic curve and follows the heavy arrow in the orthopyroxene field, because Cr is an included element in orthopyroxene. Contamination of primitive magma at A with felsic crust (F) results in magma with composition M that will crystallize only chromite until it returns to the olivine–chromite cotectic; b) mixing differentiated magma at B or C with primitive magma at A results in hybrid magmas MI or M2 that will crystallize only chromite until they return to the olivine–chromite cotectic**


**Figure 75. Pegmatitic pyroxenite. Hammer is about 40 cm long**

*and bear left onto a north-trending track for a further 1.9 km. Stop at MGA 609064E 6804383N. Walk 100 m to the west.*

Here are good examples of the dunitic and peridotitic rock types that represent the most primitive exposed part of the Narndee Igneous Complex (ultramafic zone, Fig. 60). Hornblende is abundant in thin section (Fig. 64), and phlogopite is locally present as an accessory phase. Proceed 200 m to the north, observing more leucocratic rocks on the way.

Drive north about 1.6 km (to MGA 609022E 6806230N). Examine peridotitic and gabbroic lithologies adjacent to the track. There are some costeans to the east where chromitite can be seen among the other peridotitic lithologies.

Drive east on a track from here and cross a creek to the southeast. Park and walk 100 m (to MGA 609203E 6804683N) where there is an example of a chilled contact zone between a gabbroic–anorthositic sheet and adjacent peridotitic lithologies. Note the bladed texture of amphiboles in the contact region.

# References


Ahmat, AL 1986, Petrology, structure, regional geology and age of the gabbroic Windimurra complex, Western Australia: The University of Western Australia, PhD thesis, (unpublished).

Amelin, YV 1998, Geochronology of the Jack Hills detrital zircons by precise U–Pb isotope dilution analysis of crystal fragments: Chemical Geology, v. 146, p. 25–38.

Arriens, PA 1971, Archaean geochronology of Australia: Geological Society of Australia, Special Publication 3, p. 1–23.

Baxter, JL, Wilde, SA, Pidgeon, RT and Fletcher, IR 1984, The Jack Hills Metasedimentary Belt: an extension of the early Archaean terrain in the Yilgarn Block, Western Australia, *in* Seventh Australian Geological Convention — Geoscience in the Development of Natural Resources: Geological Society of Australia, Abstracts 12, p. 56–57.

Baxter, JL, Wilde, SA, Pidgeon, RT and Collins, LB 1986, A video presentation on the geological setting of ancient detrital zircons within the Jack Hills Metamorphic Belt, WA, *in* Eighth Australian Geological Convention — Earth Resources in Time and Space: Geological Society of Australia, Abstracts 15, p. 220.

Bigourdan, N 2006, Aboriginal watercraft depictions in Western Australia: Department of Maritime Archaeology, Western Australia Museum, Report 216, p. 23–24.

Bindon, PR 1997, Aboriginal people and granite domes: Journal of the Royal Society of Western Australia, v. 80, p. 173–179.

Blichert-Toft, J and Albarède, F 2008, Hafnium isotopes in Jack Hills zircons and the formation of the Hadean crust: Earth and Planetary Science Letters, v. 265, p. 686–702.

Bowring, SA and Williams, IS 1999, Priscoan (4.00–4.03 Ga) orthogneisses from northwestern Canada: Contributions to Mineralogy and Petrology, v. 134, p. 3–16.

Bunting, JA 2004, The nickel–PGE potential of the Narndee and Windimurra intrusions: Report for Apex Minerals NL (unpublished).

Campbell, IH and Hill, RI 1988, A two-stage model for the formation of the granite–greenstone terrains of the Kalgoorlie–Norseman area, Western Australia: Earth and Planetary Science Letters, v. 90, p. 11–25.

Carey, ML 1994, Petrography and geochemistry of selected sills from the Kambalda–Kalgoorlie region, WA: The Australian National University, Canberra, BSc (Hons) thesis (unpublished).

Cassidy, KF, Champion, DC, Krapež, B, Barley, ME, Brown, SJA, Blewett, RS, Groenewald, PB and Tyler, IM 2006, A revised geological framework for the Yilgarn Craton, Western Australia: Geological Survey of Western Australia, Record 2006/8, 8p.

Cavosie, AJ, Wilde, SA, Liu, D, Weiblen, PW and Valley, JW 2004, Internal zoning and U–Th–Pb chemistry of Jack Hills detrital zircons: a mineral record of early Archean to Mesoproterozoic (4348–1576 Ma) magmatism: Precambrian Research, v. 135, p. 251–279.

Cavosie, AJ, Valley, JW, Wilde, SA and Edinburgh Ion Microprobe Facility 2005, Magmatic $\delta^{18}O$ in 4400–3900 Ma detrital zircons: a record of the alteration and recycling of crust in the Early Archean: Earth and Planetary Science Letters, v. 235, p. 663–681.

Cavosie AJ, Valley JW, Wilde, SA and Edinburgh Ion Microprobe Facility 2006, Correlated microanalysis of zircon: trace element, $\delta^{18}O$, and U–Th–Pb isotopic constraints on the igneous origin of complex >3900 Ma detrital grains: Geochimica et Cosmochimica Acta, v. 70, p. 5601–5616.

Cawthorn RG and Walraven, F 1998, Emplacement and crystallization time for the Bushveld Complex: Journal of Petrology, v. 39, p. 1669–1687.

Chambers, J 2004, Planetary accretion in the inner Solar System: Earth and Planetary Science Letters, v. 223, p. 241–252.

Champion, DC and Cassidy, KC 2007, An overview of the Yilgarn Craton and its crustal evolution, *in* Proceedings of Geoconferences (WA) Inc. Kalgoorlie '07 Conference *edited by* FP Bierlein and CM Knox-Robinson: Geoscience Australia, Record 2007/14, p. 8–13.

Chen, SF, Riganti, A, Wyche, S, Greenfield, JE and Nelson, DR 2003, Lithostratigraphy and tectonic evolution of contrasting greenstone successions in the central Yilgarn Craton, Western Australia: Precambrian Research, v. 127, p. 249–266.

Compston, W and Pidgeon, RT 1986, Jack Hills, evidence of more very old detrital zircons in Western Australia: Nature, v. 321, p. 766–769.

Compston W, Williams IS, Campbell, IH and Gresham, JJ 1986, Zircon xenocrysts from the Kambalda volcanics: age constraints and direct evidence for older continental crust below the Kambalda Norseman greenstones: Earth and Planetary Science Letters, v. 76, p. 299–311.

Coogan, LA and Hinton, RW 2006, Do the trace element compositions of detrital zircons require Hadean continental crust?: Geology, v. 34, p. 633–636.

Crowley, JL, Myers, JS, Sylvester, PJ and Cox, RA 2005, Detrital zircon from the Jack Hills and Mount Narryer, Western Australia: evidence for diverse >4.0 Ga source rocks: The Journal of Geology, v. 113, p. 239–263.

Czaja, AD, Johnson, CM, Beard, BL and Van Kranendonk, MJ in press, Iron isotope evidence for an abiological origin of a banded iron-formation from the Yilgarn Craton: 5th International Archean Symposium, Abstracts volume: Geological Survey of Western Australia, Record.

de Laeter, JR, Williams, IR, Rosman, KJR and Libby, WG 1981a, A definitive 3350 m.y. age from banded gneiss, Mount Narryer area, Western Gneiss Terrain: Geological Survey of Western Australia, Annual Report 1980, p. 94–98.

de Laeter, JR, Fletcher, IR, Rosman, KJR, Williams, IR, Gee, RD and Libby, WG, 1981b, Early Archaean gneisses from the Yilgarn Block, Western Australia: Nature, v. 292, p. 322–324.

Dunn, SJ, Nemchin, AA, Cawood, PA and Pidgeon, RT 2005, Provenance record of the Jack Hills Metasedimentary Belt: source of the Earth's oldest zircons: Precambrian Research, v. 138, p. 235–254.

Elias, M 1982, Belele, WA: Geological Survey of Western Australia, 1:250 000 Geological Series Explanatory Notes, 1st edition, 22p.

Elias, M and Williams, SJ 1980, Robinson Range, WA: Geological Survey of Western Australia, 1:250 000 Geological Series Explanatory Notes, 1st edition, 22p.

Ernst R, Buchan, K and Campbell, I 2005, Frontiers in Large Igneous Province research: Lithos, v. 79, p. 271–297.

Eriksson, KA and Wilde, SA 2010, Palaeoenvironmental analysis of Archaean siliciclastic sedimentary rocks in the west central Jack Hills belt, Western Australia with new constraints on ages and correlations: Journal of the Geological Society of London, v. 167, p. 827–840.

Fletcher, IR, McNaughton, NJ, Pidgeon, RT and Rosman, KJR 1997, Sequential closure of K–Ca and Rb–Sr isotopic systems in Archaean micas: Chemical Geology, v. 138, p. 289–301.

Froude, DO, Ireland, TR, Kinny, PD, Williams, IS, Compston, W, Williams, IR and Myers, JS 1983, Ion microprobe identification of 4100–4200 Myr-old terrestrial zircons: Nature, v. 304, p. 616–618.

Fu, B, Page, FZ, Cavosie, AJ, Fournelle, J, Kita, NT, Lackey, JS, Wilde, SA and Valley, JW 2008, Ti-in-zircon thermometry: applications and limitations: Contributions to Mineralogy and Petrology, v. 156, p. 197–215.

Gee, RD 1979, Structure and tectonic style of the Western Australian Shield: Tectonophysics, v. 58, p. 327–369.

Gee, RD, Baxter, JL, Wilde, SA and Williams, IR 1981, Crustal development in the Archaean Yilgarn Block, Western Australia, *in* Archaean Geology *edited by* JA Glover and DI Groves: Geological Society of Australia, Special Publication 7, p. 43–56.

Geological Survey of Western Australia 2008, Interpreted bedrock geology of Western Australia (1:500 000-scale digital compilation): Geological Survey of Western Australia.

Geological Survey of Western Australia 2010, Compilation of geochronology information, 2010 update: Geological Survey of Western Australia.

Grange, ML, Wilde, SA, Nemchin, AA and Pidgeon, RT 2010, Implications of Mesoproterozoic sedimentation at Jack Hills, Western Australia: evidence from zircons hosted within quartzite cobbles in the metaconglomerates: Earth and Planetary Science Letters, v. 292, p. 158–169.

Grimes, CB, John, BE, Kelemen, PB, Mazdab, FK, Wooden, JL, Cheadle, MJ, Hanghøj, K and Shwartz, JJ 2007, Trace element chemistry of zircons from oceanic crust: a method for distinguishing detrital zircon provenance: Geology, v. 35, p. 643–646.

Hallberg, JA 1993, Austin mapping project 1993, 1:25 000 map series: J Hallberg and Associates, Neerabup, Western Australia.

Hallberg, JA 2000, Hallberg Murchison 1:25 000 geology dataset, 1989–1994 (including GSWA Record 2000/20): Geological Survey of Western Australia.

Harrison, TM 2009, The Hadean crust: Evidence from >4 Ga zircons: Annual Review of Earth and Planetary Sciences, v. 37, p. 479–505.

Harrison, TM, Blichert-Toft, J, Müller, W, Albarède, F, Holden, P and Mojzsis, SJ 2005, Heterogeneous Hadean Hafnium: Evidence of Continental Crust at 4.4 to 4.5 Ga: Science, v. 310, p. 1947–1950.

Harrison, TM, Watson, EB and Aikman, AK 2007, Temperature spectra of zircon crystallization in plutonic rocks: Geology, v. 35, p. 635–638.

Harrison, TM, Schmitt, AK, McCulloch, MT and Lovera, OM 2008, Early (4.5 Ga) formation of terrestrial crust: Lu–Hf, $\delta^{18}O$, and Ti thermometry results for Hadean zircons: Earth and Planetary Science Letters, v. 268, p. 476–486.

Hopkins, M, Harrison, TM and Manning, CE 2008, Low heat flow inferred from >4 Ga zircons suggests Hadean plate boundary interactions: Nature 456, p. 493–496.

Irvine, TN 1977, Origin of chromitite layers in the Muskox intrusion and other stratiform intrusions: a new interpretation: Geology, v. 5, p. 273–277.

Ivanic, T 2009, Madoonga, WA Sheet 2444: Geological Survey of Western Australia, 1:100 000 Geological Series.

Ivanic, TJ, Wingate, MTD, Kirkland, CL, Van Kranendonk, MJ and Wyche, S 2010, Age and significance of voluminous mafic–ultramafic magmatic events in the Murchison Domain, Yilgarn Craton: Australian Journal of Earth Sciences, v. 57, p. 597–614.

Kemp, AIS, Wilde, SA, Hawkesworth, CJ, Coath, CD, Nemchin, A, Pidgeon, RT, Vervoort, JD and DuFrane, SA 2010, Hadean crustal evolution revisited: New constraints from Pb–Hf isotope systematics of the Jack Hills zircons: Earth and Planetary Science Letters, v. 296, p. 45–56.

Kent, AJR and McDougall, I 1995, $^{40}Ar$–$^{39}Ar$ and U–Pb age constraints on the timing of gold mineralization in the Kalgoorlie goldfields, Western Australia: Economic Geology, v. 90, p. 845–859.

King, EM, Valley, JW, Davis, DW and Edwards, GR 1998, Oxygen isotope ratios of Archean plutonic zircons from granite–greenstone belts of the Superior Province; indicator of magmatic source: Precambrian Research, v. 92, p. 365–387.

Kinny, PD and Nutman, AP 1996, Zirconology of the Meeberrie gneiss, Yilgarn Craton, Western Australia: an early Archaean migmatite: Precambrian Research, v. 78, p. 165–178.

Kinny, PD, Williams, IS, Froude, DO, Ireland, TR and Compston, W 1988, Early Archaean zircon ages from orthogneisses and anorthosites at Mount Narryer, Western Australia: Precambrian Research, v. 38, p. 325–341.

Kinny, PD, Wijbrans, JR, Froude, DO, Williams, IS and Compston, W 1990, Age constraints on the geological evolution of the Narryer Gneiss Complex, Western Australia: Australian Journal of Earth Sciences, v. 37, p. 51–69.

Köber, B, Pidgeon, RT and Lippolt, HJ 1989, Single-zircon dating by stepwise Pb-evaporation constrains the Archaean history of detrital zircons from the Jack Hills, Western Australia: Earth and Planetary Science Letters, v. 91, p. 286–296.

Liu, SF, Champion, DC and Cassidy, KF 2002, Geology of the Sir Samuel 1:250 000 sheet area, Western Australia: Geoscience Australia, Record 2002/14.

Liu, Y-C, Li, S-G and Xu, S-T 2007, Zircon SHRIMP U–Pb dating for gneisses in northern Dabie high T/P metamorphic zone, central China: implications for decoupling within subducted continental crust: Lithos, v. 96, p. 170–185.

Lofgren, G 1971, Spherulitic textures in glassy and crystalline rocks: Journal of Geophysical Research, v. 76, p. 5635–5648.

Lofgren, G 1974, An experimental study of plagioclase crystal morphology: isothermal crystallisation: American Journal of Science, v. 274, p. 243–273.

Maas, R, Kinny, PD, Williams, IS, Froude, DO and Compston, W 1992, The Earth's oldest known crust: a geochronological and geochemical study of 3900–4200 Ma old detrital zircons from Mt Narryer and Jack Hills, Western Australia: Geochimica et Cosmochimica Acta, v. 56, p. 1281–1300.

Martin, H, Smithies, RH, Rapp, R, Moyen F-F and Champion, D 2005, An overview of adakite, tonalite–trondhjemite–granodiorite (TTG), and sanukitoid: relationships and some implications for crustal evolution: Lithos, v. 79, no. 1–2, p. 1–24.

Mathison, CI, Perring, RJ, Vogt, JH, Parks, J, Hill, RET and Ahmat, AL 1991, The Windimurra Complex *in* Mafic–ultramafic complexes of Western Australia *edited by* SJ Barnes and RET Hill: Sixth International Platinum Symposium guidebook for the post-Symposium field excursion, Geological Society of Australia (WA Division), Excursion Guidebook no. 3, p. 45–76.

Menneken, M, Nemchin, AA, Geisler, T, Pidgeon, RT and Wilde, SA 2007, Hadean diamonds in zircon from Jack Hills, Western Australia: Nature, v. 448, p. 917–920.

Mojzsis, SJ, Harrison, TM and Pidgeon, RT 2001, Oxygen-isotope evidence from ancient zircons for liquid water at the Earth's surface 4300 Myr ago: Nature, v. 409, p. 178–181.

Mueller, AG, Campbell, IH, Schiøtte, L, Sevigny, JH and Layer, PW 1996, Constraints on the age of granitoid emplacement, metamorphism, gold mineralization, and subsequent cooling of the Archean greenstone terrane at Big Bell, Western Australia: Economic Geology, v. 91, p. 896–915.

Myers, JS 1988, Early Archaean Narryer Gneiss Complex, Yilgarn Craton, Western Australia: Precambrian Research, v. 38, p. 297–307.

Myers, JS 1990, Western Gneiss Terrane, *in* Geology and mineral resources of Western Australia: Geological Survey of Western Australia, Memoir 3, p. 13–31.

Myers, JS and Williams, IR 1985, Early Precambrian crustal evolution at Mount Narryer, Western Australia: Precambrian Research, v. 27, p. 153–163.

Nelson, DR, Robinson, BW and Myers, JS 2000, Complex geological histories extending for ≥4.0 Ga deciphered from xenocryst zircon microstructures: Earth and Planetary Science Letters, v. 181, p. 89–102.

Nemchin, AA, Pidgeon, RT and Whitehouse, MJ 2006, Re-evaluation of the origin and evolution of >4.2 Ga zircons from the Jack Hills metasedimentary rocks: Earth and Planetary Science Letters, v. 244, p. 218–233.

Nemchin, AA, Whitehouse, MJ, Menneken, M, Geisler, T, Pidgeon, RT and Wilde, SA 2008, Light carbon reservoir in the early Earth revealed by diamond and graphite inclusions in 3050 to 4250 Myr old zircon from Jack Hills, Western Australia: Nature, v. 453, p. 92–95.

Nieuwland, DA and Compston, W 1981, Crustal evolution in the Yilgarn Block near Perth, Western Australia, *in* Archaean Geology *edited by* JA Glover and DI Groves: Geological Society of Australia, Special Publication 7, p. 159–171.

Nutman, AP and Kinny, PD 1990, Migmatitic Meeberrie Gneiss west of Nookawarra Bore 37, *in* Third International Archaean Symposium, Perth, excursion guidebook *edited by* SE Ho, JE Glover, JS Myers and J Muhling: University of Western Australia, Publication 21, p. 92–93.

Nutman, AP, Kinny, PD, Compston, W and Williams, IS 1991, SHRIMP U–Pb zircon geochronology of the Narryer Gneiss Complex, Western Australia: Precambrian Research, v. 52, p. 275–300.

Nutman, AP, Kinny, PD and Price, R 1993, Large-scale crustal structure of the northwestern Yilgarn Craton, Western Australia: Evidence from Nd isotopic data and zircon geochronology: Tectonics, v. 12, p. 971–981.

Occhipinti, SA and Reddy, SM 2004, Deformation in a complex crustal-scale shear zone: Errabiddy Shear Zone, Western Australia, *in* Flow Processes in Faults and Shear Zones *edited by* GI Alsop, RE Holdsworth, KJW McCaffrey and M Hand: Geological Society of London, Special Publication, 224, p. 229–248.

Occhipinti, SA and Reddy, SM 2009, Neoproterozoic reworking of the Palaeoproterozoic Capricorn Orogen of Western Australia and implications for the amalgamation of Rodinia*, in* Ancient Orogens and Modern Analogues *edited by* JB Murphy, JD Keppie and AJ Hynes: Geological Society of London, Special Publication, 327, p. 445–456.

Occhipinti, SA, Sheppard, S, Passchier, C, Tyler, IM and Nelson, DR 2004, Palaeoproterozoic crustal accretion and collision in the southern Capricorn Orogen: the Glenburgh Orogeny: Precambrian Research, v. 128, p. 237–255.

Parks, J 1983, The geology and geochemistry of the Windimurra Hills section, Windimurra Complex, Western Australia: The University of Western Australia, BSc (Hons) thesis (unpublished).

Parks, J 1998, The Weld Range platinum group element deposit, *in* Geology of Australian and Papua New Guinean mineral deposits *edited by* DA Berkman and DH Mackenzie: Australasian Institute of Mining and Metallurgy, Monograph 22, p. 279–286.

Peck, WH, Valley, JW, Wilde, SA and Graham, CM 2001, Oxygen isotope ratios and rare earth elements in 3.3 to 4.4 Ga zircons: Ion microprobe evidence for high $\delta^{18}O$ continental crust and oceans in the Early Archean: Geochimica et Cosmochimica Acta, v. 65, p. 4215–4229.

Pidgeon, RT 1992, Recrystallisation of oscillatory zoned zircon: some geochronological and petrological implications: Contributions to Mineralogy and Petrology, v. 110, p. 463–472.

Pidgeon, RT and Hallberg, JA 2000, Age relationships in supracrustal sequences in the northern part of the Murchison Terrane, Archaean Yilgarn Craton, Western Australia: a combined field and zircon U–Pb study: Australian Journal of Earth Sciences, v. 47, p. 153–165.

Pidgeon, RT and Wilde, SA 1990, The distribution of 3.0 Ga and 2.7 Ga volcanic episodes in the Yilgarn Craton of Western Australia: Precambrian Research, v. 48, p. 309–325.

Pidgeon, RT and Wilde, SA 1998, The interpretation of complex zircon U–Pb systems in Archaean granitoids and gneisses from the Jack Hills, Narryer Gneiss Terrane, Western Australia: Precambrian Research, v. 91, p. 309–332.

Pidgeon, RT and Nemchin, AA 2006, High abundance of early Archaean grains and the age distribution of detrital zircons in a sillimanite-bearing quartzite from Mt Narryer, Western Australia: Precambrian Research, v. 150, p. 201–220.

Rasmussen, B, Fletcher, IR, Muhling, JR and Wilde, SA 2010, In situ U–Th–Pb geochronology of monazite and xenotime from the Jack Hills belt: implications for the age of deposition and metamorphism of Hadean zircons: Precambrian Research, v. 180, p. 26–46.

Riganti, A, Wyche, S, Wingate, MTD, Kirkland, CL and Chen, SF 2010, Constraints on ages of greenstone magmatism in the northern part of the South Cross Domain, Yilgarn Craton: 5th International Archean Symposium, Extended Abstracts.

Rollinson, H 2008, Ophiolitic trondhjemites: a possible analogue for Hadean felsic 'crust': Terra Nova, v. 20, p. 364–369.

Schiøtte, L and Campbell, IH 1996, Chronology of the Mount Magnet granite–greenstone terrain, Yilgarn Craton, Western Australia: implications for field based predictions of the relative timing of granitoid emplacement: Precambrian Research, v. 78, p. 237–260.

Scowen, P 1991, The geology and geochemistry of the Narndee intrusion: Australian National University, Canberra, PhD thesis (unpublished).

Spaggiari, CV 2006, Interpreted bedrock geology of the northern Murchison Domain, Youanmi Terrane, Yilgarn Craton: Geological Survey of Western Australia, Record 2006/10, 19p.

Spaggiari, CV 2007a, The Jack Hills greenstone belt, Western Australia, Part 1: Structural and tectonic evolution over >1.5 Ga: Precambrian Research, v. 155, p. 204–228.

Spaggiari, CV 2007b, Structural and lithological evolution of the Jack Hills greenstone belt, Narryer Terrane, Yilgarn Craton, Western Australia: Geological Survey of Western Australia, Record 2007/3, 49p.

Spaggiari, CV, Pidgeon, RT and Wilde, SA 2007, The Jack Hills greenstone belt, Western Australia, Part 2: Lithological relationships and implications for the deposition of >4.0 Ga detrital zircons: Precambrian Research, v. 155, p. 261–286.

Spaggiari, CV, Wartho, J-A and Wilde, SA 2008, Proterozoic development of the northern margin of the Archean Yilgarn Craton: Precambrian Research, v. 162, p. 354–384.

Sun, S-S and McDonough, WF 1989, Chemical and isotopic systematics of oceanic basalts: implications for mantle compositions and processes, *in* Magmatism in the ocean basins *edited by* AD Saunders and MJ Norry: Publication of The Geological Society of London, p. 313–345.

Ushikubo, T, Kita, NT, Cavosie, AJ, Wilde, SA, Rudnick, RL and Valley, JW 2008, Lithium in Jack Hills zircons: evidence for extensive weathering of Earth's earliest crust: Earth and Planetary Science Letters, v. 272, p. 666–676.

Valley, JW, Peck, WH, King, EM and Wilde, SA 2002, A Cool Early Earth: Geology, v. 30, p. 351–354.

Van Kranendonk, MJ 2008, New evidence on the evolution of the Cue–Meekatharra area of the Murchison Domain, Yilgarn Craton: Geological Survey of Western Australia, Annual Review 2006–07, p. 39–49.

Van Kranendonk, MJ and Ivanic, TJ 2009, A new lithostratigraphic scheme for the northeastern Murchison Domain, Yilgarn Craton: Geological Survey of Western Australia, Annual Review 2007–08, p. 34–53.

Van Kranendonk, MJ, Philippot P, Lepot, K, Bodorkos, S and Pirajno, F 2008, Geological setting of Earth's oldest fossils in the c. 3.5 Ga Dresser Formation, Pilbara Craton, Western Australia: Precambrian Research, v. 167, p. 93–124.

Wang, Q 1998, Geochronology of the granite–greenstone terranes in the Murchison and Southern Cross Provinces of the Yilgarn Craton, Western Australia: The Australian National University, Canberra, PhD thesis (unpublished).

Watkins, KP, Fletcher, IR, and de Laeter, JR 1991, Crustal evolution of Archaean granitoids in the Murchison Province, Western Australia: Precambrian Research, v. 50, p. 311–336.

Watkins, KP and Hickman, AH 1990, Geological evolution and mineralization of the Murchison Province, Western Australia: Geological Survey of Western Australia, Bulletin 137, 267p.

Watson, EB and Harrison, TM 2005, Zircon thermometer reveals minimum melting conditions on earliest Earth: Science, v. 308, p. 841–844.

Wiedenbeck, M and Watkins, KP 1993, A time scale for granitoid emplacement in the Archean Murchison Province, Western Australia, by single zircon geochronology: Precambrian Research, v. 61, p. 1–26.

Wilde, SA 2001, Jimperding and Chittering metamorphic belts, southwestern Yilgarn Craton, Western Australia — a field guide: Geological Survey of Western Australia, Record 2001/12, 24p.

Wilde, SA 2010, Proterozoic volcanism in the Jack Hills Belt, Western Australia: some implications and consequences for the World's oldest zircon population: Precambrian Research <doi:10.1016/j.precamres.2010.05.007> viewed May 2010.

Wilde, SA and Low, GH 1978, Perth, Western Australia: Geological Survey of Western Australia: 1:250 000 Geological Series Explanatory Notes, 36p.

Wilde, SA, Middleton, MF and Evans, BJ 1996, Terrane accretion in the southwest Yilgarn Craton: evidence from a deep seismic crustal profile: Precambrian Research, v. 78, p. 179–196.

Wilde, SA and Pidgeon, RT 1990, Geology of the Jack Hills metasedimentary rocks, *in* Third International Archaean Symposium, Perth, excursion guidebook *edited by* SE Ho, JE Glover, JS Myers and J Muhling: The University of Western Australia and Extension Service, Publication 21, p. 82–92.

Wilde, SA and Spaggiari, CV 2007, The Narryer Terrane, Western Australia: a review, *in* Earth's Oldest Rocks: Elsevier Special Publication 17, p. 275–304.

Wilde, SA, Valley, JW, Peck, WH and Graham, CM 2001, Evidence from detrital zircons for the existence of continental crust and oceans on the Earth 4.4 Gyr ago: Nature, v. 409, p. 175–178.

Williams, IR, Walker, IM, Hocking, RM and Williams, SJ 1983, Byro, WA: Geological Survey of Western Australia, 1:250 000 Geological Series Explanatory Notes, 1st edition, 27p.

Williams, IR and Myers, JS 1987, Archaean geology of the Mount Narryer region, Western Australia: Geological Survey of Western Australia, Report 22, 32p.

Wingate, MTD, Kirkland, CL and Ivanic, TJ 2010, Sample 191056: gabbronorite, Kockalocka Bore: Geochronology Record 898: Geological Survey of Western Australia, 4p.

Wingate, MTD, Kirkland CL and Pawley, MJ in press a, 185968, leucogabbro, Mount Sefton: Geological Survey of Western Australia, Geochronology Record 869.

Wingate, MTD, Kirkland CL and Pawley, MJ in press b, 185976, leucogabbro, Mount Warren: Geological Survey of Western Australia, Geochronology Record 870.

Woods, BK, 1997, Petrogenesis and geochronology of felsic dykes in the Kalgoorlie Terrane, Kalgoorlie, Western Australia: Curtin University of Technology, Perth, BSc (Hons) thesis (unpublished).

Wyche, S (compiler) 2008, Kalgoorlie, Youanmi, and Narryer Terranes of the Yilgarn Craton — a field guide: Geological Survey of Western Australia, Record 2008/12, 67p.

Yeats, CJ, McNaughton, NJ and Groves, DI 1996, SHRIMP U–Pb geochronological constraints on Archean volcanic-hosted massive sulfide and lode gold mineralization at Mount Gibson, Yilgarn Craton, Western Australia: Economic Geology, v. 91, p. 1354–1371.

RECORD 2010/19

# A time transect through the Hadean to Neoarchean geology of the western Yilgarn Craton — a field guide

Van Kranendonk et al.

This Record is published in digital format (PDF) and is available online at <www.dmp.wa.gov.au/GSWApublications>.
Laser-printed copies can be ordered from the Information Centre for the cost of printing and binding.

Further details of geological products produced by the Geological Survey of Western Australia can be obtained by contacting:

Information Centre
Department of Mines and Petroleum
100 Plain Street
EAST PERTH WESTERN AUSTRALIA 6004
Phone: (08) 9222 3459 Fax: (08) 9222 3444
www.dmp.wa.gov.au/GSWApublications